UNIVERSIDADE FEDERAL DO RIO GRANDE DO SUL

INSTITUTO DE PESQUISAS HIDRÁULICAS

PROGRAMA DE PÓS-GRADUAÇÃO EM RECURSOS HÍDRICOS E SANEAMENTO AMBIENTAL

IAN ROCHA DE ALMEIDA

REMOÇÃO DO FUNGICIDA CARBENDAZIM POR ADSORÇÃO EM CARVÃO ATIVADO GRANULAR

PORTO ALEGRE

2023

IAN ROCHA DE ALMEIDA

REMOÇÃO DO FUNGICIDA CARBENDAZIM POR ADSORÇÃO EM CARVÃO ATIVADO GRANULAR

Tese apresentada ao Programa de Pós-graduação em Recursos Hídricos e Saneamento Ambiental da Universidade Federal do Rio Grande do Sul, como requisito parcial à obtenção do grau de doutor.

Orientador: Antônio Domingues Benetti

PORTO ALEGRE

2023

CIP - Catalogação na Publicação

Almeida, Ian Rocha de
Remoção do fungicida Carbendazim por adsorção em carvão ativado granular / Ian Rocha de Almeida. -- 2023.
145 f.
Orientador: Antônio Domingues Benetti.

Tese (Doutorado) -- Universidade Federal do Rio Grande do Sul, Instituto de Pesquisas Hidráulicas, Programa de Pós-Graduação em Recursos Hídricos e Saneamento Ambiental, Porto Alegre, BR-RS, 2023.

1. Carbendazim. 2. Adsorção. 3. Carvão ativado granular. 4. Isotermas. 5. Ensaios Rápidos em Colunas de Escala Reduzida. I. Benetti, Antônio Domingues, orient. II. Título.

Elaborada pelo Sistema de Geração Automática de Ficha Catalográfica da UFRGS com os dados fornecidos pelo(a) autor(a).

IAN ROCHA DE ALMEIDA

REMOÇÃO DO FUNGICIDA CARBENDAZIM POR ADSORÇÃO EM CARVÃO ATIVADO GRANULAR

Tese apresentada ao Programa de Pós-graduação em Recursos Hídricos e Saneamento Ambiental da Universidade Federal do Rio Grande do Sul, como requisito parcial à obtenção do grau de doutor).

Aprovado em: Porto Alegre, 18 de agosto de 2023.

_____

Prof. Dr. Antônio Domingues Benetti – UFRGS
Orientador

_____

Profª. Drª. Maria Cristina de Almeida Silva - UFRGS
Examinadora

_____

Profª. Drª. Edumar Ramos Cabral Coelho - UFES

Examinadora

_____

Profª. Drª. Nathalia Krummenauer Haro - UNIRITTER
Examinadora

AGRADECIMENTOS

Agradeço a meus pais (Edilene Almeida e Paulo Almeida) e a meu irmão (Renan Almeida), que me acompanharam e me apoiaram em mais um grande desafio da minha vida.

Agradeço à minha companheira (Lígia Tavares) que esteve junto comigo do início ao fim dessa longa e difícil jornada. Que dividiu comigo as alegrias e as tristezas desses sete anos de vivência em Porto Alegre e sempre me deu conselhos nos momentos de indecisão e angústia.

Agradeço aos amigos (Izabella Bosisio, Barroso Júnior, Rafael Fritzen, Thaís Frota, Maria Cristina, Juliano, Ana Flávia, Louidi Albornoz, Raíssa Engroff, Maria Teresa Guedes, Marcos Ribeiro, Lucas Bohnenberger, Camila Zorzo, Juliana Andrade, Franciele Vanelli) pelos momentos de descontração e acolhimento nos períodos mais adversos que passamos durante este ciclo do doutorado.

Agradeço ao professor Antônio Benetti, meu orientador, pelos valiosos conselhos que me deu não apenas neste trabalho, mas em todas as minhas atividades do doutorado.

Aos alunos de Iniciação Científica Daphne Calazans, Daniel Moro e Geovana Keller pelo auxílio nos experimentos realizados em laboratório.

Agradeço à CAPES e ao CNPq pelo fomento à pesquisa, cujo recurso foi de fundamental importância para viabilizar o trabalho aqui desenvolvido.

RESUMO

ALMEIDA, Ian Rocha de. Remoção do fungicida Carbendazim por adsorção em carvão ativado granular. 2023. Tese (Doutorado em Recursos Hídricos e Saneamento Ambiental) — Instituto de Pesquisas Hidráulicas, Universidade Federal do Rio Grande Sul, Porto Alegre, 2023.

O estudo investigou a adsorção do fungicida Carbendazim (CBZ) em Carvão Ativado Granular (CAG) através de ensaios em batelada e em fluxo contínuo usando o método de Ensaios Rápidos em Colunas de Escala Reduzida (ERCER). Os ensaios foram realizados em meios contendo água deionizada somente e com adição de matéria orgânica, além de água pós-filtração de uma Estação de Tratamento de Água (ETA) de Porto Alegre. Foram analisados quais modelos de isoterma e cinética melhor se ajustaram à adsorção do fungicida. Foi realizado um estudo da termodinâmica do CBZ em água deionizada. Ensaios ERCER simularam a operação e remoção de CBZ em uma coluna com CAG. Nos testes foram obtidos os tempos de ruptura, saturação, taxa de transferência específica (TTE) e taxa de utilização do carvão (TUC) nas três matrizes aquosas testadas. Os resultados indicaram que a isoterma de Freundlich foi a que melhor se ajustou à adsorção do CBZ em CAG. A maioria dos experimentos mostrou que a adsorção do composto foi favorável. A remoção do fungicida é caracterizada como um processo exotérmico, espontâneo, com predominância da fisiossorção e a presença de interações dipolo-dipolo entre a superfície do CAG e o CBZ. Quanto à cinética, o modelo de pseudo-segunda ordem foi o que melhor se ajustou na adsorção do CBZ, independente das condições experimentais aplicadas e do meio no qual o CBZ estava dissolvido. A difusão intrapartícula influenciou mais na adsorção do CBZ em água da ETA. Quanto aos ERCER, o tempo de ruptura foi maior para os experimentos em AD. Não houve diferença significativa entre os pontos de saturação obtidos para este meio e nos demais. Os valores de TUC e TTE mostraram que a coluna com CBZ dissolvido somente em AD apresentou maior eficiência do que nas outras matrizes. De forma geral, a MON na forma de ácido húmico e as substâncias presentes na água filtrada da ETA impactaram no tempo de ruptura na coluna de CAG mas a interferência não foi significativa nos tempos de saturação. Analisando a competição do CBZ pelos sítios adsortivos do CAG com as substâncias presentes na água filtrada da ETA e com a matéria orgânica, observou-se que essa competição foi mais evidenciada nos estudos de isoterma e cinética, em que há a mudanças de valores dos parâmetros obtidos. A competição pelos sítios adsortivos do CAG é controlada principalmente pela distribuição dos tamanhos dos poros, uma vez que a matéria orgânica pode ocupar os macros e mesoporos do CAG, impedindo o acesso do CBZ aos microporos do adsorvente. As interações eletrostáticas entre a matéria orgânica e o carvão ativado também podem ter interferido na adsorção do CBZ, devido às características do CAG e dos compostos nas condições experimentais aplicadas. Para os experimentos utilizando o ERCER, a competição pelos sítios adsortivos do CAG não foi considerada significativa e há indícios de que a MON possa ter melhorado a eficiência do CAG. O estudo do *fouling* mostrou que a MON não impactou significativamente a curva de ruptura do CBZ.

Palavras-chave: Carbendazim; Adsorção; Carvão ativado granular; Isotermas; Cinética; Ensaios Rápidos em Colunas de Escala Reduzida.

ABSTRACT

ALMEIDA, Ian Rocha de. Removal of the fungicide Carbendazim by adsorption on granular activated carbon. 2023. Doctoral thesis (Water Resources and Environmental Engineering) — Instituto de Pesquisas Hidráulicas. Universidade Federal do Rio Grande do Sul. 2023.

The study investigated the adsorption of the fungicide Carbendazim (CBZ) on Granular Activated Carbon (GAC) through batch and continuous flow tests using Rapid Small-Scale Column Tests (RSSCT). The experimental tests were made using media containing only deionized water and with the addition of organic matter, as well as post-filtration water from a Water Treatment Plant (WTP). The study analyzed which isotherm and kinetic models best fitted the adsorption of the fungicide. A study of the thermodynamics of CBZ in deionized water was also conducted. RSSCT tests simulated the operation and removal of CBZ in a column with GAC. It was possible to estimate the breakthrough time, saturation time, specific transfer rate (STR), and carbon utilization rate (CUR) in the three aqueous matrices tested. The results indicated that the Freundlich isotherm best fitted the adsorption of CBZ on GAC. Most experiments showed that the compound's adsorption was favorable. The removal of the fungicide was characterized as an exothermic and spontaneous process, with a predominance of physisorption and the presence of dipole-dipole interactions between the surface of GAC and CBZ. Regarding kinetics, the pseudo-second-order model best fitted the adsorption of CBZ, regardless of the experimental conditions applied and the medium in which CBZ was dissolved. Intraparticle diffusion influenced CBZ adsorption more in FWTP water. As for RSSCTs, the breakthrough time was longer for experiments in post-filtration water. There was no significant difference between the saturation points obtained for this medium and the others. The CUR and STR values showed that the column with CBZ dissolved in post-filtration water presented greater efficiency than the other matrices. Overall, the NOM in the form of humic acid and substances present in filtered WTP water impacted the breakthrough time in the GAC column. However, the interference was not significant in saturation times. Analyzing the competition of CBZ for GAC adsorptive sites with substances present in filtered WTP water and organic matter, it was observed that this competition was more evident in isotherm and kinetic studies, where there was a change in the parameters' values. The distribution of pore sizes controls competition for GAC adsorptive sites since organic matter can occupy GAC's macros and mesopores, preventing CBZ access to the adsorbent's micropores. Electrostatic interactions between organic matter and activated carbon may also have interfered with CBZ adsorption due to the characteristics of GAC and the compounds in the applied experimental conditions. For the experiments using RSSCT, competition for GAC adsorption sites was not considered significant, and there are indications that NOM may have improved GAC efficiency. The fouling study showed that NOM did not significantly impact the CBZ breakthrough curve.

Keywords: Carbendazim; Adsorption; Granular activated carbon; Isotherms; Kinetics; Rapid Small-Scale Column Tests.

LISTA DE FIGURAS

LISTA DE TABELAS

LISTA DE ABREVIATURAS

AD	Água Deionizada
ANVISA	Agência Nacional de Vigilância Sanitária
CAG	Carvão Ativado Granular
CAP	Carvão Ativado Pulverizado
CBZ	Carbendazim
CD	Constant Diffusivity
CEC	Contaminants of Emerging Concern
COD_b	Carbono Orgânico Dissolvido Biodegradável
CPE	Contaminantes de Preocupação Emergente
CUR	Carbon Utilization Rate
DW	Deionized water
DWNOM	Deionized Water with Addition of Natural Organic Matter
EBCT	Empty Bed Contact Time
ERCER	Ensaios Rápidos em Colunas de Escala Reduzida
ETA	Estação de Tratamento de Água
ETE	Estação de Tratamento de Esgoto
FWTP	Filtered Water From a Treatment Plant
GAC	Granular Activated Carbon
HLR	Hydraulic Loading Rate
HPLC	High-Performance Liquid Chromatograph
HSD	Honestly Significant Difference
MON	Matéria Orgânica Natural
NOM	Natural Organic Matter
PD	Proportional Diffusivity
PZC	Point of Zero Charge
RSM	Response Surface Methodology
RSSCT	Rapid Small-Scale Column Tests
STR	Specific Transfer Rate
SW	Shapiro- Wilk
TAS	Taxa de Aplicação Superficial
TCLV	Tempo de Contato de Leito Vazio
TTE	Taxa de Transferência Específica
TUC	Taxa de Utilização do Carvão
WTP	Water Treatment Plant
ZTM	Zona de Transferência de Massa

SUMÁRIO

1. INTRODUÇÃO E JUSTIFICATIVA

O acesso à água potável é um dos desafios globais, pois este é um recurso fundamental para manutenção da salubridade ambiental e da saúde humana (SCHWARZENBACH *et al.*, 2010). Todavia, a quantidade e a qualidade desse recurso natural continuamente são impactados por ações antrópicas (BENNER *et al.*, 2013). Essas ações têm resultado na intensificação do lançamento de poluentes para o meio natural, entre os quais os contaminantes de preocupação emergente.

O interesse no estudo dos contaminantes emergentes em corpos hídricos tem crescido ao longo dos anos, uma vez que os tratamentos convencionais de água apresentam limitações na remoção desses compostos. Há, ainda, uma carência mundial no que diz respeito à regulação da emissão destes compostos (HALLÉ, HUCK e PELDSZUS, 2015). Cada vez mais, as pesquisas apontam efeitos deletérios desses poluentes para a salubridade ambiental e para a saúde pública. Os efeitos dependem da concentração e do tempo de exposição de organismos a esses compostos (PAREDES *et al.*, 2016).

Dentre os contaminantes de preocupação emergente, um grupo que se destaca são os agrotóxicos, também conhecido como defensivos agrícolas ou praguicidas. Segundo a Agência Nacional de Vigilância Sanitária (ANVISA, 2019), agrotóxicos são substâncias aplicadas em insumos agrícolas, pastagens, cuja finalidade seja alterar a composição da flora ou da fauna a fim de preservá-las da ação danosa de seres vivos considerados nocivos, bem como as substâncias e produtos empregados como desfolhantes, dessecantes, estimuladores e inibidores de crescimento. Nas últimas décadas, o Brasil tem sido um dos maiores consumidores e produtores de pesticidas no mundo, sendo o primeiro em ambos os aspectos na América Latina (BARBOSA, SOLANO e UMBUZEIRO, 2015; COELHO & ROZÁRIO, 2019; PRETE *et al.*, 2017).

O Carbendazim (CBZ) é um dos agrotóxicos mais utilizados no Brasil. O CBZ é um defensivo agrícola do grupo dos benzimidazóis (RAMA *et al.*, 2014). Esse composto é um fungicida sistêmico aplicado nas culturas de algodão, arroz, citros, feijão, maçã, milho, soja e trigo (ANVISA, 2012; RAMA, 2013). O CBZ é eficiente contra uma variedade de doenças nessas culturas causadas pelos fungos *Ascomicetos spp., Basidiomicetos e Deuteromicetos spp* (COUTINHO, GALLI, MAZO, 2007).

O CBZ já foi detectado em amostras de água de abastecimento da cidade de Porto Alegre, juntamente com outros 26 agrotóxicos (BRASIL, 2020). A Agência Nacional de Vigilância Sanitária (ANVISA) proibiu o uso deste composto (ANVISA, 2022), entretanto, a eliminação do produto está sendo gradual, uma vez que o CBZ é largamente utilizado por agricultores brasileiros nas plantações de feijão, arroz, soja e de outros produtos agrícolas importantes para a economia brasileira (PEDUZZI, 2022).

A reavaliação toxicológica do CBZ, realizada pela ANVISA entre 2020 e 2022, concluiu que o fungicida apresenta potencial carcinogênico, induz mutações em células germinativas e pode causar toxicidade reprodutiva em seres humanos. Além disso, a Agência apontou que não foi possível encontrar um limiar de dose segura para a população quanto às características de mutagenicidade e toxicidade reprodutiva (ANVISA, 2022).

Com o intuito de mitigar os impactos ao meio ambiente e à saúde humana provocados pela exposição de organismos às concentrações de pesticidas consideradas tóxicas, diversos estudos têm sido realizados sobre tecnologias de tratamento para a remoção destes compostos. Dentre as técnicas apresentadas, o processo de adsorção em carvão ativado é amplamente estudado, apresentando moderado custo de aplicação e manutenção, comparando-se outras técnicas de tratamento avançado (CRITTENDEN *et al.*, 1987).

Diante do exposto, o presente documento detalha a pesquisa de doutorado que aborda a remoção de Carbendazim por adsorção em carvão ativado granular, em batelada e em fluxo contínuo, em amostras com água deionizada, água efluente do filtro de uma Estação de Tratamento de Água (ETA) e água deionizada com adição de ácido húmico para investigar a interferência da matéria orgânica na adsorção. A tese de doutorado foi escrita no formato de artigos, que compuseram a seção de Resultados e Discussões.

2. OBJETIVO

2.1. OBJETIVO GERAL

Avaliar a remoção do fungicida Carbendazim por adsorção em carvão ativado granular (CAG) através de ensaios em batelada e Ensaios Rápidos em Colunas de Escala Reduzida (ERCER) de leito fixo.

2.2. OBJETIVOS ESPECÍFICOS

a) Determinar os parâmetros da cinética e termodinâmica de adsorção do CBZ em carvão ativado através de ensaios em batelada;

b) Identificar a isoterma que melhor se ajusta à adsorção do CBZ em ensaios em batelada através de métodos não lineares;

c) Identificar parâmetros operacionais, como os tempos de ruptura e de saturação da coluna de adsorção, para o Carbendazim dissolvido em água deionizada somente, em amostra efluente de filtro rápido de Estação de Tratamento de Água, e em água deionizada com matéria orgânica;

d) Verificar se há competição pelos sítios adsortivos do carvão ativado entre o CBZ e as substâncias presentes nas amostras de água da ETA e a matéria orgânica.

3. REVISÃO BIBLIOGRÁFICA

3.1. CARVÃO ATIVADO

Nesse tópico serão abordados o uso de carvão ativado na remoção de poluentes de água potável, com foco no uso do Carvão Ativado Granular (CAG).

3.1.1. Adsorção em carvão ativado

A adsorção é um processo de transferência de fase em que os átomos, íons ou moléculas no estado gasoso, líquido ou sólido se acumulam na fase sólida. O composto que se deposita na superfície é definido como o adsorvato enquanto o sólido que fornece a superfície é o adsorvente (METCALF & EDDY, 2014). Nos processos de tratamento de água, a adsorção é, geralmente, um dos processos mais econômicos para reduzir as concentrações de contaminantes dissolvidos (BENJAMIN & LAWLER, 2013).

Diversos fatores podem influenciar no processo de adsorção de um composto ao adsorvente, podendo-se citar as propriedades do fluido (pH, temperatura, por exemplo), características e concentração do poluente, além da presença de outros compostos que podem competir pelos sítios de adsorção. A afinidade entre adsorvato e adsorvente é essencial para a eficiência do processo, além de determinar os mecanismos de adsorção que podem incluir troca iônica, interações eletrostáticas, precipitação na superfície, reações químicas ou a combinação de todos esses fatores (BONILLA-PETRICIOLET, MENDOZA-CASTILLO, DIDILIA ILEANA, 2017). A aplicação de condições apropriadas maximiza o fator de separação e melhora a eficiência de remoção do poluente no sistema desejado.

O carvão ativado é normalmente produzido pela decomposição térmica de material carbonáceo seguido por ativação com vapor ou dióxido de carbono a temperaturas elevadas (700º – 1100º C). O processo de ativação envolve essencialmente a remoção de produtos de carbonização formados durante a pirólise, abrindo os poros do material (RUTHVEN, 1984).

De acordo com Crittenden *et al* (1999), Li *et al* (2002) e Schoonenberg *et al* (2010), a técnica de adsorção em carvão ativado remove preferencialmente compostos orgânicos hidrofóbicos através de interações de van der Waals entre o

carvão e o soluto. Através dessas particularidades, a remoção de compostos mais insolúveis e apolares são favorecidas nos processos de adsorção em carvão ativado.

O processo de adsorção pode ocorrer de forma física (fisiossorção) ou química (quimiossorção). As particularidades que distinguem os dois tipos de adsorção são apresentadas no Quadro 3.1. Vários estudos apontam que quase todo tipo de processo de separação adsortivo depende da adsorção física (RUTHVEN, 1984).

Quadro 3.1 - Diferenças entre adsorção física e química de compostos ao carvão ativado.

Adsorção Física	**Adsorção Química**
Baixo calor de adsorção (duas ou três vezes menor que o calor de evaporação), 5 a 40 kJ/mol	Alto calor de adsorção (duas ou três vezes maior que o calor de evaporação), 40 a 800 kJ/mol
Não específica.	Altamente específico.
Monocamada ou multicamada, sem dissociação de espécies envolvidas. Significante somente em temperaturas relativamente baixas.	Monocamada somente. Pode envolver dissociação. Possível em uma ampla faixa de temperatura.
Rápida, não ativada, reversível. Sem transferência de elétrons, contudo pode ocorrer polarização do adsorvato.	Ativada. Pode ser lenta e irreversível. Transferência de elétrons levando à formação de ligações entre adsorvato e adsorvente.

Fonte: Adaptado de Ruthven, 1984.

Os processos de adsorção envolvem vários aspectos de engenharia, que devem ser otimizados para maximizar a remoção de contaminantes. A Figura 3.1 mostra esses aspectos que devem estar alinhados com as propriedades texturais, além da química da superfície dos adsorventes usados (BONILLA-PETRICIOLET, MENDOZA-CASTILLO, DIDILIA ILEANA, 2017).

Figura 3.1 - Aspectos de engenharia envolvidos no processo de adsorção.

Fonte: Adaptado de Bonilla-Petriciolet, Mendoza-Castillo, Didilia Ileana, 2017.

Quanto aos processos de adsorção em Estações de Tratamento de Água (ETA), a transferência de massa de um ou mais contaminantes (adsorvatos) é realizada predominantemente da fase líquida para a fase sólida (JULIANO, 2010). Nesse processo, as moléculas presentes na fase fluida são depositadas na superfície do adsorvente. O carvão ativado é o adsorvente mais utilizado em ETAs que aplicam a adsorção para a remoção de poluentes específicos (COELHO *et. al.*, 2005).

A utilização de carvão ativado no tratamento de água pode ocorrer na forma de Carvão Ativado Granular (CAG) ou Carvão Ativado Pulverizado (CAP), dependendo do tipo de água bruta, da ETA e do poluente que se deseja remover. Há uma grande variedade de carvões sendo fabricados e comercializados (BRANDÃO & SILVA, 2006), sendo a escolha do tipo de carvão dependente dos fatores técnico-econômicos, de funcionalidade operacional da ETA, além de aspectos cinéticos envolvidos na adsorção (JULIANO, 2010).

O uso de CAP é feito visando principalmente a remoção de gosto e odor da água de abastecimento, bem como na remoção de baixas concentrações de pesticidas e outros microcontaminantes. A praticidade no uso deste tipo de carvão ativado se dá pela possibilidade de aplicação em certas épocas do ano (geralmente quando há floração de algas no reservatório de água bruta), bem como poder ser

adicionado em pontos distintos ao longo das etapas que constituem o tratamento de água (CRITTENDEN, 2012).

O CAG é usado principalmente na remoção de contaminantes-traço e de carbono orgânico dissolvido em pequenas concentrações. Nesse tipo de carvão ativado pode haver atividade microbiana com o crescimento do biofilme na superfície do carvão, caso se tenham condições adequadas. Nas ETAs, o CAG pode ser utilizado como meio filtrante ou como adsorvente após o decantador ou o filtro de areia (CRITTENDEN, 2012).

O Quadro 3.2 mostra as principais vantagens e desvantagens do uso de CAG e CAP, segundo Lima (2014).

Quadro 3.2 - Vantagens e desvantagens do uso dos tipos de carvão.

	CAG	CAP
Vantagens	Regeneração; Recomendável na presença contínua de microcontaminantes.	Menor custo inicial comparado ao CAG; Possibilidade de alteração na dosagem e emprego sazonal
Desvantagens	Maior custo comparado ao CAP.	Dificuldade de regeneração; Eventual dificuldade na disposição de lodo; Eventuais sobredosagens quando aplicado na captação ou na unidade de mistura rápida Eventual redução do tempo de vida dos filtros de areia, quando aplicado antes dessa etapa

Fonte: Adaptado de Lima (2014).

A adsorção em carvão ativado granular tem sido utilizado para a remoção de contaminantes emergentes da água (NOWOTNY *et al.*, 2007; REUNGOAT *et al.*, 2011; SNYDER *et al.*, 2007; WESTERHOFF *et al.*, 2005). O uso dessa técnica está relacionado com a relativa facilidade de operação e manutenção, conferindo ao CAG um custo moderado para a remoção de poluentes (JOSS, SIEGRIST e TERNES, 2008).

Lewoyehu (2021) comparou os custos, formação de subprodutos e ação desinfetante relacionados ao tratamento da água por carvão ativado com outras técnicas de tratamento avançado. A comparação dos custos está apresentada no Quadro 3.3.

Quadro 3.3 - Comparação da performance da adsorção por carvão ativado com outras técnicas avançadas de tratamento de água

Técnica de tratamento	Custo/demanda energética	Formação de subproduto	Desinfeta
Adsorção pro carvão ativado	Moderado	Não	Não
Ozonização	Baixo para moderado	Sim	Sim
Oxidação por ClO_2	Baixo para moderado	Sim	Sim
Nanofiltração/ Osmose reversa	Alto	Não	Não
Adsorção por zeólita	Incerto	Não	Não

Fonte: Adaptado de Lewoyehu, 2021.

O CAG tem sido utilizado como uma unidade de tratamento avançado tanto para os sistemas de abastecimento de água quanto para os sistemas de tratamento de esgoto. Em ETEs, o CAG é utilizado como tratamento terciário e tem demonstrado uma boa eficiência na remoção de perturbadores endócrinos, fármacos e produtos de cuidado pessoal (GROVER *et al.*, 2011).

A aplicação do carvão ativado como adsorvente é favorecida por sua ampla área superficial por unidade de massa, permitindo acumular grandes quantidades de adsorvato em pequenas quantidades de adsorvente. Além disto, apresenta forte afinidade por uma ampla gama de moléculas hidrofóbicas (por exemplo, solventes, pesticidas, substâncias húmicas, toxinas e compostos odoríferos gerados por algas). Também, exibe relativa inércia em relação às interações com a água e a maioria dos solutos hidrofílicos (BENJAMIN & LAWLER, 2013).

3.1.2. Isotermas de adsorção

Isotermas de adsorção são a representação matemática da relação entre a quantidade de adsorvato extraído pelo adsorvente e a quantidade de adsorvato remanescente na fase líquida quando a solução se encontra em equilíbrio dinâmico a uma determinada temperatura. Nos sistemas de adsorção da fase líquida para a fase sólida, as isotermas são importantes devido aos seguintes aspectos (PICCIN *et al*, 2017):

a) É possível calcular a capacidade máxima de adsorção de um determinado adsorvente em diferentes condições experimentais;

b) É possível obter informações sobre os pontos de vista energéticos, estéricos e de afinidade;

c) Fornecer informações sobre o mecanismo de interação que ocorre entre adsorvato e adsorvente, possível através do formato da curva;

d) Permitir a modelagem da taxa de adsorção, assumindo-se um equilíbrio local a fim de resolver as equações diferenciais parciais. Esse equilíbrio local é matematicamente descrito pelas isotermas de adsorção;

e) É possível determinar parâmetros termodinâmicos, como a energia livre de Gibbs (ΔG^0), a variação de entalpia (ΔH^0) e a variação da entropia (ΔS^0), importantes para identificar a espontaneidade e a natureza do processo adsortivo.

Ruthven (1984) dividiu o formato das isotermas por adsorção física em 5 classes, conforme ilustrado na Figura 3.2. O Tipo I geralmente ocorre com adsorventes cujo tamanho do poro não é muito maior do que o diâmetro molecular do adsorvato. Esse formato é característico pois há a indicação de que há um limite de saturação, resultado do preenchimento total dos microporos. Ocasionalmente, se os efeitos da atração intramolecular forem grandes no sistema, a isoterma Tipo V é observada.

Figura 3.2 - Classificação Brunauer das isotermas.

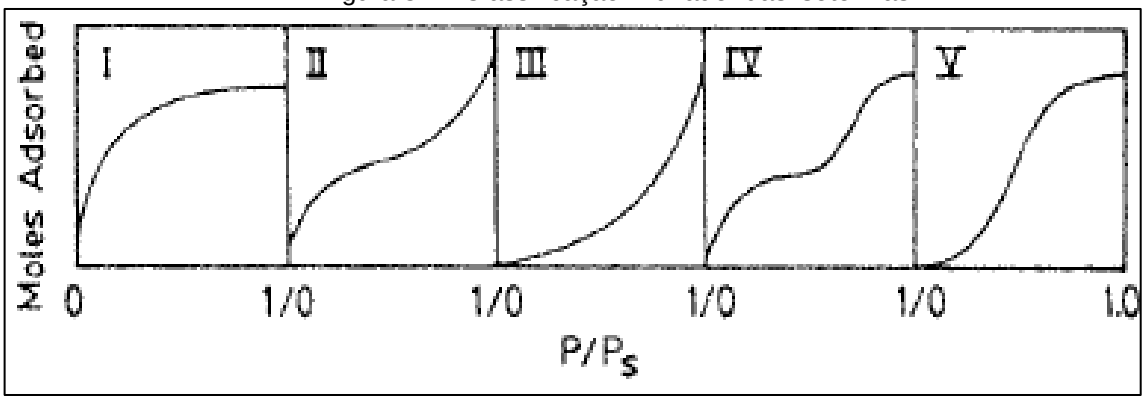

Fonte: Ruthven (1984)

Uma isoterma Tipo IV sugere a formação de duas camadas superficiais na superfície plana ou na parede de um poro muito maior que o diâmetro molecular do adsorvato. Isotermas Tipo II e III são geralmente observadas em adsorventes onde há uma grande variedade de tamanho de poros. Neste caso, há uma progressão contínua com o aumento da carga da monocamada para a adsorção multicamada e depois para a condensação capilar. O aumento da capacidade de adsorção em altas pressões é devido à condensação capilar ocorrendo em poros de diâmetro crescente à medida que a pressão aumenta (RUTHVEN, 1984).

A seguir são apresentados os modelos de isotermas explorados na presente pesquisa: Langmuir, Freundlich, Sips, Liu e Redlich-Peterson.

a) Modelo de Langmuir

O modelo de Langmuir foi inicialmente idealizado para representar a quimiossorção em um conjunto de sítios de adsorção distintos (RUTHVEN, 1984). O modelo é fundamentado nos seguintes princípios, segundo Piccin *et al* (2017), Atkins e De Paula (2006) e Dehghani, Karri e Lima (2021):

- A adsorção não pode ocorrer além da cobertura de monocamada;
- Não há interações entre os compostos na solução;
- Os compostos são adsorvidos em um número fixo de locais ativos;
- Cada sítio pode conter apenas uma molécula de adsorvato;
- O adsorvente atinge um máximo de saturação dos sítios ativados;
- Todos os sítios do carvão ativado são energicamente equivalentes e a superfície é uniforme;
- A capacidade de uma molécula de adsorver em um determinado sítio é independente da vizinhança.

O modelo de isoterma de Langmuir estabelece que há uma máxima capacidade adsortiva do carvão, ocorrendo sua saturação em uma monocamada. Uma das formas de expressão da isoterma de Langmuir é descrita na Equação 1.

$$q_e = q_{máx.} \frac{b \,.\, C_e}{1 + b \,.\, C_e} \qquad (1)$$

Em que: q_e - Concentração de equilíbrio do adsorvato no carvão ativado (Massa de adsorvato /Massa de adsorvente); $q_{máx}$ - (Massa de adsorvato/Massa de adsorvente) C_e – Concentração de equilíbrio do adsorvato na solução (Massa do contaminante/Volume do líquido); q_{max} - concentração máxima de contaminante no carvão ativado (Massa de adsorvato/Massa de adsorvente), e; b = constante de adsorção de Langmuir do contaminante (Volume/Massa).

b) Modelo de Freundlich

A Isoterma de Freundlich foi a primeira descrição conhecida de adsorção reversível, e esse modelo não se restringe à formação de monocamada (FREUNDLICH, 1906 apud HARO, 2017). Segundo Freundlich (1906) apud Piccin *et*

al (2017), esse tipo de isoterma pressupõe que a adsorção ocorra de forma heterogênea na superfície. O modelo é fundamentado nos seguintes princípios (DEHGHANI, KARRI e LIMA, 2021).

- Não há saturação do adsorvente, o que significa que a capacidade de sorção dele aumenta exponencialmente à medida que a concentração do adsorvato aumenta;
- O modelo de Freundlich assume multicamadas de adsorvato cobrindo o adsorvente;
- Existe a possibilidade de formar uma segunda camada antes que a primeira seja concluída;
- Por se tratar de adsorção multicamadas, ocorre a interação dos adsorvatos;
- A energia de cada sítio ativo não é homogênea.

No trabalho realizado por Maataqui *et al.* (2017), a isoterma de Freundlich foi a que melhor se ajustou à adsorção de Carbendazim em argilas *homoionic-montmorillonite*, sendo melhor representado pelo modelo não-linear do que o linear. Além disso, há vários estudos na literatura que mostram o melhor ajuste da isoterma de Freundlich na adsorção do CBZ em CAG (JIN *et al*., 2013; LI *et al*., 2011; PASZKO, 2006; RIZZI *et al*., 2020; WANG *et al*., 2020).

A Isoterma de Freundlich é representada pela Equação 2.

$$q_e = k_f . C_e^{1/n} \quad (2)$$

Em que: q_e - Concentração de equilíbrio do contaminante no carvão ativado (Massa de adsorvato/ Massa de adsorvente); C_e – Concentração de equilíbrio do contaminante na solução (Massa do contaminante/Volume); k_f – constante de equilíbrio de Freundlich [(Massa do adsorvato/Massa adsorvente).(Volume/Massa do adsorvato)$^{1/n}$]. Segundo Anfar *et al*. (2020), o expoente 1/n indica se o processo de adsorção é favorável (0,1 < 1/n < 1) ou desfavorável (1/n > 1). Valores mais próximos de 1 significam as condições mais favoráveis de adsorção.

c) Modelo de Sips

O modelo de Sips combina as expressões de Langmuir e Freundlich, sendo elaborado para modelar os sistemas de adsorção heterogêneos, contornando a

limitação da crescente concentração de adsorvato associada ao modelo de Freundlich. Em baixas concentrações de adsorvato, a equação se reduz à isoterma e Freundlich, enquanto, em altas concentrações, o modelo se assemelha à isoterma de Langmuir devido à previsão de uma capacidade de adsorção em monocamada (HARO, 2017; FOO & HAMEED, 2010). O método de Sips possui as seguintes características (DEHGHANI, KARRI e LIMA, 2021).

- A saturação do adsorvente é prevista (q_{max});
- Podem ocorrer multicamadas do adsorvato sobre o adsorvente;
- É possível iniciar a segunda camada sem a necessidade de a primeira camada ser concluída;
- Os sítios de ativação podem ter energias diferentes;
- Podem ocorrer interações entre os adsorvatos em solução.

O modelo de Sips é expresso na Equação 3.

$$q_e = \frac{q_{max}.K_s.C_e^{1/ns}}{1 + K_s.C_e^{1/ns}} \quad (3)$$

Em que: $0 < \frac{1}{n_s} \leq 1$; q_e - Concentração de equilíbrio do contaminante no carvão ativado (Massa adsorvato/Massa de adsorvente); q_{max} - concentração máxima de contaminante no carvão ativado (Massa adsorvato/Massa adsorvente); K_s – Constante de equilíbrio de Sips (Volume/Massa)$^{1/ns}$; C_e – Concentração de equilíbrio do adsorvato na solução (Massa/Volume); e n_s – expoente de Sips, adimensional.

Em baixas concentrações de adsorvato (1>> $K_s.C_e^{1/ns}$), o modelo assume a forma da isoterma de Freundlich (Equação 4). Para ns = 1, o modelo assume o formato da isoterma de Langmuir (Equação 5).

$$q_e = q_{máx}.k_s.C_e^{1/ns} \quad (4)$$

$$q_e = \frac{q_{max}.k_s.C_e}{1 + k_s.C_e} \quad (5)$$

d) Modelo de Liu

O modelo de Liu é um modelo empírico que também associa as isotermas de Langmuir e Freundlich. Possui mesmas características do modelo de Sips com a exceção de que o expoente da isoterma de Liu deve apresentar valores positivos ($n_L > 0$) (DEHGHANI, KARRI e LIMA, 2021). A Equação 6 apresenta o modelo de Liu

$$q_e = \frac{q_{max}.\left(k_g.C_e\right)^{n_L}}{1 + \left(k_g.C_e\right)^{n_L}} \quad (6)$$

Em que: K_g – constante que representa a afinidade entre adsorvente-adsorvato (Volume/Massa) e n_L é o expoente de Liu, adimensional.

e) Modelo de Redlich-Peterson

O modelo de Redlich-Peterson é empírico e é representado pela Equação 7.

$$q_e = \frac{k_{RP}.C_e}{1+ a_{RP}.C_e^{ß}} \text{ sendo } 0 < ß \leq 1 \quad (7)$$

Em que: a_{RP} - a constante de equilíbrio de Redlich-Peterson (Volume/Massa)^{ß}; k_{RP} - a constante que contém a máxima capacidade de sorção e descreve a afinidade adsorvente-adsorvato (Volume/Massa); ß – expoente da isoterma de Redlich-Peterson, adimensional. Quando ß=1, o modelo assume a forma da isoterma de Langmuir (Equação 8), enquanto para baixas concentrações de adsorvato, o modelo assume o formato linear (Equação 9).

$$q_e = \frac{q_{max}.a_{RP}.C_e}{1+a_{RP}.C_e} \quad (8)$$

$$q_e = k_{RP}.C_e \quad (9)$$

Em que: $k_{RP} = q_{max}.a_{RP}$

f) Determinação da isoterma de adsorção por regressão não-linear

A determinação dos parâmetros das isotermas podem ser obtidos através de métodos de regressão não-linear. Da mesma forma, permite a obtenção dos

parâmetros do método termodinâmico de Van't Hoff (ELOUAHLI *et al.*, 2018; LIMA, GOMES, TRAN, 2020; MAATAOUI *et al.*, 2017; PRETE, DE OLIVEIRA, TARLEY, 2017; WEFER-ROEHL *et al.*, 2001; ZANELLA *et al.*, 2016). De forma geral, alguns trabalhos afirmam que os resultados obtidos pelo método não-linear apresentam resultados mais robustos e com menor erro que os estimados com método linear (OSMARI *et al.*, 2013). Para a aplicação desse método de regressão podem ser utilizadas ferramentas computacionais como o *Solver* do *Microsoft Office Excel* (SUMMERS, KNAPPE and SNOEYINK, 2011).

3.1.3. Termodinâmica de adsorção

Através das variáveis obtidas pelas isotermas, é possível se conhecer os parâmetros termodinâmicos da adsorção de um composto. O método de Van't Hoff é uma metodologia pela qual se pode estimar as variações de entalpia (ΔH, kJ/mol), entropia (ΔS, J/mol.K) e energia Livre de Gibbs (ΔG, kJ/mol) (HARO *et al.*, 2021; MANSOURIIEH, SOHRABI, KHOSRAVI, 2016; PRETE, DE OLIVEIRA, TARLEY, 2017; SELIN & EMIK, 2018). Os valores de ΔH e ΔS são calculados através da Equação 10.

$$\ln K_e = \frac{\Delta S}{R} - \frac{\Delta H}{RT} \quad (10)$$

Em que: K_e é a constante de equilíbrio (adimensional), R é a constante universal dos gases ideais (8,314 J/mol.K) e T é a temperatura (K).

A constante de equilíbrio de adsorção pode ser expressa pela relação entre a concentração de equilíbrio do contaminante no carvão ativado pela concentração de equilíbrio do contaminante na solução (Equação 11). Já os valores de ΔH e ΔS são obtidos a partir da inclinação da reta do gráfico de Van't Hoff (Equação 10).

$$K_e = \frac{q_e}{C_e} \quad (11)$$

A variação da energia livre (ΔG) é calculada pela Equação 12.

$$\Delta G = -RTlnK_e \quad (12)$$

Parâmetros termodinâmicos como o ΔH informam dados importantes quanto ao processo de adsorção. A Figura 3.3 mostra os valores de ΔH característicos para os processos de fisiossorção e quimiossorção.

Figura 3.3 - Tipos de adsorção e as variações de entalpia em cada processo.

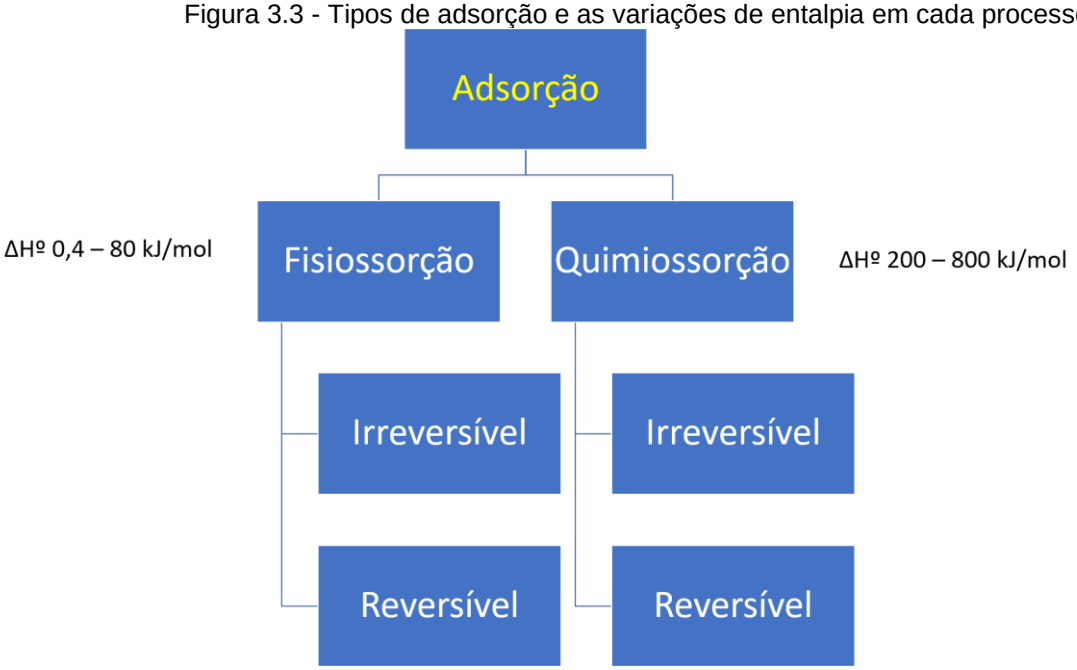

Fonte: Adaptado de Dehghani, Karri e Lima, 2021.

3.1.4. Cinética de adsorção

O estudo da cinética é importante pois permite identificar o tempo de contato necessário para atingir o equilíbrio de adsorção entre adsorvente e adsorvato, representando a velocidade do processo (HARO, 2017), além da avaliação da eficiência da adsorção (ZANELLA *et al.*, 2016). Os principais modelos que descrevem a cinética de adsorção são os modelos de pseudo-primeira ordem e pseudo-segunda ordem (HO & MCKAY, 1998), além do modelo de difusão intrapartícula. Vários trabalhos tem abordado o estudo da cinética de adsorção de contaminantes emergentes (HARO *et al.*, 2021; MANSOURIIEH, SOHRABI, KHOSRAVI, 2016; ÖZCAN & ÖZCAN, 2004; PRETE, DE OLIVEIRA, TARLEY, 2017; ABDELHAMEED *et al.*, 2018; ZANELLA *et al.*, 2016).

3.1.4.1. Modelo de pseudo-primeira ordem

Esse modelo, desenvolvido por Lagergren (1898), foi a primeira equação de taxa estabelecida para um sistema de adsorção sólido/líquido. Nele, assume-se que

a velocidade de remoção do adsorvato é diretamente proporcional à diferença entre a quantidade adsorvida e o número de sítios ativos do adsorvente (HARO, 2017).

O modelo de pseudo-primeira ordem descreve de forma satisfatória processos de adsorção em que a etapa determinante do processo precede a difusão superficial (HARO, 2017). Este método avalia se a cinética de adsorção é majoritariamente controlada por difusão externa e independe da concentração do adsorvato (DA SILVA *et al.*, 2018). A Equação 13 representa o modelo de primeira-ordem.

$$q_t = q_e(1 - e^{-k_1 t}) \quad (13)$$

Em que: q_t – Quantidade de adsorvato removida por unidade do adsorvente no tempo t, em Massa de adsorvato/Massa de adsorvente; q_e – Quantidade de adsorvato adsorvida por unidade do adsorvente no equilíbrio (Massa do adsorvato/Massa do adsorvente); k_1 – constante da taxa de pseudo-primeira ordem (Massa/Massa.Tempo) ; t – tempo de contato.

3.1.4.2. Modelo de pseudo-segunda ordem

Esse método, proposto por Ho & Mckay (1998), também descreve o processo de adsorção de sólido/líquido. Nele é possível prever o processo de adsorção ao longo do tempo, o ajuste satisfatório da remoção do adsorvente no adsorvato e a predominância da natureza química do processo (HARO, 2017). A taxa de adsorção no modelo de pseudo-segunda ordem é dependente da quantidade da espécie química adsorvida na superfície do adsorvente e a quantidade adsorvida no estado de equilíbrio (DA SILVA *et al.*, 2018). A Equação 14 mostra o modelo de pseudo-segunda ordem (HO, 2006):

$$q_t = \frac{q_e^2 k_2 t}{1 + q_e k_2 t} \quad (14)$$

Em que: k_2 – constante da taxa de pseudo-segunda ordem (Massa/Massa. Tempo).

3.1.4.3. Modelo de difusão intrapartícula

Em alguns processos de adsorção, a etapa que controla o processo é a difusão no interior dos poros (HARO, 2017). Dessa forma, Weber e Morris (1963) propuseram um método em que a transferência de massa intrapartícula é o processo limitante da difusão. A Equação 15 mostra o modelo de difusão intrapartícula.

$$q_t = k_{di} . t^{0,5} + C \quad (15)$$

Em que: k_{di} – Constante de difusão intrapartícula (Massa/Massa.Tempo^{0,5}); C – Constante relacionada com a resistência à difusão (Massa/Massa).

Segundo Haro (2017) e Allen, Mckay e Khader (1989), o gráfico obtido através do modelo Weber-Morris pode apresentar uma multilinearidade que caracteriza os diferentes estágios na adsorção: transferência de massa externa seguida por difusão intrapartícula no macro, meso e microporo. O modelo diz que se nos estágios iniciais de adsorção o coeficiente linear for igual a zero, então a difusão dentro do poro controla o processo de adsorção. Entretanto, se o coeficiente linear for diferente de zero, o processo que controla a adsorção pode ser uma difusão intrafilme cuja espessura é atribuída ao coeficiente linear.

3.1.5. Ensaios em colunas de leito fixo

Algumas variáveis, como tempos de ruptura e de saturação, são importantes para se analisar a eficiência de adsorção de um poluente em uma coluna de leito fixo com carvão ativado. Tipicamente, o ponto de ruptura é atingido quando o efluente apresenta 5% da concentração inicial (C_0) do poluente ou quando é atingido um Valor Máximo Permitido (VMP) proposto por uma legislação específica. A Equação 16 mostra a descrição matemática da curva de ruptura, que depende do tempo de ruptura (t) ao longo da coluna de carvão, no ponto em que há a saturação do leito ($Z_{máx}$) (HENDRICS, 2011).

$$C(t)_Z = Z_{máx} \quad (16)$$

Em que: $C(t)_Z$ – curva de ruptura e $Z_{máx}$ é o comprimento da coluna saturada (geralmente em cm).

O ponto de saturação geralmente é atingido quando o efluente (C) apresenta 90% ou 95% da concentração inicial do poluente. Na exaustão completa da coluna, a concentração do contaminante no afluente e no efluente é a mesma ($C = C_0$) (METCALF & EDDY, 2014).

Outro conceito importante do processo de adsorção é a Região de Transferência de Massa Ativa (RTMA), também chamada de Zona de Transferência de Massa (ZTM), que é a região em que está ocorrendo a adsorção na coluna com

carvão ativado. Quando a água com o contaminante atravessa a região do leito cuja extensão é igual à ZTM, a concentração do contaminante é reduzida ao valor mínimo devido à adsorção deste pelo carvão. Considerando um fluxo descendente de adsorção em uma coluna de CAG, inicialmente não ocorre adsorção na camada da coluna inferior à ZTM. À medida que as camadas superiores forem saturando, a ZTM também vai descendo ao longo do leito até alcançar a saída da coluna, quando ocorre a ruptura da concentração do contaminante. Desta forma pode-se calcular o valor do tempo de ruptura. Prosseguindo-se com a operação da coluna, pode-se chegar a sua saturação, com seu correspondente tempo (METCALF & EDDY, 2014).

A Figura 3.4 ilustra esse processo de adsorção em uma coluna de CAG, mostrando também o deslocamento da ZTM até que a coluna como um todo esteja saturada.

Figura 3.4 - Curva de ruptura típica de uma coluna com CAG, mostrando o deslocamento da RTMA.

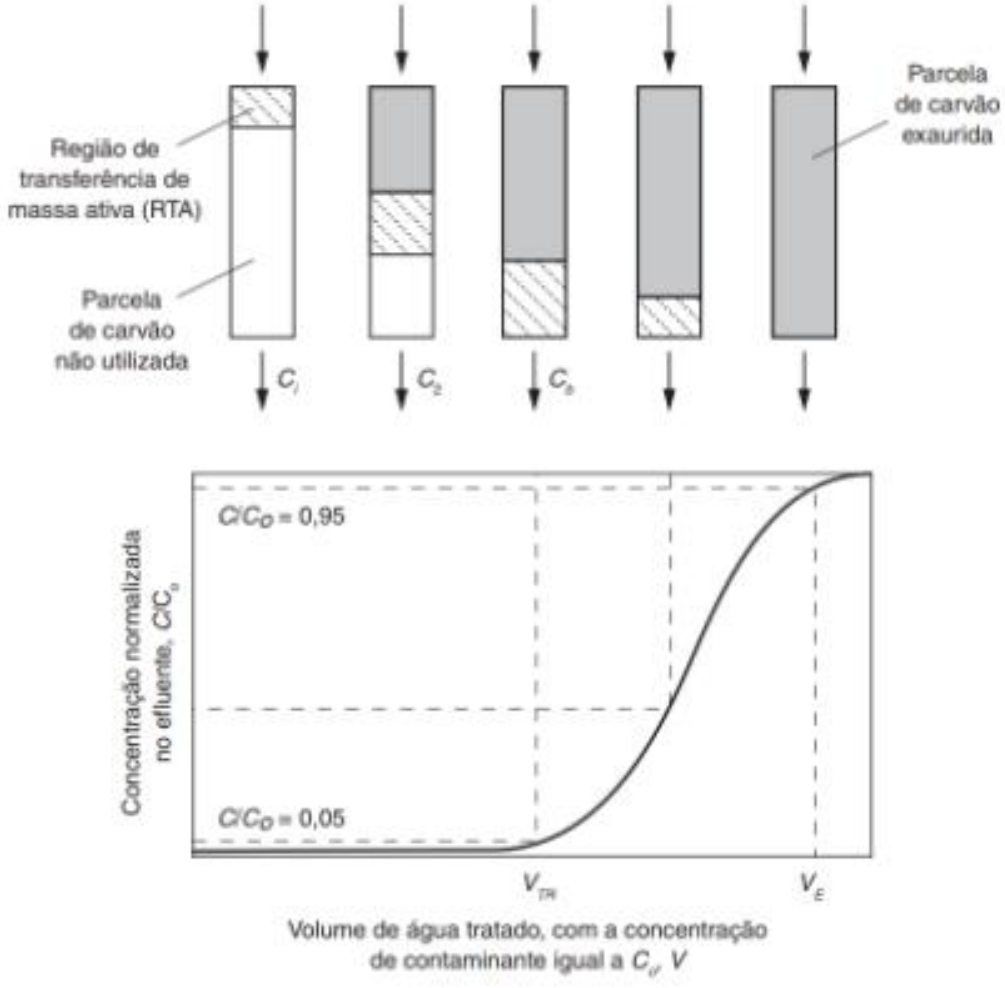

Fonte: Metcalf & Eddy (2014).

A Figura 3.4 mostra os conceitos de Volume do Tempo de Ruptura (V_{TR}) e Volume de Exaustão (V_E), que correspondem aos volumes de água tratada antes de obtidos os pontos de ruptura e de exaustão da coluna com carvão ativado. Em geral, o tamanho da ZTM é dado em função das características do carvão ativado, da taxa de aplicação hidráulica e da cinética de adsorção do contaminante. Se a taxa de aplicação hidráulica for muito alta, a ZTM será maior do que o comprimento da coluna de carvão e o contaminante não será removido apropriadamente (METCALF & EDDY, 2014).

A presença de substâncias não adsorvíveis e biodegradáveis na água de alimentação da coluna impactam na curva de ruptura de adsorção do contaminante de interesse na coluna com carvão ativado. Os compostos não adsorvíveis aparecerão no efluente da coluna desde o início da sua operação. Também, a presença de compostos biodegradáveis possibilita o crescimento de atividade biológica na superfície do carvão, impactando na relação C/C_0, que não atinge a unidade (METCALF & EDDY, 2014).

Desta forma, a presença de compostos não adsorvíveis e biodegradáveis faz com que a curva de ruptura não se inicie no 0 (início da operação da coluna) e não termine em 1 ($C = C_0$) (SUMMERS, KNAPPE E SNOEYINK, 2011). Esse efeito é comum em colunas com carvão ativado utilizados em estações de tratamento de água e esgotos devido principalmente à presença de Carbono Orgânico Dissolvido Biodegradável (COD_b). A Figura 3.5 mostra o impacto dessas substâncias na curva de ruptura.

Figura 3.5 - Impacto da presença de substâncias adsorvíveis, não adsorvíveis e biodegradáveis na curva de ruptura.

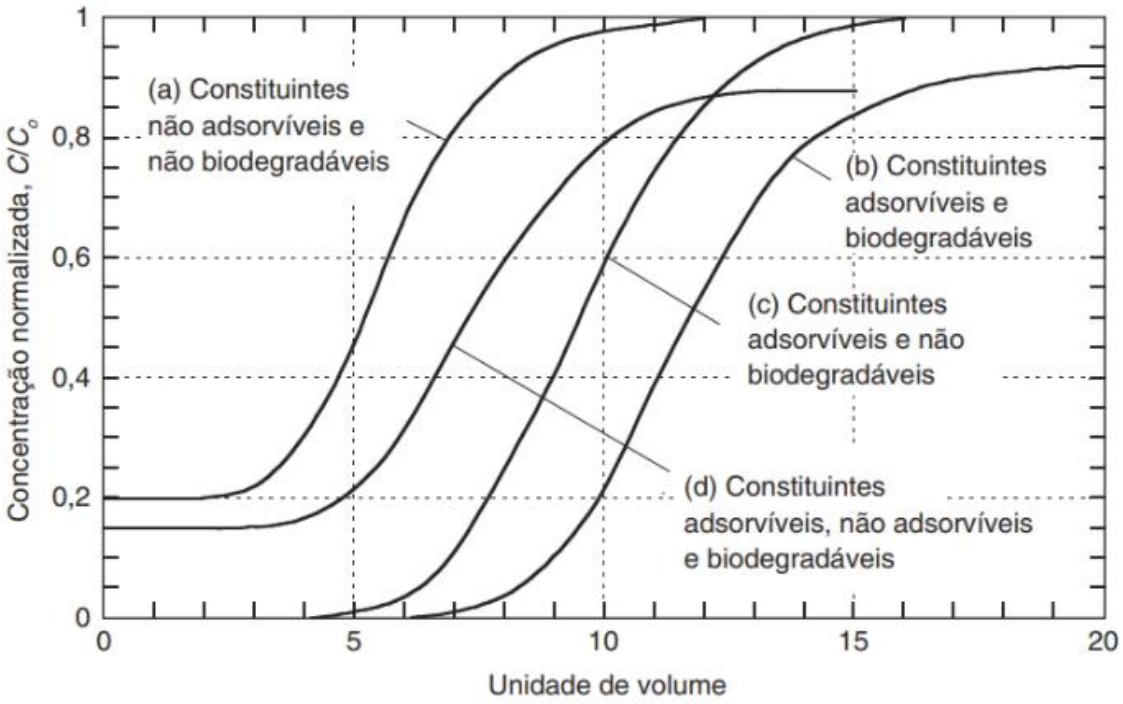

Fonte: Adaptado de Metcalf & Eddy (2014); Summers, Knappe e Snoeyink (2011).

Um dos métodos para se estimar o funcionamento de uma coluna de leito fixo de carvão ativado em escala real são os Ensaios Rápidos em Colunas de Escala Reduzida (ERCER), conhecidos como *Rapid Small-Scale Column Tests* (RSSCT), em inglês. Esse método consiste na determinação de curvas de ruptura e outros parâmetros operacionais do uso de uma coluna com CAG em escala real a partir de ensaios em escala reduzida sem o uso de métodos matemáticos complexos, através de modelos de transferência de massa baseados em leitos fixos (CRITTENDEN *et al.*, 1991).

O método foi proposto inicialmente por Crittenden *et al* (1987; 1986) para determinar de forma prática, simplificada e consistente, os parâmetros operacionais de uma coluna de CAG, assim como a sua eficiência em escala reduzida de bancada. O ERCER oferece dados operacionais tão relevantes quando os testes de isotermas. Pelo fato de serem realizados em pequena escala de laboratório, é econômico, prático e não necessita de um grande tempo de operação (CRITTENDEN *et al* 1987; 1986).

Plattner *et al.* (2018) utilizaram ERCER para a predição de um sistema de pós-tratamento a partir da aplicação de outras técnicas de remoção de pesticidas remanescentes, como a aplicação de membranas. Coelho e Rozário (2019) aplicaram essa técnica para a remoção de 2,4-Diclorofenoxiacético (2,4-D) em amostras de

águas ultrapura e de água filtrada proveniente de ETA. Em outro estudo, Voltan *et al*. (2016) avaliaram a remoção dos herbicidas Diuron e Hexazinona em CAG utilizando este método.

O ERCER utiliza o Tempo de Contato de Leito Vazio (TCLV), também chamado de *Empty Bed Contact Time* (EBCT), a taxa de aplicação hidráulica e a granulometria do CAG para representar o processo de adsorção. Algumas correlações também são realizadas, como a razão entre os diâmetros médios das partículas de carvão, com o intuito de se prever o desempenho de uma coluna de CAG em escala real (EPA, 1996; CRITTENDEN *et al.*, 1991).

O método de ERCER apresenta duas formas de aplicação, que dependem do modelo de difusidade intrapartícula do CAG. O primeiro é o modelo de difusividade constante, que pressupõe que a difusidade intrapartícula não depende da variação da partícula de CAG. O segundo é o modelo de difusividade proporcional ou não constante, que considera a existência de uma proporcionalidade linear entre a difusividade intrapartícula e o tamanho de partícula de CAG (CRITTENDEN *et al.*, 1991). No modelo constante, é assumido que a dispersão é negligenciável pois a taxa de aplicação hidráulica é alta no ERCER e a transferência de massa ocorre como resultado da difusão do filme. No modelo proporcional é assumido que a dispersão é negligenciável também devido à alta taxa de aplicação hidráulica, contudo a transferência de massa ocorre como resultado da difusão intrapartícula (METCALF & EDDY, 2014).

O TCLV do ERCER é determinado a partir de resistências de transferência de massa intrapartícula. Conhecendo-se a dependência do coeficiente de difusão entre poros e superfícies sobre o tamanho de partícula, a relação entre as modelagens matemáticas pode ser alcançada ao equiparar os grupos adimensionais que consideram a resistência à difusão intrapartícula em colunas de pequena e grande escala. Se as frações de vazios, densidades e capacidades aparentes são idênticas para os carvões utilizados no ERCER e em escala piloto ou real, a razão entre os TCLVs das colunas de pequena e grande escala podem ser determinados a partir da Equação 17 (CRITTENDEN *et al.*, 1991; CRITTENDEN, BERRIGAN e HAND, 1986).

$$\mathrm{TCLV_{red}} = \mathrm{TCLV_{real}} \cdot \left(\frac{\mathrm{d_{p.red}}}{\mathrm{d_{p.real}}}\right)^{2-X} = \frac{\mathrm{t_{red}}}{\mathrm{t_{real}}} \qquad (17)$$

Em que: $\mathrm{TCLV_{red}}$- TCLV na coluna de escala reduzida (min); $\mathrm{TCLV_{real}}$ – TCLV na coluna de escala real (min); $\mathrm{d_{p.red}}$ – diâmetro médio das partículas da coluna em escala reduzida (mm); $\mathrm{d_{p.real}}$ – diâmetro médio das partículas da coluna em escala real (mm); X - coeficiente de dependência do tamanho da partícula na difusividade intrapartícula, sendo 0 quando a difusividade é constante e 1 quando ela é proporcional ao tamanho da partícula; $\mathrm{t_{red}}$ – Tempo de operação da coluna em escala reduzida (min); $\mathrm{t_{real}}$ – Tempo de operação da coluna em escala real (min).

Quando as condições de difusidade intrapartícula são consideradas constantes (X = 0) e independentes do diâmetro das partículas, a expressão que relaciona a relação entre o TCLV da coluna em escala reduzida e em escala real é dada pela Equação 18:

$$\mathrm{TCLV_{red}} = \mathrm{TCLV_{real}} \cdot \left(\frac{\mathrm{d_{p.red}}}{\mathrm{d_{p.real}}}\right)^2 = \frac{\mathrm{t_{red}}}{\mathrm{t_{real}}} \qquad (18)$$

Para esse caso de difusidade intrapartícula constante, a condição de difusidade requer também que os números de Reynolds para as colunas piloto e real sejam iguais. Dessa forma, tem-se a Equação 19:

$$\frac{\mathrm{TAS_{red}}}{\mathrm{TAS_{real}}} = \frac{\mathrm{d_{p.real}}}{\mathrm{d_{p.red}}} \qquad (19)$$

Em que: $\mathrm{TAS_{red}}$ – Taxa de aplicação superficial em escala reduzida (m/h); $\mathrm{TAS_{real}}$ – Taxa de aplicação superficial em escala real (m/h).

No caso em que a difusidade intrapartícula é considerada proporcional (X=1), a relação entre os TCLVs das colunas em escala reduzida e real é dada pela Equação 20.

$$\mathrm{TCLV_{red}} = \mathrm{TCLV_{real}} \cdot \left(\frac{\mathrm{d_{p.red}}}{\mathrm{d_{p.real}}}\right) = \frac{\mathrm{t_{red}}}{\mathrm{t_{real}}} \qquad (20)$$

Além das equações apresentadas, é utilizado o domínio da transferência de massa interna sobre a transferência de massa externa, com o intuito de se reduzir o tamanho da coluna operacionalizada. Para isso, considera-se que a $\mathrm{TAS_{red}}$ pode ser reduzida a um valor abaixo da $\mathrm{TAS_{real}}$ desde que este esteja acima da TAS mínima

na qual a coluna ERCER pode operar. Deste modo, a transferência de massa interna continua dominando. Para isso, é utilizada a Equação 21 (CRITTENDEN *et al.*, 1991):

$$TAS_{red} = \frac{R_{red.min} \cdot \varepsilon \cdot \upsilon}{d_{p.red}} \quad (21)$$

Em que: $R_{red.min}$ – Número de Reynolds mínimo (0,5); ε – Porosidade; υ – viscosidade cinemática (10^{-6} m²/s a 20º C).

A Equação 22 é utilizada para calcular a massa de CAG na coluna ERCER, minimizando o impacto da densidade aparente e das diferenças de porosidade entre as colunas piloto e ERCER.

$$M_{red} = H_{red} \cdot \rho_{F.red} \cdot A \quad (22)$$

Em que: M_{red} – massa de CAG em coluna em escala reduzida (g); H_{red} - altura do leito de CAG na coluna ERCER (cm); $\rho_{F.red}$ – densidade aparente da coluna de pequena escala (g/cm³); A – área da coluna de pequena escala (cm²).

Quanto ao diâmetro de CAG utilizado em testes com coluna ERCER, identificou-se que diâmetros de grãos inferiores a 60 x 80 mesh conferem uma maior perda de carga ao meio, além de reduzir o tempo de ruptura e influenciar no coeficiente de difusão intrapartícula que decresce consideravelmente com menores diâmetros de carvão. Desse modo, não é recomendado o uso de CAG com diâmetro inferior a 60 X 80 mesh em colunas ERCER a não ser que haja mudanças da estrutura da coluna capazes de solucionar essas limitações (CRITTENDEN *et al.*, 1991).

3.1.6. Impactos da matéria orgânica na adsorção

Em condições naturais e em estações de tratamento, a Matéria Orgânica Natural (MON) pode estar presente em diferentes concentrações. MON é uma mistura complexa de compostos orgânicos tais como ácidos fúlvico e húmico, ácidos hidrofílicos, e compostos específicos tais como hidratos de carbono e proteínas, todos de origem natural (SUMMERS, KNAPPE e SNOEYINK, 2011).

O estudo do impacto da matéria orgânica natural na adsorção é de fundamental importância, visto que na maioria dos casos ela reduz a capacidade de adsorção do carvão ativado e o seu desempenho na remoção de CPE (DOMERGUE *et al*., 2022). Essa redução é devida a capacidade da MON em competir pelos sítios adsortivos ou

bloqueio dos poros do CAG (ERSAN *et al*., 2016). Portanto, o desempenho do CAG na remoção de um adsorvato de interesse pode ser afetado pela presença de MON na solução.

Estudos mostram que o peso molecular da matéria orgânica é muito maior do que as das outras substâncias envolvidas em um processo adsortivo. Por isso, a MON pode obstruir a passagem dos poros no carvão ativado, dificultando a entrada das moléculas de substâncias como os CPE aos sítios de adsorção (MOUSSAVI, HOSSEINI e ALAHABADI, 2013; DOMERGUE *et al*., 2022). Mesmo as menores frações de MON podem competir com os contaminantes de interesse pelos sítios remanescentes (DOMERGUE *et al*., 2022). Por apresentarem tamanhos moleculares distintos, essa competição pelos sítios é devida principalmente à distribuição dos poros do CAG, uma vez que a matéria orgânica pode ocupar os macros e mesoporos, impedindo o acesso do CBZ aos microporos do adsorvente. Dessa forma, o mecanismo de competição é controlado pela distribuição dos poros do CAG (PELEKANI & SNOEYINK, 1999). Os microcontaminantes em água potável estão usualmente presentes em concentrações que são menores de três a seis ordens de magnitude do que matéria orgânica natural. Baseado somente neste fato, não é surpreendente que possa haver uma redução significativa da capacidade de adsorção do CAG na presença de MON (DOMERGUE *et al*., 2022).

Outro fator de interferência no processo adsortivo são as interações eletrostáticas entre a matéria orgânica e o carvão ativado, que podem favorecer a sua adsorção. A matéria orgânica na forma de ácido húmico é carregada negativamente na faixa de pH neutro, podendo competir com os ânions da solução pelos poros do carvão ativado carregados positivamente (MOUSSAVI *et. al*., 2013). A presença de MON na água interfere ainda na cinética da adsorção, que é influenciada pela interação entre ela com moléculas-traço e a competição pelos sítios adsortivos do CAG. Com isso, a MON afeta a remoção de contaminantes-alvo, reduzindo a eficiência do carvão ativado (DOMERGUE *et al*., 2022).

Ainda que não seja comum, a presença da MON pode influenciar positivamente na remoção de um adsorvente, melhorando a eficiência do CAG. Isso ocorre, pois, a presença de substâncias húmicas pode alterar algumas características de poluentes orgânicos (CARTER & SUFFET, 1982). Guillossou *et al*. (2020) identificaram que um

pré-equilíbrio de 24h entre os micropoluentes orgânicos e a matéria orgânica dissolvida melhorava a sua remoção em CAP. Os resultados mostraram a formação de complexos em solução que aumentaram a remoção dos compostos, especialmente em tempos de contato curtos com o adsorvente. Do mesmo modo, Zhu *et al.* (2023) mostraram que a presença de matéria orgânica dissolvida aumentava a adsorção de metais pesados em CAG a concentrações de 5 mg/L de matéria orgânica. O mesmo já foi detectado, também, em estudos de adsorção de CPE utilizando água de ETA como matriz (COELHO *et al.*, 2020).

3.2. CARBENDAZIM

O Carbendazim teve o seu uso autorizado no Brasil no ano de 1985, por meio de uma publicação da então Secretaria Nacional de Vigilância Sanitária (SNVS) do Ministério da Saúde (MS) (RAMA, 2013). No ano de 2009 o Carbendazim foi o 10º ingrediente ativo de agrotóxico mais comercializado no Brasil e de 2009 a 2012 permaneceu entre os pesticidas mais consumidos do país (BARBOSA, SOLANO e UMBUZEIRO, 2015).

Na última década, o CBZ foi o principal pesticida usado de forma irregular no Brasil, sendo detectado em culturas não autorizadas assim como acima dos níveis máximos permitidos pela legislação brasileira (RAMA *et al.*, 2014). O intenso lançamento de CBZ no meio ambiente, associado também ao seu grande consumo, reflete-se no aparecimento desse produto em insumos presentes na dieta alimentar brasileira. Bastos (2013) identificou a presença do Carbendazim em amostras de leite distribuído a crianças de 4 meses a três anos de idade, frequentadoras de uma instituição pública com fins filantrópicos, em concentrações acima do limite ou no limiar dos valores máximos permitidos pelo CODEX *Alimentarius* (conjunto de padrões alimentares adotado internacionalmente) e pela Comunidade Europeia.

Estudos anteriores detectaram a presença de CBZ em concentrações variadas em ambientes aquáticos, tais como águas superficiais, subterrâneas e até água potável (LI *et al*., 2022). Pereira (2018) aponta que o CBZ foi identificado em mananciais de abastecimento de água de todos os estados das Regiões Sul, Sudeste e Centro-Oeste do país, além dos estados do Tocantins, Paraíba e Sergipe. Em alguns desses estados foram encontradas concentrações acima do limite permitido (120 µg/L) pela Portaria nº 888 de 4 de maio de 2021, do Ministério da Saúde (BRASIL,

2021). Esta portaria estabelece os procedimentos de controle e de vigilância da qualidade da água para consumo humano e seu padrão de potabilidade no Brasil.

O CBZ tem sido identificado em águas superficiais de vários países. De acordo com um levantamento realizado por Merel *et al*. (2018), o CBZ estava presente em corpos hídricos do Brasil, Chile, China, Colômbia, Dinamarca, Alemanha, Grécia, Portugal, Romênia, Sérvia, Espanha e Suíça, com concentrações variando de 10 ng/L a 6,00 mg/L.

Apesar de seu uso intenso em zonas agrícolas, o Carbendazim também é identificado em efluentes domésticos de centros urbanos. A presença desse composto nessas zonas pode se dar pelo seu uso em jardins, parques, ou demais áreas verdes urbanas, em que eventos chuvosos podem lixiviar o agrotóxico. Outra hipótese para o surgimento desse químico em zonas urbanas é o seu uso em domicílios. Ele pode estar em papeis ou produtos têxteis eventualmente impregnados, uma vez que o CBZ pode ser usado como conservante de filme e de fibra (MEREL *et al.*, 2018).

Segundo o levantamento bibliográfico feito por Rama (2013), o CBZ é um composto altamente absorvido, amplamente distribuído aos tecidos e possuindo baixo potencial de bioacumulação. Pode ser biotransformado e é excretado principalmente pela urina. Como a toxicidade aguda do CBZ é relativamente baixa, este não é o principal foco de preocupação toxicológica do composto, além do fato de que, segundo a autora, o conjunto de evidências científicas não possibilita afirmar que o Carbendazim causa mutações gênicas herdáveis.

Ainda segundo Rama (2013), os estudos crônicos e de carcinogenicidade demonstraram que o CBZ apresenta potencial carcinogênico para fígado de camundongos, com dose-dependência. Em ratos, o composto causou aumento do peso do fígado, proliferação nas células parafoliculares da tireoide e atrofia testicular, sendo este mesmo efeito identificado em cães, acompanhado da inibição da espermatogênese.

A avaliação de risco realizada por Rama (2013) alerta que a exposição dietética ao CBZ pela população brasileira apresenta risco inaceitável, assim como a exposição ocupacional considerando a maioria dos cenários de exposição dos trabalhadores no Brasil. As evidências analisadas mostraram que o composto apresenta potencial carcinogênico, tóxico-reprodutivo e alterações hormonais. Outros trabalhos

mostraram que doses na faixa de 300-600 mg/kg de CBZ por dia podem afetar os tecidos do fígado e dos rins dos ratos e provocar alguns efeitos adversos nos parâmetros hematológicos e bioquímicos destes organismos (LI *et al*., 2022).

Segundo Coutinho, Galli e Mazo (2007), a *Pesticide Action Network* (PAN, 2020) e a *International Programme on Chemical Safety* (IPCS, 2020), o Carbendazim é um composto que apresenta potencial carcinogênico, sendo considerado, também, um possível desregulador endócrino. Possui pequeno efeito toxico sobre a comunidade microbiana presente no solo, porém mostrou-se letal para minhocas. É um composto altamente tóxico para a comunidade aquática: anfíbios (efeitos genéticos e mortalidade), plantas aquáticas (reprodução), crustáceos (mortalidade), peixes (bioacumulação e mortalidade), fungos, (desenvolvimento e reprodução), moluscos (intoxicação e mortalidade) e plâncton (intoxicação, crescimento, reprodução e mortalidade). É pouco tóxico para pássaros e atóxico para abelhas.

A estrutura química do CBZ está representada na Figura 3.6. Observa-se a presença do anel benzimidazólico, que aumenta a resistência à quebra da molécula por biodegradação. (POURREZA, RASTEGARZADEH and LARKI, 2015).

Figura 3.6 - Estrutura do Carbendazim.

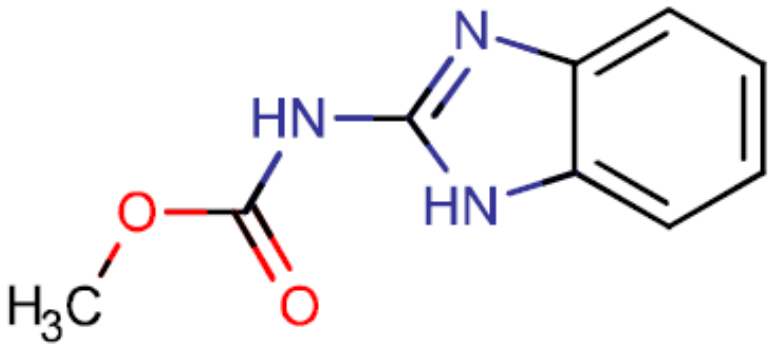

Fonte: Chemicalize (2021).

O Quadro 3.4 apresenta algumas características gerais físico-químicas do CBZ.

Quadro 3.4 - Características gerais do Carbendazim.

Propriedade	**Valor**
Fórmula	$C_9H_9N_3O_2$
Massa Molar	191,19 g/mol
Solubilidade em água (24º C)	29 mg / L a pH 4; 8 mg / L a pH 7; 1,49 mg / L a pH 8
Coeficiente de partição octanol/água	log Kow = 1,52
Constante de dissociação	pKa = 4,29
Meia-vida na água	34 dias
Constante de Henry a 20º C (adimensional)	$8,82 \times 10^{-7}$
Coeficiente de adsorção normalizado em função do conteúdo orgânico - K_{oc} (cm^3/g)	200 cm^3/g
Polaridade	Polar
Classe	Fungicida
Classe toxicológica	Medianamente tóxico
IDA*	0,02 mg/Kg.dia

*Ingestão Diária Aceitável.
Fonte: PubChem (2020) e Pereira (2018).

Através do Quadro 3.4 é possível observar que o CBZ apresenta baixa solubilidade em água (menor do que 50 mg/L) de acordo com a *International Union of Pure Applied Chemistry* (IUPAC). Isso favorece a adesão e persistência desse composto em meio suporte como o solo, por exemplo (SINGH *et al.*, 2016). Analisando exclusivamente essa particularidade, verifica-se que a adsorção do CBZ na superfície do CAG é favorecida.

A meia-vida do CBZ indica que ele é bastante estável no meio aquoso (IUPAC, 2020). Em solos, a baixa decomposição do CBZ faz com que o mesmo persista por mais tempo, de 6 a 12 meses (SINGH *et al.*, 2016).

O coeficiente de partição octanol/água indica que o CBZ possui baixa tendência a se associar à fração sólida hidrofóbica, ou seja, pode ser considerado hidrofílico e com grande capacidade de difusão em ambientes aquosos. Isso se deve ao fato de que o seu Log K_{ow} ser menor do que 2,5 (ROGERS, 1996) e também pela polaridade da molécula. Essa particularidade pode impactar na eficiência de remoção por adsorção, dependendo também das características do adsorvente utilizado.

A constante adimensional de Henry (K'_h) indica a volatilidade dos compostos, sendo este processo expressivo para compostos com $K'_h > 10^{-4}$, o que não é verificado para o Carbendazim. Nesse sentido, é possível inferir que o composto não apresenta uma expressiva volatilidade e que as perdas de CBZ da água para a atmosfera são improváveis (PEREIRA, 2018).

O Coeficiente de Adsorção de Carbono Orgânico no solo (K_{oc}) indica a tendência de um composto em aderir nesse meio. Quanto maior for o valor de K_{oc}, maior será a tendência de sorção no solo, e menor será sua mobilidade (K_{oc}>10000 indica sorção forte ao solo) (PEREIRA, 2018). Dessa forma, o CBZ é considerado moderadamente móvel (BARCELÓ & HENNION, 1997). Essa particularidade está em consonância com o coeficiente de partição octanol/água, mostrando que o CBZ possui afinidade e estabilidade no meio aquoso.

O pKa permite estimar a distribuição de espécies iônicas (desprotonadas) e não iônicas (neutras) de determinado composto. Se o pH do meio for maior que o pKa, a concentração da fração aniônica será predominante. Do contrário, se o pH for menor que o pKa, a fração neutra ou eventualmente protonada do composto será predominante. Segundo Barceló e Hennion (1997), compostos aniônicos tendem a ser lixiviados mais facilmente no solo. Dessa forma, em pH próximo à neutralidade, o CBZ pode se lixiviar com certa facilidade devido à repulsão eletrostática com as partículas negativas do solo. Caso o pH do meio seja inferior ao pKa, só haverá interação de natureza hidrofóbica do composto com a matéria orgânica ou com minerais menos hidrofílicos (BARCELÓ & HENNION, 1997).

Vários estudos identificaram a remoção de CBZ por carvão ativado. Kegel, Rietman e Verliefde (2010) verificaram que a combinação de osmose reversa seguida de adsorção por carvão ativado foi capaz de remover mais de 99% do CBZ presente na água em uma ETA na Holanda, além de outros poluentes orgânicos emergentes.

Estudo realizado por Pereira *et al*. (2021; 2018) abordou a remoção do fungicida por carvão ativado pulverizado em amostras de água clarificada em escala de laboratório, de alta e baixa turbidez, além da associação dessas amostras com ozonização e ciclo completo com posterior cloração. O primeiro teste de remoção do composto foi feito somente com o CBZ e os coagulantes (sulfato de alumínio, cloreto de polialumínio e cloreto férrico); no segundo momento o teste de remoção do fungicida abrangeu a adição do coagulante associada à adsorção por carvão ativado em pó (CAP). No último teste foi avaliada a remoção de CBZ após coagulação e cloração com hipoclorito de sódio.

Nesse trabalho foi observado que na clarificação, em águas de alta turbidez, o cloreto férrico foi o coagulante mais eficiente na remoção do CBZ enquanto, em águas

de baixa turbidez, o cloreto de polialumínio se destacou em relação aos demais. Foi verificado que a turbidez influencia diretamente na remoção do fungicida, sendo maior em águas menos turvas. Essa é uma informação relevante na compreensão do comportamento do CBZ em ETAs, visto que em períodos sazonais em que a água bruta apresenta menor turbidez, a remoção do CBZ possivelmente será maior considerando somente a etapa de coagulação/floculação. A adsorção com CAP adicionado juntamente com o coagulante ou utilizado como pós-tratamento não apresentou melhoria considerável à etapa de clarificação como um todo.

A associação da etapa de cloração com hipoclorito de sódio após a coagulação aumentou a eficiência na remoção de Carbendazim, alcançando concentração inferior ao limite de quantificação do método analítico utilizado. Nessa etapa foram identificados dois compostos químicos possivelmente oriundos da degradação do Carbendazim por cloração.

As informações apresentadas no trabalho de Pereira (2018) servem de base para a predição do comportamento do CBZ em ETAs convencionais, ainda que a etapa de filtração não tenha sido testada. A partir do observado, têm-se como pressuposto de que a adição de carvão ativado juntamente com a etapa de coagulação não apresenta melhorias significativas e pode vir a reduzir o tempo de vida útil dos filtros, diminuindo o intervalo entre as retrolavagens. Uma alternativa é a adição de carvão ativado granular na etapa de filtração, visando promover uma maior remoção do composto.

No Brasil há vários estudos sobre o uso de carvão ativado em escala de bancada para a análise da remoção de outros microcontaminantes. Voltan *et al* (2016) avaliaram a remoção dos herbicidas Diuron e Hexazinona com uma coluna de CAG em escala piloto. Os autores visaram identificar os mecanismos de transportes por difusão predominantes entre o carvão ativado e os contaminantes estudados. O trabalho concluiu que a difusão pode ser considerada constante em relação ao diâmetro do grão de carvão ativado granular, ao invés de proporcional. Ao final do experimento, foi observado que a técnica pôde remover com eficiência os contaminantes avaliados.

Gorza (2012) avaliou a remoção dos agrotóxicos através das técnicas de pré-oxidação e adsorção em carvão ativado granular do tipo betuminoso em uma unidade

de tratamento piloto da Companhia Espírito Santense de Saneamento (CESAN). O estudo mostrou que a adsorção em CAG apresentou os melhores resultados para a remoção de 2,4-D e 2,4-Diclorofenol (2,4-DCP), sendo uma alternativa para a remoção desses compostos associada ao tratamento convencional em ETAs

Em estudo de remoção de agrotóxicos de efluentes através de um biorreator de membranas, Lopes (2019) demostrou que o CBZ foi biodegradado pelos microrganismos com eficiências médias de remoção de 69%, com um tempo de contato de 50 – 98h. Após a adição de uma coluna de carvão ativado, o CBZ foi totalmente removido do sistema.

3.3. ANÁLISES ESTATÍSTICAS

Os testes estatísticos são ferramentas importantes para a análise de dados. O método de Kruskal-Wallis, por exemplo, é um teste estatístico não paramétrico que avalia se duas ou mais amostras são retiradas da mesma distribuição. É habitualmente utilizado em várias áreas de estudo, e este teste visa descobrir se um grupo de amostras provém da mesma população (GUO, ZHONG and ZHANG, 2013). Este método é utilizado quando os dados experimentais não apresentam uma distribuição normal e são adequados especialmente nos casos em que a dimensão dos dados é pequena. Geralmente o método de Kruskal-Wallis é utilizado em situações em que se quer analisar dois ou mais grupos independentes, de tamanhos iguais ou não, com variável resposta quantitativa (HOLLANDER & WOLFE, 1973).

Quanto à avaliação da distribuição das amostras, o teste de hipótese paramétrico de Shapiro- Wilk (SW) de normalidade composta é um método bastante conhecido e usado para a análise da normalidade dos dados. O teste de SW é um dos mais conhecidos e aplicados para verificar a normalidade de uma determinada distribuição quando o tamanho da amostra é pequeno (YAMANAPPA *et al*., 2018). A distribuição normal, também chamada de Gaussiana, é importante por ser frequentemente usada para modelar fenômenos naturais. Dessa forma, a partir do método de SW, podemos testar a hipótese nula de que uma amostra retirada de uma população possui ou não distribuição normal (ROYSTON, 1982).

Um método estatístico bastante utilizado na análise de dados é o teste da diferença honestamente significativa (*honestly significant difference* - HSD) de Tukey, que engloba comparações múltiplas. O teste de Tukey consiste em comparar todos

os pares de médias de uma série de dados e se baseia na diferença mínima significativa entre elas, considerando os percentis do grupo (TUKEY, 1949; COPENHAVER & HOLLAND, 1988). O método de Tukey é considerado rigoroso e prático, e já foi aplicado no estudo de cinética e termodinâmica de adsorção da Eritrosina B em carvão ativado para análise dos resultados gerados, a exemplo (OKOYE, ONUKWULI and OKEY-ONYESOLU, 2019).

A correlação é um conceito importante e muito utilizado, e é normalmente ensinado através de uma explicação por palavras ou de uma descrição gráfica acompanhada de uma medida numérica. Um dos métodos bastante utilizados é o método de Kendall (KENDALL, 1938). Este método pode ser representado por visualizações gráficas ou modelos matemáticos, mostrando uma tendência ou como os dados são afetados pelas por outras variáveis independentes (DAVIS & CHEN, 2007). O coeficiente de regressão de Kendall indica em que medida a variável de resposta pode ser aproximada por uma função estritamente crescente das variáveis preditoras (LIEBSCHER, 2021). Este método já foi utilizado na análise de absorção e lixiviação de inseticida em solos agrícolas (BROZNIĆ *et. al.*, 2021).

Para se otimizar as condições de remoção de um determinado composto através do processo de adsorção em carvão ativado são necessários ensaios laboratoriais para identificar os melhores parâmetros operacionais, tais como temperatura, tempo de contato e massa de carvão ativado empregada. A metodologia curva de superfície resposta (*Response Surface Methodology* – RSM) é uma coleção de técnicas estatísticas e matemáticas utilizadas para desenvolver, otimizar e aprimorar processos, em que a RSM é empregada para avaliar a significância relativa de fatores que afetam uma resposta dos dados (ZHOU, ZHANG and CHENG, 2015). Em linhas gerais, o objetivo da RSM é otimizar simultaneamente os níveis das variáveis experimentais para obter o melhor desempenho do sistema (BEZERRA *et al*., 2008).

Os métodos estatísticos descritos neste tópico auxiliaram nas análises realizadas neste trabalho e foram fundamentais para as conclusões da pesquisa.

4. METODOLOGIA

A tese foi escrita no formato de artigos, que compuseram os capítulos referente a sessão de resultados e discussões do manuscrito. Cada trabalho possui introdução e metodologia próprias, com resultados e conclusões que atenderam aos objetivos gerais e específicos. Optou-se por manter o idioma no qual os artigos foram publicados e/ou submetidos.

O artigo "*Carbendazim Adsorption on Granular Activated Carbon of Coconut Shell: Optimization and Thermodynamics*", apresentado no item 5.1, foi publicado na revista *Revista AIDIS de Ingeniería y Ciencias Ambientales* (https://doi.org/10.22201/iingen.0718378xe.2023.16.2.82890). O artigo "*Carbendazim Adsorption on Granular Activated Carbon in Deionized and Filtered Water from Treatment Plant - Isotherms, Kinetics, and Rapid Small-Scale Column Tests*", apresentado no item 5.2, está em processo de conclusão para submissão em um periódico. O artigo "*Adsorption of the Fungicide Carbendazim on Activated Carbon: Analysis of Isotherms, Kinetics, Rapid Small-Scale Column Tests and Impacts of the Presence of Organic Matter*", apresentado no item 5.3, foi finalizado e submetido para publicação na revista *Water Practice and Technology.*

A Figura 4.1 mostra, de forma gráfica, as etapas de elaboração do trabalho. A tese de doutorado foi desenvolvida durante as restrições de trabalho presencial nas instalações da Universidade Federal do Rio Grande do Sul (UFRGS) devido à pandemia de COVID-19, que foram de 2020 a 2022. Dessa forma, o tempo de permanência no laboratório influenciou na adoção dos tempos de contato dos testes em batelada dos artigos, principalmente.

Outra limitação desta pesquisa foi quanto a troca do CAG utilizado no Artigo 1 (CAG de casca de coco) para os Artigos 2 e 3 (CAG de osso), devido à granulometria indicada na literatura para realização dos ERCER. Ressalta-se que, antes da aplicação do CAG de osso nos artigos, foram realizados testes preliminares em condições similares às realizadas com o CAG de casca de coco, que apresentaram resultados similares aos dispostos no Artigo 1.

Figura 4.1 - Fluxograma de elaboração da tese de doutorado.

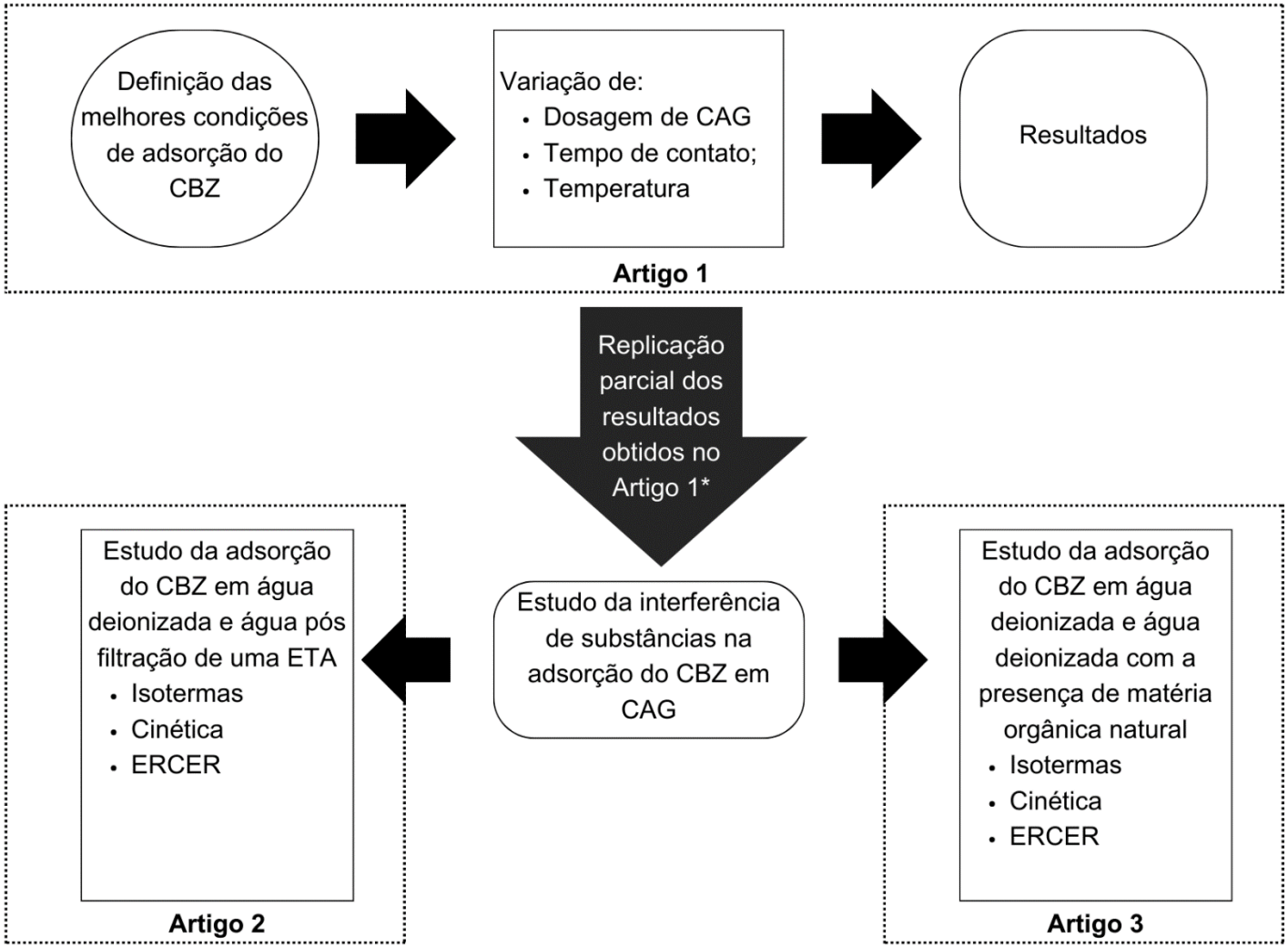

*Devido às limitações na aplicação do ERCER, trocou-se CAG utilizado no Artigo 1. Também se aumentaram os tempos de contato e as dosagens de CAG.

5. RESULTADOS

5.1. CARBENDAZIM ADSORPTION ON GRANULAR ACTIVATED CARBON OF COCONUT SHELL: OPTIMIZATION AND THERMODYNAMICS

5.1.1. Abstract

The adsorption of the fungicide Carbendazim (CBZ) on granular activated carbon (GAC) of coconut shell was investigated through batch tests in deionized water. The most favorable conditions for the adsorption of CBZ were examined through the variation of the mass of GAC, temperature, and contact time. The Response Surface Methodology (RSM) was applied, seeking the best adsorption condition to optimize future tests. A thermodynamic analysis was carried out using the Van't Hoff method. The tests with the dosage of 10 mg of GAC and temperatures of 25º C and 30º C showed higher adsorption of the fungicide. The Freundlich isotherm adjusted best to the adsorption of the compound. The Freundlich intensity parameter had a result that contrasted with the value of ΔG regarding a spontaneous change. Physisorption predominates the adsorption of CBZ on GAC. It is an exothermic and spontaneous process that reduces the degree of disorder of the adsorbent/solution interface.

Keywords: Carbendazim adsorption, Granular Activated Carbon, Adsorption optimization, Response Surface Methodology, Adsorption thermodynamics.

5.1.2. Introduction

The release of contaminants from point and diffuse sources derived from human activities impacts water quality. Among the pollutants are Contaminants of Emerging Concern (CEC), which are chemical compounds present at low concentrations (usually at levels of µg/L or ng/L) in water and sewage that cause risks to human health and ecosystems (BENNER *et al*., 2013). They result from various human activities in urban areas, industry, and agriculture. Pesticides, pharmaceuticals, and flame retardants are examples of CEC that can be found in water (KÜMMERER, 2011).

Interest in the study of CEC in water bodies has grown over the years, considering their impacts on aquatic ecosystems and water sources used for human consumption. Conventional water treatment processes have limitations in removing several CEC, and there is a global need to regulate the emission of most of these contaminants (HALLÉ *et al*., 2015). Studies have shown that these contaminants may

have deleterious effects on the environment and public health, depending on the concentration and exposure time of the organisms (PAREDES *et al*., 2016).

Among the CEC, a group that stands out is pesticides. According to the Brazilian National Health Surveillance Agency (ANVISA, 2019), pesticides are substances applied to crops, pastures, and the environment to control the action of harmful plants and insects. They are used as defoliants, desiccants, growth stimulators, and inhibitors. In recent decades, Brazil has been one of the largest consumers and producers of pesticides in the world, being the first in both aspects in Latin America (BARBOSA *et al*., 2015; PRETE *et al*., 2017; COELHO & ROZÁRIO, 2019).

One of the most applied pesticides in Brazil is Carbendazim (CBZ), the commercial name for methyl benzimidazole-2-ylcarbamate. CBZ is an agricultural defensive from the group of benzimidazoles (RAMA *et al.*, 2014). It is considered a systemic fungicide with authorized application in Brazil for cotton, rice, citrus, beans, apple, corn, soybean, and wheat crops (RAMA, 2013). CBZ is efficient against various fungal diseases in these crops caused by the fungi *Ascomycetes spp*., *Basidiomycetes*, and *Deuteromycetes* spp (COUTINHO *et al.*, 2007).

CBZ is used in agriculture to protect and eradicate several pathogens that affect fruits, nuts, vegetables, and other crops. Also, it can be applied in post-harvest storage and pre-planting seeds. Figure 5.1 shows the chemical structure of CBZ (CHEMICALIZE, 2019). The benzimidazole ring provides resistance to molecule breakdown and slow degradation, persisting in the environment for a long time (POURREZA *et al.*, 2015).

Figure 5.1 - Chemical structure of Carbendazim.

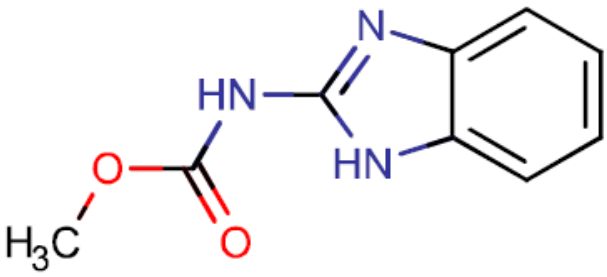

Source: Chemicalize (2021).

CBZ is one of Brazil's most commercialized pesticide-active ingredients (BARBOSA *et al*., 2015). In 2012, the American Food and Drug Administration (FDA) detected CBZ in concentrated orange juice exported from Brazil to the United States (YUKHANANOV, 2012). This finding caused a decline in the application of CBZ in Brazil. In the last decade, CBZ was the main pesticide used irregularly in Brazil, being detected in unauthorized crops and above the maximum levels allowed by Brazilian legislation (RAMA *et al*., 2014).

CBZ has been identified in surface waters in several countries. According to a survey carried out by Merel *et al.* (2018), CBZ was identified in water bodies in Brazil, Chile, China, Colombia, Denmark, Germany, Greece, Portugal, Romania, Serbia, Spain, and Switzerland with concentrations ranging from 10 ng/L to 6,000 ng/L. In Brazil, it is not possible to assess the population's exposure to CBZ and other pesticides due to inconsistencies in the drinking water monitoring system (BARBOSA *et al*., 2015). Brazilian regulation sets an upper limit of 120 µg/L for CBZ in drinking water (BRAZIL, 2021).

According to Coutinho *et al*. (2007), the Pesticide Action Network (PAN, 2020), and the International Program on Chemical Safety (IPCS, 2020), CBZ is a compound that has carcinogenic potential in addition to being a possible endocrine disruptor. It is a highly toxic compound for the aquatic community: amphibians (genetic effects and mortality), aquatic plants (reproduction), crustaceans (mortality), fish (bioaccumulation and mortality), fungi (development and reproduction), mollusks (intoxication and mortality) and plankton (intoxication, growth, reproduction, and mortality).

To mitigate the impacts on the environment and human health caused by the exposure of organisms to concentrations of pesticides considered toxic, several studies have been carried out on treatment technologies to remove these compounds. Activated carbon has become one of the most used adsorbents to remove complex contaminants in aqueous solutions (CRITTENDEN *et al*., 1987; RATHI & KUMAR, 2021).

In drinking water treatment, Granular Activated Carbon (GAC) is used as an adsorbent to remove contaminants such as pesticides, drugs, and organic compounds from industrial sources, among other CEC (KEARNS *et al*., 2020). The use of GAC is

justified by the relative practicality of operation and maintenance and its effectiveness compared to other treatment techniques (JOSS *et al*., 2008; ANFAR *et al*., 2020).

To optimize the removal conditions of a given compound by adsorption on activated carbon, laboratory tests are needed to identify the best operational parameters such as temperature, contact time, and mass of activated carbon used. The Response Surface Methodology (RSM) is a collection of statistical and mathematical techniques used to develop, optimize, and improve the operation of processes (RIFI *et al*., 2022). RSM is used to assess the relative significance of factors that affect a data response (ZHOU *et al*., 2015). This methodology aims to optimize the levels of experimental variables to obtain the best system performance (BEZERRA *et al.*, 2008; RIFI *et al*., 2022).

RSM has been used to optimize and model the adsorption process to identify the best operating conditions to achieve greater efficiency in removing the compound of interest, studying the effect of parameter variation (TAKTAK *et al*., 2015). The RSM is based on a multivariate nonlinear model, allowing the determination of mathematical equations with a better correspondence with the data obtained in experimental tests (ANFAR *et al.*, 2020).

This research studied the removal of CBZ by adsorption on GAC in batch tests. The GAC mass, water temperature, and contact time were varied, and the best condition for CBZ removal was identified using RSM. The adjustment of the experimental data to Langmuir and Freundlich isotherms was verified. The thermodynamics of CBZ adsorption in GAC was also investigated. A literature review did not find a similar approach for CBZ adsorption on GAC from coconut shell, the adsorbent used in the experiments.

5.1.3. Methodology

5.1.3.1. Adsorbate and adsorbent

Adsorption tests were made using commercial GAC produced from coconut shells. Table 5.1 indicates the characteristics of the GAC used in the experiments. The tests were carried out with particle sizes in the range of sieves 20 × 50 mesh (0.841 x 0.297 mm). GAC was previously washed and soaked repeatedly with abundant

deionized water to remove fine particles. In sequence, the material was dried in an oven at a temperature of 105ºC for 24 h.

Table 5.1 - Coconut shell GAC Specifications.

Specifications		**Value**
Iodine number (mg/g)		883
Ashes (%)		Max. 10
Moisture (%)		Max. 10
Apparent density (g/cm^3)		0.45 – 0.55
Granulometry (Nominal, mesh)		6×10 – 6×12 - 8×16 - 12×25 – 8×30 - 12×40 – 20×50
Hardness (%)		Min. 90
Uniformity Coefficient		1,59
BET surface area (m²/g)		1,218
Pores distribution (%)	Primary Micropores (pore <0,8 nm)	54,1
	Secondary Micropores (0,8 nm < pore <2 nm)	34,5
	Mesopores (2 nm < pore <50 nm)	8,8
	Macropores (50 nm > pore)	2,6

Source: Teixeira (2014); Mavaieie Júnior (2019).

Granular Activated Carbons manufactured from coconut shells have most of their total void volume as micropores (CRITTENDEN *et al*., 2012). The surface area and iodine number of GAC are, respectively, in the range of 700-1,300 m^2/g and 600-1,100 mg/g (METCALF & EDDY, 2003). The iodine number generally correlates well with the surface area available for the adsorption of small molecules (SUMMERS *et al*., 2011; NARBAITZ & MCEWEN, 2012). The values for ash, apparent density, and uniformity coefficient are also in the range presented by these authors.

CBZ from Sigma-Aldrich with 97% purity was used. Synthetic solutions were prepared with deionized water to a final CBZ concentration of 5.0 mg/L and neutral pH. For this research, a concentration of 5.0 mg/L was chosen. This level of concentration is not likely to be found in the environment, but it was believed it would allow better monitoring of the adsorption process and the thermodynamic data. Also, this concentration had a good fit with the curve calibration at this concentration. Analyzes were performed in a Shimadzu High-Performance Liquid Chromatograph (HPLC) (LC20A) equipped with a diode array detector (DAD, SPD-20AV) and an autosampler (SIL-20A). The HPLC was operated at a 1 mL/min flow rate, and the detector was set at λ = 285 nm. The stationary phase was HyperCloneTM 5 µm ODS C18 column (4.6 mm × 100 mm, Phenomenex). The mobile phase was phosphate buffer and acetonitrile

(75:25%). An injection volume of 20 µL was used. In these conditions, the CBZ retention time was 2.7 min (Machado *et al*., 2022).

The mass of GAC used in the batch tests were 0.0; 0.2; 0.5; 1.0; 1.5; 2.0; 5.0 and 10.0 mg. The tests were carried out at temperatures of 30ºC and contact times of 2h (E-1), 3h (E-2), and 4h (E-3), 25ºC (E-4, E-5, and E-6, respectively for 2, 3, and 4h), and 40ºC (E-7, E-8, and E-9, for 2, 3, and 4h). The solutions containing CBZ and GAC were stored in a Dubnoff Bath Shaker equipment, model TE-053, allowing the control of temperature and agitation. Due to restrictions on the time of access and stay at the laboratory due to the COVID-19 pandemic in Brazil, the variation of parameters was restricted to 3 different temperatures and a maximum contact time of 4 hours. All experiments were conducted in triplicate.

5.1.3.2. Adsorption Isotherms

The experimental results of CBZ adsorption on GAC were fitted to the Langmuir and Freundlich isotherms. The R^2 coefficients and trend lines were determined with Microsoft Office Excel (MOE) 2019 software. The Solver function was used to calculate the isotherm variables. The Langmuir and Freundlich isotherms are represented, respectively, by Equations 23 and 24 (CRITTENDEN *et al*., 2012).

$$q_e = q_{max} . \frac{b . C_e}{1 + b . C_e} \quad (23)$$

$$q_e = k_f . {C_e}^{1/n} \quad (24)$$

Where: C_e is the equilibrium concentration of adsorbate in solution after adsorption (mg/L); q_e is the quantity sorbed at equilibrium (mg/g); $q_{máx}$ is the maximum adsorption capacity (mg/g); b is the Langmuir adsorption equilibrium constant (L/mg); k_f is the Freundlich constant, representing the adsorption capacity [(mg/g) $(L/mg)^{1/n}$]; $1/n$ is the Freundlich intensity parameter. (METCALF & EDDY, 2003).

For comparative purposes, the linearized forms of the models were also investigated (Equations 25 and 26).

$$\frac{C_e}{q_e} = \frac{1}{b . q_{max}} + \frac{C_e}{q_{max}} \quad (25)$$

$$\ln q_e = \ln k_f + \frac{1}{n} . \ln C_e \quad (26)$$

5.1.3.3. Thermodynamic analysis

For the thermodynamic analysis, the variations in enthalpy (ΔH, kJ/mol), entropy (ΔS, J/mol.K), and Gibbs Free Energy (ΔG, kJ/mol) were quantified using equations 27 to 29 (NEKOUEI *et al.*, 2015; HARO *et al.*, 2021). The values of ΔH and ΔS were obtained using the Van't Hoff graph (lnKe as a function of 1/T) represented by Equation 27.

$$\ln K_e = \frac{\Delta S}{R} - \frac{\Delta H}{RT} \quad (27)$$

Where: *Ke* is the equilibrium constant; *R* is the universal gas constant, 8.314 J/mol.K; and *T* is Temperature (K).

The adsorption equilibrium constant can be expressed by the ratio of the equilibrium concentration of the contaminant in the activated carbon to the equilibrium concentration of the contaminant in the solution expressed in Equation 28 (MANSOURIIEH *et al*., 2016; PRETE *et al*., 2017).

$$K_e = \frac{q_e}{C_e} \quad (28)$$

The variation of free energy (ΔG) was calculated with Equation 29.

$$\Delta G = -RT\ln K_e \quad (29)$$

5.1.3.4. Statistical analysis

Response Surface Methodology (RSM) curves were performed for each contact time tested, totaling 3 curves. For these statistical tests, two independent variables were adopted: Y (temperature of 25º C, 30º C, and 40º C) and X (Mass of GAC from 0.0 to 10.0 mg) and a dependent variable Z (Efficiency of CBZ removal). The quadratic model was used to optimize the responses as a function of the independent variables. The application of the RSM was performed with the Statistica 13.5 software.

Statistical tests were used to check if the CBZ removal percentages had significant differences. The block design method was applied using the "Mass GAC" treatment. The "Time" and "Temperature" factors were combined to build the block variable. The variance model (ANOVA) was fitted to the data, and the F test was used to test the null hypothesis of no difference between the means. Tukey's honestly significant difference (HSD) test for multiple comparisons was used to detect which groups differed from one another. The 5% significance level was adopted in all

analyses (p = 0.05). Boxplot graphs were created to present the distribution of the response variable (dependent variable). These analyzes were performed using R software version 4.0.4.

5.1.4. Results and discussion

Table 5.2 shows the results obtained in the adsorption experiments for the contact time, temperature, and GAC mass that were tested. The initial concentration of CBZ was 5 mg/L CBZ.

Table 5.2 - Removal of CBZ in the adsorption tests (%).

Tests	GAC (mg)							
	0	**0.2**	**0.5**	**1.0**	**1.5**	**2.0**	**5.0**	**10.0**
E-1	0.0	1.1	2.8	6.5	7.5	10.5	23.2	29.8
E-2	0.0	0.4	8.6	12.1	16.7	18.1	21.8	25.7
E-3	0.0	3.5	8.7	14.9	17.9	18.8	27.7	31.6
E-4	0.0	6.5	13.8	15.3	18.7	21.3	24.3	25.4
E-5	0.0	3.5	5.9	10.1	10.7	10.7	15.6	25.8
E-6	0.0	9.5	11.0	18.7	20.3	21.1	27.0	33.3
E-7	0.0	6.7	10.4	15.2	15.8	20.5	21.5	23.5
E-8	0.0	11.3	11.6	13.8	14.9	20.4	23.0	26.0
E-9	0.0	6.7	8.7	10.1	12.7	15.8	16.6	22.3

E-1: 2 h, 30ºC; E-2: 3 h, 30ºC; E-3: 4 h, 30ºC; E-4: 2 h, 25ºC; E-5: 3 h, 25ºC; E-6: 4 h, 25ºC; E-7: 2 h, 40ºC; E-8: 3 h, 40ºC; E-9: 4 h, 40ºC;

The highest CBZ removal efficiencies occurred in tests E-3 and E-6, which presented 31.6% and 33.3%, with a contact time of 4 h, 10 mg of GAC, and temperatures of 30 ºC and 25 ºC, respectively. Contact time and carbon mass influenced the removal efficiency of CBZ in batch tests. It is possible that the use of the higher mass of GAC and longer contact time would improve CBZ removal by adsorption. The block stratification shown in Figure 2 corroborates the best performances of CBZ adsorption in tests at 25 ºC and 30 ºC (E-6 and E-3) and a contact time of 4h. In Figure 5.2, blocks include efficiencies considering all GAC masses applied in each test.

Figure 5.2 - Distribution of stratified CBZ removal percentage by block. Each block considered efficiencies achieved by all GAC masses applied to each box.

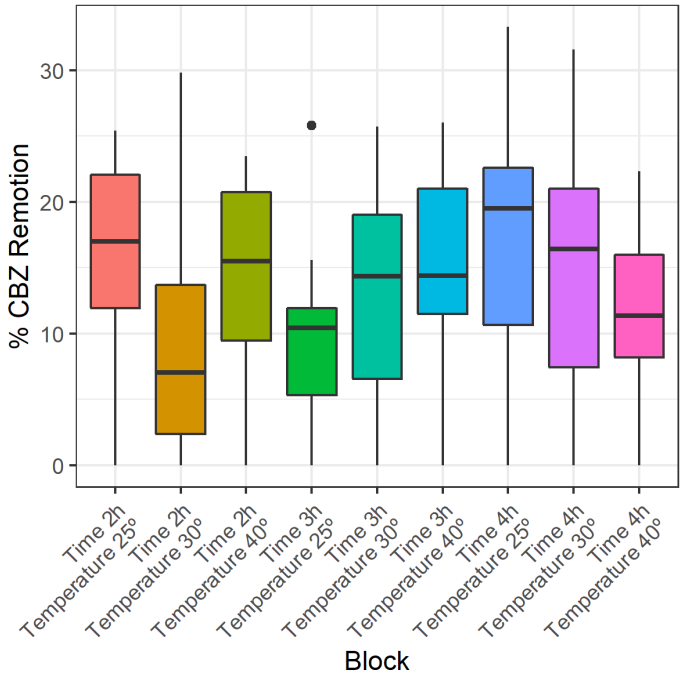

Figure 5.2 shows the highest removal efficiency at E-3 and E-6, above 30%. E-1 presented the lowest efficiency values in the second and third quartiles but showed maximum efficiency close to 30%. Only E-5 presented an outlier.

Table 5.3 shows the difference between the averages of CBZ removal efficiency by GAC mass, the lower and upper limits (LL and UL, respectively), and the adjusted p-value considering the 5% significance level. The approach aimed to investigate whether there were significant differences between the ranges of GAC masses adopted to execute the experiments.

Table 5.3 - Differences between treatment means (GAC mass), 95% confidence intervals (CI), and adjusted p-value (Tukey's HSD).

Breaks (mg)	Differences	LL – CI 95%	UL – CI 95%	p adjusted
0.2-0	0.0548	0.0155	0.0941	0.0012
0.5-0	0.0906	0.0514	0.1299	0.0000
1-0	0.1298	0.0905	0.1690	0.0000
1.5-0	0.1503	0.1110	0.1896	0.0000
2-0	0.1747	0.1354	0.2140	0.0000
5-0	0.2228	0.1835	0.2621	0.0000
10-0	0.2705	0.2312	0.3098	0.0000
0.5-0.2	0.0358	-0.0035	0.0751	0.0985
1-0.2	0.0749	0.0357	0.1142	0.0000
1.5-0.2	0.0955	0.0562	0.1348	0.0000
2-0.2	0.1199	0.0806	0.1592	0.0000
5-0.2	0.1680	0.1287	0.2073	0.0000
10-0.2	0.2157	0.1764	0.2550	0.0000
1-0.5	0.0391	-0.0002	0.0784	0.0517
1.5-0.5	0.0596	0.0204	0.0989	0.0003
2-0.5	0.0841	0.0448	0.1234	0.0000
5-0.5	0.1322	0.0929	0.1715	0.0000
10-0.5	0.1799	0.1406	0.2192	0.0000
1.5-1	0.0205	-0.0188	0.0598	0.7216
2-1	0.0450	0.0057	0.0843	0.0144
5-1	0.0931	0.0538	0.1324	0.0000
10-1	0.1408	0.1015	0.1800	0.0000
2-1.5	0.0244	-0.0148	0.0637	0.5177
5-1.5	0.0725	0.0333	0.1118	0.0000
10-1.5	0.1202	0.0810	0.1595	0.0000
5-2	0.0481	0.0088	0.0874	0.0068
10-2	0.0958	0.0565	0.1351	0.0000
10-5	0.0477	0.0084	0.0870	0.0075

Most of the results showed significant differences ($p < 0.05$), indicating that variations in temperature, contact time, and adsorbent mass influenced the adsorption of CBZ on GAC. However, there were no significant differences in the concentration intervals between 0.5-0.2 mg, 1.0-0.5 mg, 1.5-1.0 mg, 2.0-1.0 mg and 2.0-1.5 mg. In these ranges of GAC masses, the results showed similar behaviors.

Table 5.4 shows the means of CBZ removal by GAC mass. The letters “a” to “g” indicate the groupings between the treatment removals considering the significance level of 5%. It is observed that the average of CBZ removal for 10, 5, and 0 mg presented unique behaviors, and they are not grouped with other GAC masses. The other masses showed similar means of removal to the upper or lower level. That was the reason why some experiments had more than one letter ("cd", for example), representing similar behavior to the upper or lower levels.

Table 5.4 - Averages of % removal by GAC mass.

GAC (mg)	Removal (%)	Groupings
10.0	27.05	a
5.0	22.28	b
2.0	17.47	c
1.5	15.03	cd
1.0	12.98	de
0.5	9.06	ef
0.2	5.48	f
0.0	0.00	g

Tests in which 10 mg of GAC was used presented a significant difference in the CBZ removal mean compared to all other masses ($p < 0.05$). The stratified block analysis shown in Figure 5.3 indicates that the assays performed by this GAC dosage showed greater fungicide removal. Likewise, the figure suggests an increase in the adsorbed concentration of CBZ, with the increase in the mass of adsorbent employed. The addition of GAC in amounts greater than 10 mg would probably result in higher CBZ removal.

Figure 5.3 - Distribution of CBZ removal stratified by GAC in tests.

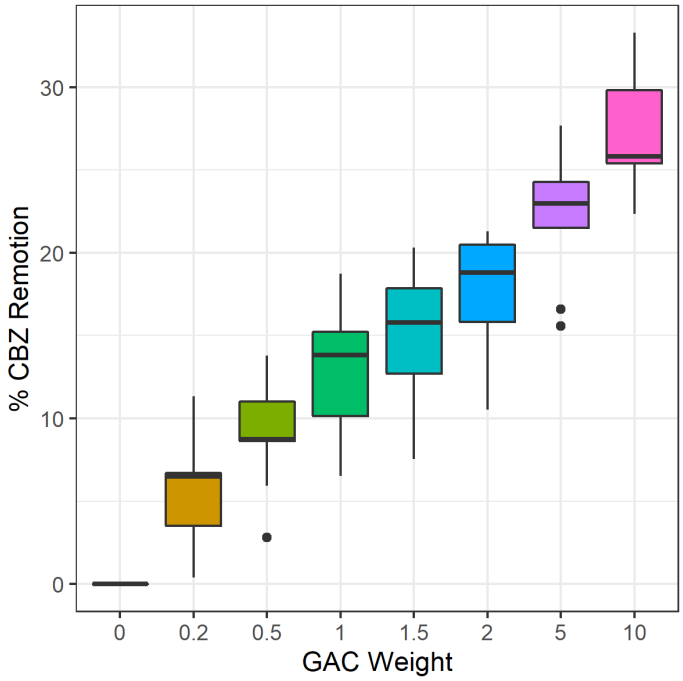

CBZ has constant dissociation (pKa) equal to 4.29 (PUBCHEM, 2020). It means that if the pH of the medium is higher than the pKa, the concentration of the anionic fraction of the pesticide will be predominant, and the compound tends to be leached more easily (BARCELÓ & HENNION, 1997). All batch adsorption tests were made with pH close to 7.0, favoring leaching and reducing adsorption.

CBZ has an octanol/water partition coefficient (log K_{ow}) and organic carbon adsorption coefficient in soil (K_{oc}) equal to 1.52 and 200 cm^3/g, respectively. CBZ can be considered hydrophilic (ROGERS, 1996) and moderately mobile, with a moderate tendency to sorption in the soil (BARCELÓ & HENNION, 1997).

Surface curves relating to GAC mass, contact time, and temperature were prepared using adsorption data from Table 5.2. The results are shown in Figure 5.4.

Figure 5.4 - Surfaces curves for removal of CBZ as a function of GAC mass and temperature at 2h (a), 3h (b), and 4h (c).

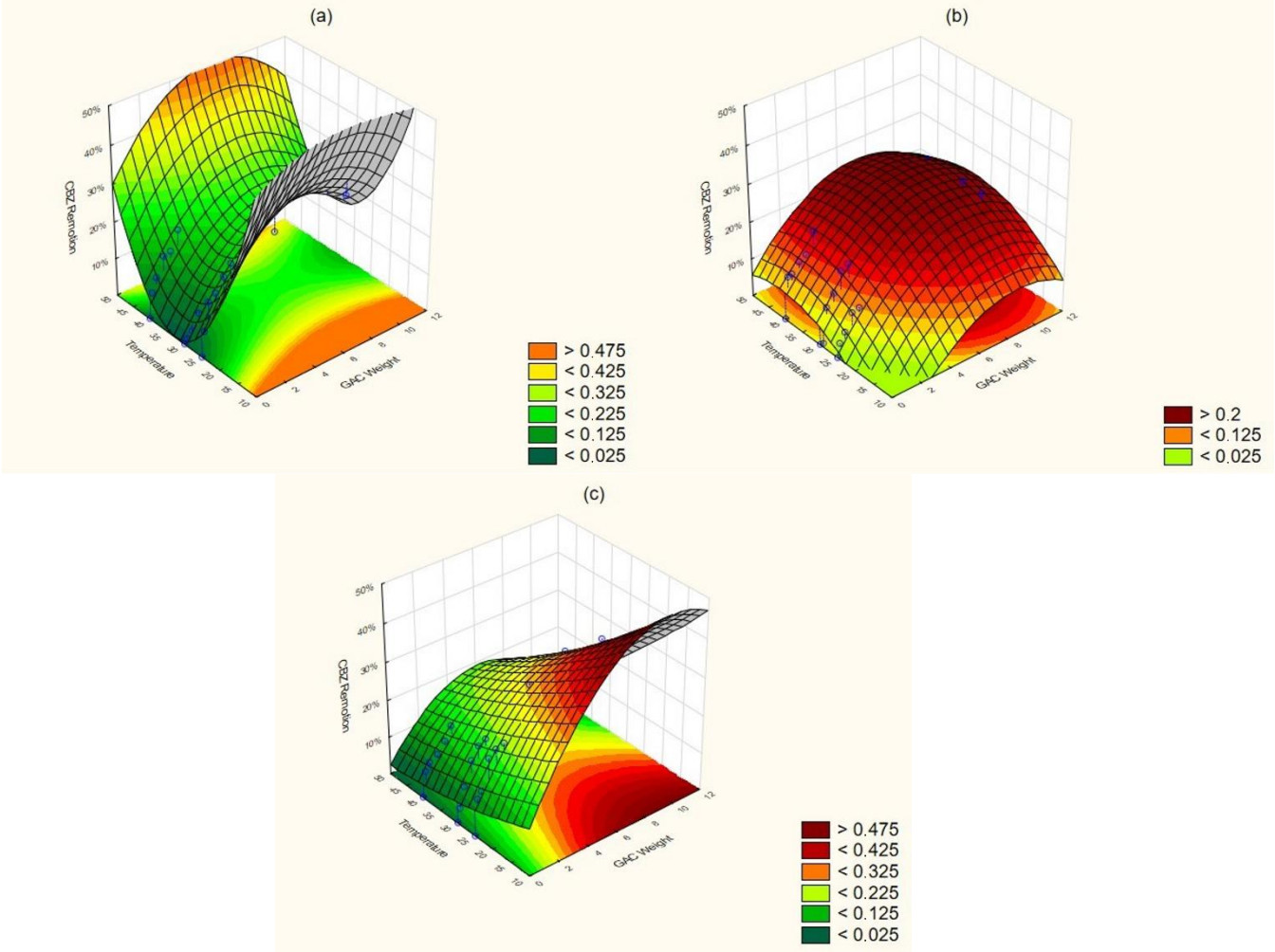

Figure 5.4a shows that the curve for 2 h presents two elevations and does not provide evidence of the optimization of CBZ adsorption on the GAC. Hence, it is not possible to identify a favorable condition for removing the fungicide. This behavior probably occurred due to the short contact time, which might have prevented consistent adsorption.

Figure 5.4b exhibits a curve flattening with increases in temperature and GAC mass. This scenario suggests that the increase in temperature and GAC mass favors the adsorption of CBZ. However, as shown in Table 5.2, the fungicide removal efficiencies were not significantly different for the temperatures of 25, 30, and 40º C ($p<0.05$), respectively 25.8%, 25.7%, and 26.0%. Due to results that had similar behaviors, it was not possible to identify a tendency in Figure 5.4b.

In Figure 5.4c it is possible to observe that there is a trend in which the greatest CBZ removal occurs at the lowest temperatures associated with the highest GAC mass, with the removals of 33.3%, 31.6%, and 22.3%, respectively for the temperatures of 25º C, 30º C, and 40º C. Thus, for the contact time of 4h the adsorption of CBZ on GAC was favored at the lowest temperature (25ºC), suggesting an exothermic process, as expected for adsorption (RATHI & KUMAR, 2021). RSM suggests that tests could be carried out at temperatures below 30ºC, reducing the number of analyzes.

Equation 30 shows the quadratic model representing Figure 5.4c. With this equation is possible to estimate the CBZ removal, giving temperature and GAC weight.

$$\mathrm{CBZ_{remotval}}(\%) = 0.174 + 0.087\mathrm{X} - 0.005\mathrm{Y} - 0.004\mathrm{X}^2 - 0.001\mathrm{XY} + 4.577\,.\,10^{-5}\mathrm{Y}^2 \qquad (30)$$

Where X is GAC mass (mg) and Y is the temperature (ºC).

Table 5.5 shows the parameters and the correlation coefficients of the Freundlich (F) and the Langmuir (L) isotherms, determined using the linear and the nonlinear methods (Equations 23 to 26). Test E-2 (2 h, 30ºC) had a poor correlation for both isotherms, and it was not further considered for analysis.

Table 5.5 - Langmuir (L) and Freundlich (F) isotherm coefficients for each test.

Parameters			Test							
			E-1	**E-3**	**E-4**	**E-5**	**E-6**	**E-7**	**E-8**	**E-9**
Linear	F	Kf	20.18	0.38	$3x10^{-4}$	0.03	0.05	$6x10^{-6}$	$7x10^{-7}$	$8x10^{-8}$
		1/n	1.73	5.13	10.63	7.35	8.12	11.73	12.90	13.77
		R^2	0.78	0.92	0.87	0.81	0.94	0.87	0.83	0.89
	L	b	-0.14	-0.20	-0.23	-0.25	-0.28	-0.19	-0.18	-0.18
		qmax	-277.78	-92.59	-42.74	-34.01	-53.48	-42.19	-41.84	-29.67
		R^2	0.41	0.76	0.59	0.82	0.88	0.61	0.83	0.86
Nonlinear	F	Kf	2.65	0.26	$4x10^{-3}$	$2.15x\ 10^{-5}$	$2x10^{-3}$	$1.22x\ 10^{-5}$	$3.98x\ 10^{-10}$	$5.68x\ 10^{-10}$
		1/n	1.55	3.81	7.25	11.18	9.00	9.88	16.07	15.43
		R^2	0.75	0.89	0.87	0.92	0.83	0.96	0.65	0.89
	L	b	$1.08x\ 10^{-4}$	$5.86x\ 10^{-6}$	$4.64x\ 10^{-5}$	$8.27x\ 10^{-6}$	$6.49x\ 10^{-6}$	$4.95x\ 10^{-6}$	$4.28x\ 10^{-6}$	$3.42x\ 10^{-6}$
		qmax	$5.42x\ 10^{4}$	$2.46x\ 10^{6}$	$4.1x\ 10^{5}$	$1.17x\ 10^{6}$	$3.53x\ 10^{6}$	$3.47x\ 10^{6}$	$5.08x\ 10^{6}$	$4.13x\ 10^{6}$
		R^2	0.75	0.95	0.93	0.70	0.73	0.92	0.50	0.67

Variable units: Kf - $[(mg/g)\ (L/mg)^{1/n}]$; b - L/mg; $q_{máx}$ - mg/g.

The linear model of the Langmuir isotherm showed negative values, which do not have a coherent physical meaning (Zhiltsova *et al*., 2020). The nonlinear model had determination coefficients above 0,90 (tests E-3, E-4, and E-7), a value not reached in the linear regression model. However, some q_{max} values were very high while b values were low. These values may indicate that the Langmuir isotherm is not the most adequate to represent the adsorption of CBZ in the GAC for the analyzed conditions.

For Freundlich isotherm, the linear model had a better fit in 4 tests. The nonlinear equation had two higher determination coefficients. In the other two, fits for the linear and nonlinear were equal. Overall, considering the results of the tests, the Freundlich isotherm represented better the adsorption of CBZ on GAC than the Langmuir isotherm.

Equation 31 shows the Freundlich isotherm for the data from E-3 test for illustrative purposes. Figure 5.5 shows the respective Freundlich graph. The model presents a positive concavity in relation to the axes. It shows that the greater the concentration of CBZ, the higher the fraction of CBZ adsorbed on the GAC until equilibrium is reached.

$$q_e = 0.38 \,.\, C_e^{\,5.13} \tag{31}$$

Figure 5.5 - Freundlich isotherm for CBZ adsorption on granular activated carbon from Equation 31.

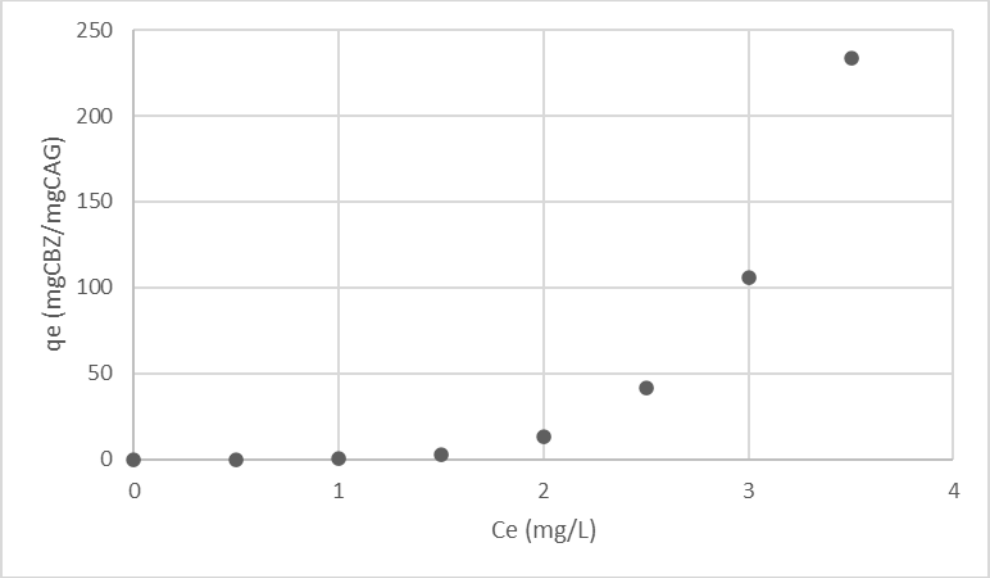

Freundlich's isotherm is not restricted to monolayer formation but occurs in heterogeneous multilayer formation (HARO *et al*., 2021). According to Piccin *et al*. (2017), the Freundlich isotherm assumes that the adsorption occurs heterogeneously on the surface. Thus, the adsorption of CBZ on the GAC probably occurs heterogeneously on the surface and predominantly through the formation of multilayers. This particularity does not exclude monolayer adsorption, which can also occur in the process.

Table 5.5 shows that almost all 1/n values were higher than unity (1/n > 1.0). This fact suggests that fungicide adsorption on the analyzed GAC is an unfavorable process under the conditions analyzed (maximum 4 hours of contact time) (CHEN *et al*., 2003; ANFAR *et al*., 2020; RIZZI *et al*., 2020). Comparing the data obtained with other studies carried out with CBZ, Hgeig *et al*., (2019) found a value of 1/n equal to 0.38 for the fungicide adsorption on activated carbon produced from coffee grounds.

For other adsorbents, Jin *et al*. (2013) obtained a 1/n value of 0.71 for the adsorption of CBZ in soils composed mainly of silt, sand, clay, and a small fraction of organic matter, indicating that the adsorption in this medium is also favorable. The same was identified by Li *et al*. (2011), with 1/n <1 for all tests carried out with Burozem and Phaeozem soils at temperatures of 25º and 40ºC. For polyethylene (PE) agricultural soil films (WANG *et al*., 2020) and for Sandy, Loess, and Loamy soils (PASZKO, 2006), the CBZ adsorption also showed values of 1/n <1. The same was identified for the adsorption of CBZ on bentonite clay (RIZZI *et al*., 2020). However,

Kanjilal *et al*. (2018) measured 1/n equal to 1.57 for the biosorption of CBZ in the strain isolated from the bacterium *Brevibacillus sp*. C17. Thus, the authors characterized CBZ biosorption as an unfavorable process considering the 1/n value.

The studies that were cited showed that the coefficient 1/n of the Freundlich model is mostly smaller than unity, indicating that CBZ adsorption is a favorable process in activated carbon from coffee grounds and soils. It is observed that the adsorption of CBZ in coconut GAC did not follow the trend observed in these studies, except for the one reported on the biosorption of the fungicide in the bacterium C17. To complement information on whether CBZ adsorption is favored in GAC for the applied conditions, Gibbs Free Energy thermodynamic analysis is discussed in sequence.

The analysis of thermodynamic parameters considered the 3.37 mg/L CBZ concentration present in water after 4 h of contact time at 30º C and 10 mg of GAC. Applying this value to Equation 31, the concentration of CBZ adsorbed on the GAC (qe) was 193.43 mgCBZ/gGAC. Substituting the values of qe and Ce in Equations 27, 28, and 29, the enthalpy, entropy, and Gibbs Free energy could be calculated. The data are presented in Table 5.6, considering the temperature variations of 25, 30, and 40 ºC and 4h contact time for ΔG.

Table 5.6 - Thermodynamic parameters of Carbendazim adsorption on GAC.

ΔG (kJ/mol)			**ΔH (kJ/mol)**	**ΔS (J/mol.K)**
25º C	30º C	40 º C		
-9.62	-10.20	-8.03	-37.31	-91.84

Table 5.6 shows that the enthalpy variation in the CBZ adsorption process is negative, indicating that the adsorption of CBZ in coconut shell GAC is an exothermic process. The negative value of ΔG indicates the reaction is favorable. Similar results were found for adsorption of other pesticides on activated carbon, such as Atrazine, Methoxychlor, Parathion-methyl (GUPTA *et al*., 2011), and Fenitrothion (LULE & ATALAY, 2014).

The study by Wang *et al*. (2019) showed that the adsorption of CBZ on straw activated carbon was also characterized as an exothermic and favorable process. The same was identified in the adsorption of CBZ on activated carbon produced from coffee grounds (HGEIG *et al*., 2019), Burozem, and Phaeozem type soils (LI *et al*., 2011), and with nano-carbon (PRETE *et al*., 2017). Concerning enthalpy and Gibbs free energy, the adsorption of CBZ on GAC is in accordance with reported research.

The negative values of ΔG indicate that the adsorption of CBZ in GAC is a spontaneous process for all temperatures used. The lowest ΔG occurred in the test performed at the temperature of 30 °C, and the free energy decreased at 25 ºC and 40 ºC.

It was observed that the favorable characteristic of the CBZ adsorptive process contrasts with the 1/n values of the Freundlich equation, which was higher than unity. In this research, it has been suggested that adsorption of the compound onto the adsorbent is a favorable process (CHEN *et al*., 2004; ANFAR *et al*., 2020; RIZZI *et al*., 2020). Therefore, the analysis of CBZ adsorption process in GAC must include not only the 1/n Freundlich coefficient but also the variation of the Gibbs free energy.

According to Zanella *et al*. (2016) and Yu *et al*. (2004), Gibbs Free Energy values between 0 to –20 kJ/mol and -80 to -400 kJ/mol generally characterize, respectively, physisorption and chemisorption processes. The values of Gibbs Free Energy measured in this study were in the range -8.03 and -10.20, suggesting that CBZ adsorption on GAC was predominantly governed by physisorption.

Physisorption or physical adsorption occurs when the adsorbate binds to the surface of the adsorbent due to less strong chemical bonds, such as the van der Waals forces. It is a process that occurs more quickly than chemisorption, and there is usually the formation of multilayers. Physisorption is a reversible process that occurs at low temperatures (RATHI & KUMAR, 2021). According to Ruthven (1984), some characteristics of physisorption are low heat of reaction; monolayer or multilayer adsorption; no dissociation of species involved; significant process only at low temperatures; and without electron transfer. Added to these characteristics is the predominance of permanent or induced dipole-dipole interactions between the adsorbate molecules and the adsorbent (DELLE SITE, 2001). The exothermic characteristic of CBZ adsorption on GAC, the predominance of physisorption, and the reasonable adjustment to the Freundlich isotherm suggest that the mentioned aspects characterize the fungicide adsorption on the studied activated carbon.

Positive values of ΔS indicate that the reaction increases the degree of disorder in the solid/solute interface during adsorption (NEKOUEI *et al*., 2015; HARO *et al*., 2021), with a strong affinity between the adsorbate and the adsorbent (ZANELLA *et al*., 2016). The value obtained for ΔS, -91.84 kJ/mol, indicates a reduction in the degree

of disorder between the surface of the activated carbon and the CBZ molecules after adsorption.

5.1.5. Conclusions

The results showed that variations in temperature, contact time, and adsorbent mass influenced the adsorption of CBZ into GAC. The tests with 10 mg of GAC dosage presented greater efficiencies for fungicide removal. GAC dosages used in the experiments showed statistically significant results in most cases.

The application of RSM methodology found that, for the longest contact time, the adsorption of Carbendazim in coconut shell GAC was more efficient at temperatures of 25 and 30°C, characterizing an exothermic process that was later confirmed by thermodynamic analysis. The RSM curves indicated that adsorption at 25 ºC and 30 ºC and a contact time of 4h would achieve higher fungicide removal than at higher temperatures.

The Freundlich isotherm adjusted better to the adsorption of CBZ on GAC. In the larger part of the tests, satisfactory results were obtained by both linear and nonlinear regression models. It was found that the adsorption of the fungicide occurs predominantly in a heterogeneous and multilayered way. The Freundlich 1/n parameter presented information that contrasted with the thermodynamic analysis regarding the promotion of CBZ adsorption on GAC. The results diverge from previous studies that investigated the adsorption of CBZ on activated carbon and other adsorbents. Thus, the analysis of spontaneity should consider not only the 1/n Freundlich parameter but also the variation of the Free Energy of Gibbs, based on the conditions applied in this study. For ΔG, this study agreed with previous investigations regarding the spontaneity of the adsorptive process.

At temperatures ranging from 25º C to 40º C, the adsorption of CBZ in GAC was spontaneous. Physisorption seems to be the dominant process, with dipole-dipole interactions between the GAC surface and the fungicide. The ΔS value indicated a reduction in the degree of disorder at the adsorbent/solution interface. The fungicide adsorption on activated carbon is a reversible process without electron transfer.

The results presented in this article contribute to a better understanding of CBZ adsorption on GAC, providing support for ongoing works that aim to achieve higher CBZ removal by activated carbon in water.

Conflict of interests

The authors declare no conflicts of interest.

Acknowledgement

The first author would like to thank CNPq (Conselho Nacional de Desenvolvimento Científico e Tecnológico) for the scholarship granted for his graduate studies and research.

5.2. CARBENDAZIM ADSORPTION ON GRANULAR ACTIVATED CARBON IN DEIONIZED AND FILTERED WATER FROM TREATMENT PLANT - ISOTHERMS, KINETICS, AND RAPID SMALL-SCALE COLUMN TESTS

Highlights

- Bovine bone GAC removed Carbendazim in both aqueous matrices.
- Freundlich isotherm and pseudo-second-order equation fitted the adsorption of CBZ on both matrices.
- Intraparticle diffusion played a significant role in FWTP.
- CBZ breakthrough was achieved earlier in FWTP than in DW, while column saturation occurred at similar times in both matrices.
- The substances present in the FWTP interfered in CBZ adsorption but did not compromise the fungicide removal.

Graphical Abstract

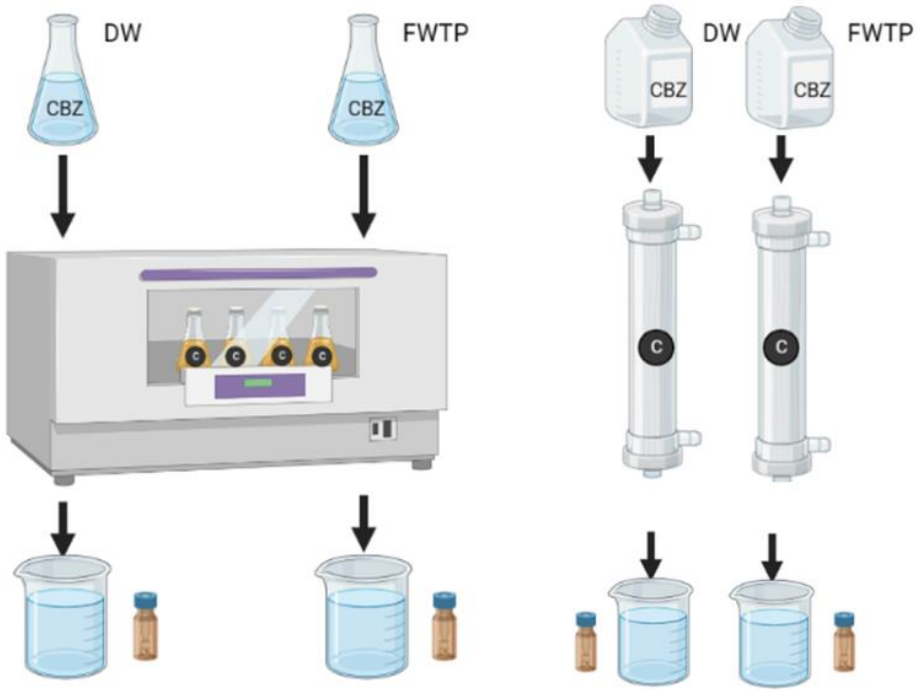

5.2.1. Abstract

Carbendazim (CBZ) adsorption on bovine bone granular activated carbon (GAC) was investigated in deionized water (DW) and filtered water from a treatment plant (FWTP). The study included isotherms, kinetics, and rapid small-scale column tests (RSSCT). Statistical methods were applied to compare the results and verify the interference of substances in filtered water in adsorption. The Freundlich model represented better the fungicide adsorption in DW and FWTP, although other models

evaluated also fitted the data. For the kinetics study, all models evaluated fitted well the CBZ adsorption in FWTP, while the pseudo-second-order was the best fit for the adsorption of CBZ on DW. Intraparticle diffusion played a significant role in FWTP. In RSSCT tests, the CBZ breakthrough was reached faster in FWTP, while the column saturation occurred at similar times in DW and FWTP. The substances present in the FWTP interfered in the adsorption of CBZ on bone GAC but did not compromise the fungicide removal.

Keywords: Carbendazim, filtered water, activated carbon adsorption, isotherms, adsorption kinetics, rapid small-scale column tests.

5.2.2. Introduction

Contaminants of emerging concern (CEC) are chemical compounds present at low concentrations in water bodies, sanitary sewage, and sometimes in treated water for human consumption. They can be harmful to human health and aquatic ecosystems. CECs are released into the environment because of human activities. Generally, they are not regulated in drinking water or the environment. Many pesticides are included in the category of CEC (KÜMMERER, 2011).

Carbendazim - methyl benzimidazole-2-ylcarbamate (CBZ) is a pesticide from the benzimidazole group (RAMA *et al.,* 2014). It is widely used in Brazil to control crop diseases caused by the fungi *Ascomycetes spp*., *Basidiomycetes*, and *Deuteromycetes spp*. (COUTINHO *et al*., 2006). CBZ is a fungicide with carcinogenic potential and an endocrine disruptor (COUTINHO *et al*., 2006). In the last decade, CBZ was Brazil's most irregularly applied pesticide. The fungicide was detected in unauthorized crops and frequently above the maximum levels allowed by Brazilian legislation in surface water. (RAMA *et al*., 2014).

Recently, the Brazilian National Health Surveillance Agency (ANVISA) banned using CBZ in Brazil (ANVISA, 2022). According to the Agency, the toxicological re-evaluation of CBZ concluded that it has carcinogenic and reproductive toxicity potentials to humans besides inducing germ cell mutations. In addition, the Agency pointed out that it was not possible to find a safe dose threshold regarding the characteristics of mutagenicity and reproductive toxicity (ANVISA, 2022). However, the elimination of the product will be gradual since CBZ is widely used by Brazilian farmers

in the plantations of beans, rice, soybeans, and other important agricultural products (PEDUZZI, 2022).

Several studies have analyzed advanced treatment technologies for removing CECs from drinking water to mitigate the health impacts caused by the exposition. Adsorption on activated carbon is a technique that has been widely studied for the removal of microcontaminants from water. It is very efficient and has low operation and maintenance costs comparing to other advanced water treatment techniques. (SUMMERS *et al*., 2011).

Adsorption isotherms tests are essential for analyzing the performance of activated carbon in removing a certain adsorbate. Isotherms are the mathematical representation of the amount of adsorbate extracted by the adsorbent and the amount of adsorbate remaining in the liquid phase when the solution is in dynamic equilibrium at a given temperature (METCALF & EDDY, 2014).

Kinetic models have been used to evaluate and analyze experimental data to investigate the sorption mechanism and control steps such as mass transport and chemical reaction processes. The pseudo-first-order, the pseudo-second-order, and the intraparticle diffusion models are among the most studied kinetic models (HARO *et al*., 2021; HO & MCKAY, 1998).

One method that can be used to predict the performance of full-scale granular activated carbon filters is called Rapid Small-Scale Column Tests (RSSCT). According to Crittenden *et al.* (1991), RSSCT presents the following advantages: 1º) the tests take a fraction of time and costs when compared to pilot studies; 2º) they predict accurately full-scale GAC performance concerning the specific contaminant being tested, and 3º) small volumes of water are required. The similarity between RSSCT and full-large-scale column is obtained by setting conditions that result in identical adsorbate transport. RSSCT can evaluate the breakthrough curve, GAC selection, empty-bed contact time (EBCT), and saturation.

This research investigated the removal of CBZ by adsorption on Granular Activated Carbon (GAC) through isotherm, kinetics, and RSSCT tests. The experiments were performed in two different aqueous matrices: deionized water (DW) and effluent from a rapid sand filter from a drinking water treatment plant (FWTP). The study also investigated the interference of substances present in FWTP in the

adsorptive process. The interference analysis covered the comparison of the results obtained for both matrices and the statistical analysis of the data.

5.2.3. Methodology

5.2.3.1. Granular Activated Carbon

The granular activated carbon used was produced from bovines' bones by Bonechar Company, Brazil. The diameter of the grains used in the experiments was 60 x 80 mesh. Table 5.7 shows the characteristics of the activated carbon.

Table 5.7 - Bone GAC Specifications.

Properties	**Specifications**
Carbon	9 - 11%
Acid-soluble ash	< 3%
Insoluble ash	0.7
Tricalcium phosphate	70 - 76%
Calcium carbonate	7 - 9%
Calcium sulfate	0.1 – 0.2%
pH	8.5 – 9.5
Point of zero charge (PZC)	8.40
Total specific surface area (BET N^2)	57.78 m^2/ g
Carbon surface area	50 m^2/g
Iron	< 0.3%
Pore size	0.48 - 14.93 nm
Pore volume	0.0077 cm^3/g
Iodine number	93 mg/g
Humidity	< 5%
Apparent density	0.60 – 0.70 g/cm^3
Hardness	> 80
Aspect	Granulated and powdered solid
Smell	odorless

* Except Point of Zero Charge (PZC), BET specific surface area and pore volume.
Source: Bonechar (2021).

The PZC was calculated by the 11- point method by varying the pH from 2 to 12 using 1 N solutions of HCl and NaOH (GIACOMNI *et al*., 2017). Total specific surface area analysis and pore volume quantification followed the BJH/DH method in a Quantachrome NovaWin equipment using the temperature of 77.350 K, molar mass of Nitrogen of 28.013 Kg/Kmol, cross-section of 16.20 Â², net density of 0.808 g/cc and Boer's method of calculation (DE BOER *et al*., 1966). The pore sizes of the carbon ranged from 0.5 to 15 nm, with a volume of 0.0077 cm^2/g, characterizing the carbon as microporous (METCALF & EDDY, 2014). The complete characterization of the GAC was described and discussed in section of the results and discussions.

5.2.3.2. Filtrated Water from the Drinking Water Treatment Plant (FWTP)

Two aqueous matrices were used to analyze the efficiencies of CBZ adsorption on GAC. These matrices were deionized water and effluent from a rapid sand filtration in a drinking water treatment plant. It was possible to compare a medium in which there was no competition for the adsorptive sites of the GAC (DW) to another, where different compounds present in water would try to occupy the sites intended for CBZ removal.

The water used in the tests was collected from the effluent of a rapid sand filter from the Moinhos de Vento Water Treatment Plant, located in Porto Alegre, Brazil. The collected material was characterized to identify components that might have competed with CBZ for the GAC sites. The parameters analyzed were pH, color, turbidity, alkalinity, free residual chlorine, monochloramine, dichloramine, total organic carbon (TOC), conductivity, and ions. Table 5.8 shows the methodology and equipment used for each parameter.

Table 5.8 - Parameters and analytical methods used to characterize the FWTP.

Parameter	**Analytical Method**
pH	Digimed DM-22 pHmeter
Apparent Color (mg Pt-Co/L)	Pro-Analise UV-1600 Spectrophotometer
Turbidity	Hach 2100N Turbidimeter
Alkalinity	Standard Methods 2320 B
Chlorine	Standard Methods 4500Cl F
TOC	NPOC 10.m Control L Report.
Conductivity	Digimed DM-32 Conductivimeter
Ions	Eco IC Metrohm 2.925.0020

5.2.3.3. Carbendazim

The Carbendazim was acquired from Sigma-Aldrich with 97% purity. The concentrations were determined with a Shimadzu LC20A High-Performance Liquid Chromatograph (HPLC) equipped with a diode array detector (DAD, SPD-20AV) and autosampler (SIL-20A). The concentration of CBZ used in the experiments was 5 mg/L, dissolved in deionized (DW) and filtered (FWTP) waters. The experiments were performed at a pH range between 7 and 8. This concentration of CBZ was determined due to better monitoring of the adsorptive process and has already been used in similar experiments with higher concentrations (LI *et al*., 2022).

5.2.3.4. Preliminary study with pH

A preliminary study was conducted to identify the pH at which the activated carbon would present the best performance. 5 mg/L CBZ in DW and 1 g/L bone GAC

concentration were used at pHs 2, 4, 6, 8, and 10. A Student's t-Test was applied to verify whether there were significant differences between the pHs. A previous analysis using the Shapiro-Wilk test found that the results followed a normal distribution.

5.2.3.5. Adsorption isotherms

In isotherm tests, different concentrations of activated carbon (0.25, 0.50, 1.00, 2.00, and 5.00 g/L) were placed in Schott flasks containing 100 mL of water with a constant concentration of CBZ (5 mg/L). The flasks were placed in a water bath in shaker equipment at 25°C for 24 hours. After this period, aliquots were removed from the flasks, passed through filters with a pore size of 0.45 µm, and analyzed. The experiments were performed in triplicate, in DW, and FWTP.

The results were analyzed to determine which isotherm, Langmuir, Freundlich, Sips, Liu, or Redlich-Peterson (Equations 32 through 36, respectively), best fitted the experimental data. The isotherm parameters were determined through the nonlinear method using the Solver tool of Microsoft Office Excel 2019.

$$q_e = q_{max.} \frac{b \,.\, C_e}{1 + b \,.\, C_e} \quad (32)$$

$$q_e = k_f \,.\, C_e{}^{1/n} \quad (33)$$

$$q_e = \frac{q_{max}.\, K_s.\, C_e^{1/ns}}{1 + K_s.\, C_e^{1/ns}} \quad (34)$$

$$q_e = \frac{q_{max}.\, (k_g.\, C_e)^{n_L}}{1 + (k_g.\, C_e)^{n_L}} \quad (35)$$

$$q_e = \frac{k_{RP}.\, C_e}{1 + a_{RP}.\, C_e^{ß}} \quad (36)$$

Where: C_e = equilibrium concentration of CBZ in solution after adsorption (mg/L); q_e = adsorbed amount of CBZ at equilibrium (mg/g); $q_{máx}$ = maximum adsorption capacity (mg/g); b = Langmuir equilibrium adsorption constant (L/mg); k_f = Freundlich constant, [(mg/g) (L/mg)$^{1/n}$]; $1/n$ = Freundlich intensity parameter; K_s = Sips equilibrium constant (L/mg)$^{1/ns}$; n_s = Sips exponent, dimensionless; K_g = constant representing the adsorbent-adsorbate affinity (L/mg); n_L = Liu exponent, dimensionless; a_{RP} = Redlich-Peterson equilibrium constant (L/mg)^{ß}; k_{RP} = constant incorporating the maximum sorption capacity and describing the adsorbent-adsorbate affinity (L/mg); and ß = exponent of the Redlich-Peterson isotherm, dimensionless.

5.2.3.6. Kinetics

The kinetics study was conducted for 24h in the same shaker and temperature (25ºC) used in the isotherm's tests. Aliquots were collected from Scott flasks containing 100 mL of CBZ 5 mg/L solution with 1 g/L of GAC (constant concentration of adsorbent). Samples were collected at 0, 10, 20, 30, 60, 120, 120, 180, 240, 300, and 360 min. The experiments were performed in triplicate, in DW and FWTP.

The kinetics parameters were determined using the nonlinear method of Microsoft Office Excel 2019 via the Solver function. The pseudo-first-order, pseudo-second-order, and intraparticle diffusion models (Equations 37, 38, and 39, respectively) were evaluated to estimate the best fit.

$$q_t = q_e(1 - e^{-k_1 t}) \quad (37)$$

$$q_t = \frac{q_e{}^2 k_2 t}{1 + q_e k_2 t} \quad (38)$$

$$q_t = k_{di} \cdot t^{0,5} + C \quad (39)$$

Where: q_t = quantity of adsorbate removed per unit of adsorbent in time t (mg/g); q_e = quantity of adsorbate adsorbed per unit of adsorbent at equilibrium (mg/g); k_1 = first order rate constant (min^{-1}); t = contact time (min); k_2 = second-order rate constant (g/mg.min); k_{di} = intraparticle diffusion constant ($mg/g.min^{0,5}$); C = linear coefficient.

According to the intraparticle diffusion model, the linear coefficient (C) in Equation 39 is equal to zero if diffusion within the pore controls the adsorption process in the initial stages of adsorption (AHMED & THEYDAN, 2012).

5.2.3.7. Rapid Small-Scale Columns Tests (RSSCT)

Parameters from a full-scale column were used to determine those of the bench-scale column. The Empty Bed Contact Time (EBCT) for the small column was calculated using Equation 40 (CRITTENDEN *et al*., 1991; 1986).

$$EBCT_{sc} = EBCT_{lc} \cdot \left(\frac{d_{p.sc}}{d_{p.lc}}\right)^{2-x} \quad (40)$$

Where: $EBCT_{sc}$ = EBCT in the small-scale column (min); $EBCT_{lc}$ = EBCT in the large column (min); $d_{p.sc}$ = mean particle diameter of the small-scale column (mm); $d_{p.lc}$ = mean particle diameter of the large-scale column (mm); x = coefficient of dependence of particle size on intraparticle diffusivity, being 0 when diffusivity is constant (CD) and 1 when diffusivity is proportional (PD) to particle size.

Crittenden *et al*. (2012) suggest that the hydraulic loading rate (HLR) and the EBCT in adsorptive beds should be, respectively, 120 to 360 $m^3/m^2.day$ and 5 to 30 minutes. EBCT of 5 min and HLR of 120 $m^3/m^2.day$ (0.083 $m^3/m^2.min$) were adopted for the full-scale column. Applying the 5 min EBCT and the proper diameters for small and large-scale columns in Equation 40, a time of 0.72 min was obtained for the small-scale. With the HLR and EBCT values, the small-scale column height was calculated using Equation 41.

$$\mathrm{H_{sc}} = \mathrm{HLR_{sc}} \,.\, \mathrm{EBCT_{sc}} \tag{41}$$

Where: $\mathrm{H_{sc}}$ = small-scale bed height (m); $\mathrm{HLR_{sc}}$ = small-scale hydraulic loading rate, 120 $m^3/m^2.day$.

Equation 42 was used to calculate the flow rate for the small-scale adsorptive column. According to Summers, Knappe & Snoeyink (2011), for constant diffusivity (CD), the flowrates vary from 50 to 150 mL/min; for proportional diffusivity (PD), the flow rates vary from 5 to 20 mL/min.

$$\mathrm{Q_{red}} = \mathrm{HLR_{red}} \,.\, \mathrm{A_{red}} \tag{42}$$

Where: $\mathrm{Q_{red}}$ = flowrate (mL/min); and $\mathrm{A_{red}}$ circular section area of the column in small-scale (cm^2).

The internal diameter of the column used was 1.20 cm. Table 5.9 details the design parameters for RSSCT, with the corresponding values for a small and full-scale column.

Table 5.9 - RSSCT parameters and dimensions and the equivalent values for full-scale.

Parameter	Unit	Full Scale	Small-scale
GAC Granulometry	Mesh	8 x 30	60 x 80
The average diameter of the grains	mm	1.49	0.21
EBCT	Min	5	0.72
Hydraulic loading rate	$m^3/m^2.day$	120	120
	$m^3/m^2.min$	0.083	0.083
Flow rate	mL/min	-	9.42
Apparent density	g/cm^3	0.65	0.65
GAC bed volume	cm^3	-	6.82
GAC bed height	cm	-	6.03

Breakthrough time and $\mathrm{EBCT_{ls}}$ using results measured in the tests made it possible to calculate STR and CUR using Equations 43 and 44.

$$\mathrm{STR} = \frac{\mathrm{t_{breakthrough}}}{\mathrm{EBCT}_{ls} \,.\, \rho_{\mathrm{GAC}}} \tag{43}$$

$$\mathrm{CUR} = \frac{1}{\mathrm{STR}} \quad (44)$$

Where: STR = specific transfer rate (cm³/g); ρ_{GAC} = density of bone GAC, equal to 0.65 g/cm³; and CUR = carbon use rate (g/L).

Due to laboratory restrictions for night work, analyses could not be performed in this period, resuming in the morning of the following day. For this reason, there was a 12 hours gap, during which no samples were collected. The experiments lasted 28 hours, after which the saturation points were reached. For the breakthrough and saturation times, 5% and 90% of the initial CBZ concentration were considered, respectively. The experiments were performed in quadruplicate.

5.2.3.8. Statistical treatment of the data

Statistical analyses were performed to verify the result's consistency and analyze the interference in the adsorptive process of substances present in the FWTP, compared to the DW. Correlation and significance tests were performed using the software R version 4.0.4. For the correlation test, the Kendall method was applied, aiming to identify if there was a linear correlation between the applied doses of GAC and the remaining concentrations of CBZ.

The results obtained from isotherms, kinetics, and RSSCT in DW and FWTP matrices have been tested for the significance tests. Also, the results obtained for all the GAC dosages and contact times within the same aqueous matrices were analyzed using the Kruskal-Wallis method. For all significance tests, $p < 0.05$ was adopted.

The results from DW and FWTP analyses considering the same doses of GAC and contact times were compared to determine whether there were significant differences, indicating interferences of substances present in the FWTP compared to the DW. The approach encompassing the results within the same matrix was made to validate the methodology. This was also applied to confirm whether there would be a significant difference between the concentrations of CBZ and the dosages of CAG and contact times applied.

5.2.4. Results and discussion

5.2.4.1. Characterization of the activated carbon

The considerations in this topic refer to Table 5.7, which shows the GAC characterization.

The presence of calcium carbonate, calcium sulfate, and tricalcium phosphate in the GAC may favor the adsorption of organic matter. Bivalent cations such as calcium can interact with organic matter, increasing its adsorption capacity by forming complexes (SUMMERS, KNAPPE & SNOEYINK, 2011).

The bulk density value is in the same range as bituminous, lignite, and coconut shell-activated carbons (0.35 to 0.65 g/cm³) (SUMMERS, KNAPPE & SNOEYINK, 2011). Compared to the values recommended by AWWA (2005) for adsorption on granular activated carbon in water supply systems, the specific surface area value (58 m²/g) is lower than suggested (600 - 1,000 m²/g). This is also observed for the iodine number, lower than 600 to 1,100 mg/g cited by Metcalf & Eddy (2014). Although these parameters are indicators of the adsorptive capacity of activated carbon, laboratory-scale or pilot-scale experiments can best predict the performance of GAC in adsorbing specific contaminants (SUMMERS, KNAPPE & SNOEYINK, 2011).

The experiments occurred in the pH range in solution between 7 and 8, below the PZC of 8.4, a value found in previous studies for activated carbon (MIYITTAH *et al*., 2016). Thus, the carbon surface showed a slightly cationic characteristic, more prone to adsorb substances with anionic nature.

The pKa allows the estimate of the distribution of ionic (deprotonated) and non-ionic (neutral) species of a given compound. If the pH of the medium is greater than the pKa of the compound, the concentration of the anionic fraction of the chemical will be predominant. Otherwise, if the pH is lower than the pKa, the compound's neutral or possibly protonated fraction will be predominant (BARCELÓ & HENNION, 1997). The pKa of CBZ is 4.53 ± 0.07 (MAZELLIER *et al*., 2002), and the anionic form prevailed in the 7 – 8 pH range of the DW and FWTP media used in the experiments. On the other hand, the surface of GAC has a cationic characteristic (MAZELLIER *et al*., 2002). Thus, considering the configuration of the GAC and CBZ surface molecules, there may be an electrostatic attraction between the compounds, favoring adsorption.

Crittenden *et al*. (2012) state that molecules with a molar mass of around 10^2 g/mol have a particle size of less than 0.01 nm. Considering that the molar mass of CBZ is 191.19 g/mol and the porosity of GAC varies between 0.48 - 14.93 nm, it can be concluded that the CBZ molecules could access the pores of GAC.

5.2.4.2. Filtered Water Characterization

Table 5.10 shows the characterization of the water collected from the treatment plant's rapid sand filter.

Table 5.10 - Physicochemical characteristics of the filtered water from treatment plant (n=3).

Parameter	**Mean**	**Variance**	**Standard Deviation**
pH	7.6	1.6	1.3
Turbidity (uT)	0.30	<0.01	0.03
Apparent Color (uH)	<0.01	<0.01	<0.01
Free residual chlorine (mg/L)	0.08	<0.01	0.06
Monochloramine (mg/L)	0.10	<0.01	0.05
Dichloramine (mg/L)	0.20	<0.01	<0.01
Alkalinity ($mgCaCO_3$/L)	10.83	0.08	0.29
TOC (mg/L)	3.12	<0.01	<0.01
Conductivity (µS/cm)	107	<0.01	0.01
Sodium (mg/L)	5.47	1.60	2.57
Lithium (mg/L)	0.00	0.00	0.00
Ammonium (mg/L)	1.40	0.29	0.08
Potassium (mg/L)	3.86	0.36	0.13
Magnesium (mg/L)	3.38	0.13	0.02
Calcium (mg/L)	0.48	0.43	0.18
Fluoride (mg/L)	1.22	<0.01	0.01
Chloride (mg/L)	17.48	0.01	0.12
Bromide (mg/L)	0.43	<0.01	0.03
Nitrite (mg/L)	0.00	0.00	0.00
Nitrate (mg/L)	1.71	<0.01	0.01
Sulfate (mg/L)	5.33	<0.01	0.03
Phosphate (mg/L)	0.00	0.00	0.00

The measured values of turbidity, apparent color, sodium, fluoride, chloride, nitrite, nitrate, and sulfate in the filtered water complied with the requirements established by the Potability Ordinance Nº 88/2021 (BRAZIL, 2021), which states the maximum contaminant levels (MCL) in drinking water. The presence of small chlorine concentrations in filtered water is due to the inter-chlorination of decanted water practiced in the water treatment plant. According to the plant operator, the practice inhibits biofilm formation in the filters.

The Potability Ordinance does not regulate alkalinity and total organic carbon. The alkalinity concentration in filtered water is low, requiring alkalinization after water disinfection. The total organic carbon concentration indicates the presence of organic matter, which competes for the adsorption sites in the activated carbon.

Considering that the carbon surface was positively charged, the adsorption of cations in water was probably low due to electrostatic repulsion. Hence, competition for the GAC adsorptive sites may have occurred between CBZ, organic matter, free and combined residual chlorine and anions. The physical-chemical characteristics of the filtered water sample were compatible with what was expected from sand filter effluent.

5.2.4.3 pH Tests

Figure 5.6 shows the percentage removal of CBZ in GAC as a function of pH. The best performance of the GAC was in an acidic medium (pH 2 and 4) compared to neutral (6 and 8) and basic (10) mediums. The lowest CBZ removal occurred at pH 10, above the PZC (8.4). The highest removals were 92% when pH was between 2 and 4.

Figure 5.6 - CBZ removal relative to pH.

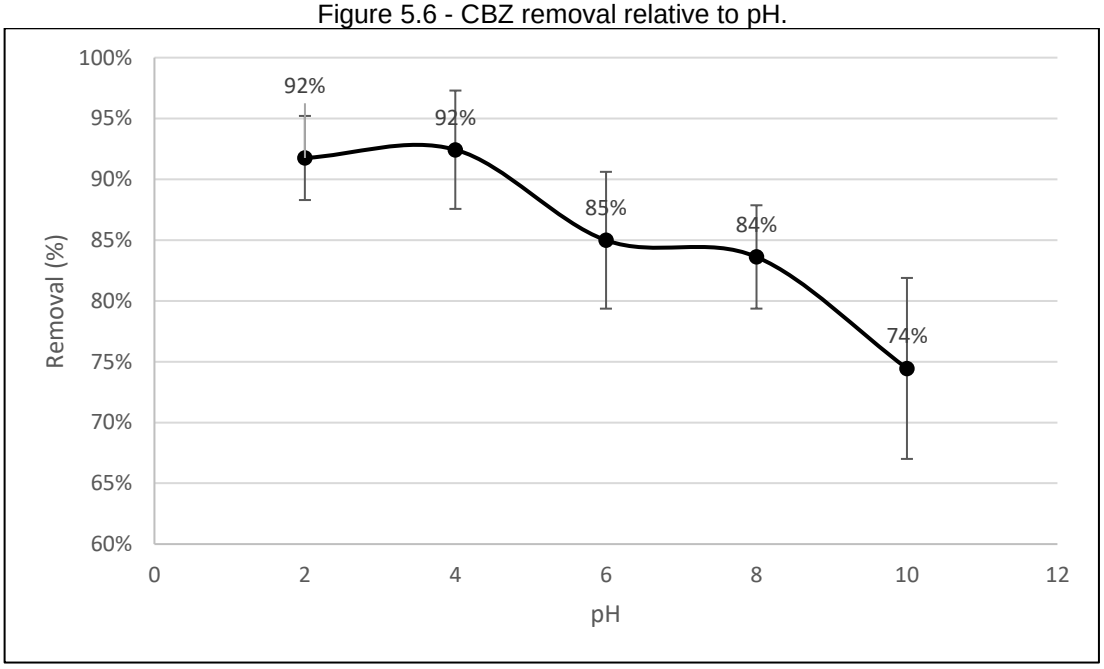

Thus, for the conditions analyzed, the best performance of CBZ removal by GAC occurred when the carbon surface presented cationic characteristics, ranging from 74 to 92%, depending on the pH of the medium.

Table 5.11 shows the results from the application of the T-test to identify significant differences between the analyzed samples. For pH 8, there was no

significant difference in results compared to pH 2, 4, and 6. Considering this result, the operational convenience, and conditions close to those measured in the FWTP (pH 7.6), the isothermal, kinetics, and RSSCT experiments were performed in the pH range between 7 and 8.

Table 5.11 - T-test result for samples at different pH.

p-valor				
pH	2	4	6	8
4	0.8308			
6	0.0142	0.0014		
8	0.1968	0.1518	0.8743	
10	0.0096	0.0066	0.0870	0.2456
legend				
> 0.05	H_0	The difference between the averages equals zero		
< 0.05	H_1	The difference between the means is not equal to zero		

5.2.4.4. Isotherms

The results of the isotherm tests are presented in Table 5.12. The correlations were high for all isotherm models in deionized water (DW), while Freundlich was the best fit for adsorption in filtered water from the treatment plant (FWTP). For comparative purposes, the Freundlich isotherm was adopted for the adsorption of CBZ in DW.

Table 5.12 – Isotherm parameters estimated from experimental results.

Model	**Parameter**	**CBZ in DW**	**CBZ in FWTP**
Freundlich	k_F $(mg/g)(L/mg)^{1/n}$	60.49	61.65
	1/n	0.67	0.52
	R^2	0.98	0.95
Langmuir	$q_{máx}$ (mg/g)	159.10	114.80
	b (L/mg)	0.49	1.57
	R^2	0.97	0.89
Sips	$q_{máx}$ (mg/g)	159.10	869,460.22
	K_s $(L/mg)^{1/ns}$	0.49	2.18×10^{-5}
	ns	1.00	1.00
	R^2	0.98	0.86
Liu	$q_{máx}$ (mg/g)	198,424.95	18,940.63
	K_g (L/mg)	3.76×10^{-6}	8.02×10^{-7}
	n_L	0.67	0.40
	R^2	0.96	0.89
Redlich-Peterson	a_{RP} $(L/mg)^{ß}$	0.00	101,352.15
	k_{RP} (L/mg)	32.72	6,797,750.23
	ß	0.00	0.62
	R^2	0.93	0.92

The high values for $q_{máx}$, a_{RP} and k_{RP} for FWTP may indicate that these isotherm models could not be the most adequate to represent the adsorption of CBZ in GAC for the analyzed conditions. These peculiarities and given the R^2 it was considered that

the Freundlich model best describe the adsorption of Carbendazim on both matrices. The mathematical models for DW and FWTP are described in Equations 45 and 46, respectively. Figure 5.7 shows the plots from the application of these equations.

$$q_e = 60.49 \text{ x } C_e^{0.67} \quad (45)$$

$$q_e = 61.65 \text{ x } C_e^{0.52} \quad (46)$$

Figure 5.7 - Freundlich isotherms for CBZ tests in DW and FWTP.

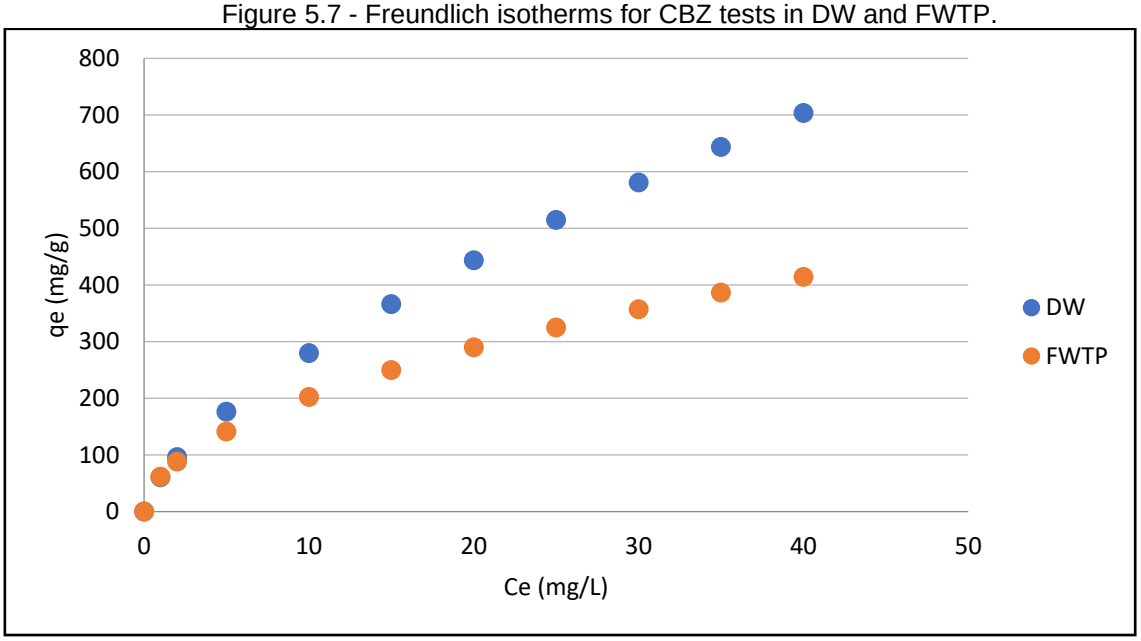

For the same range of equilibrium concentration (C_e), the amount of CBZ adsorbed per gram of GAC (q_e) is higher in deionized water than in filtered water. This was expected since no substances competed for adsorption sites in DW, contrary to FWTP. It can be seen that the adsorption capacity of the adsorbate by the GAC (q_e) increases as the equilibrium concentration increases. Although the adsorption was interfered with, the removal of CBZ was satisfactory in both matrices. Thus, bovine bone CAG was efficient in removing CBZ in both matrices.

The parameter 1/n was less than unity for both matrices analyzed, suggesting that the adsorption of CBZ on bone GAC is a favorable process (ANFAR *et al*., 2020). This agrees with previous studies conducted with CBZ on other adsorbents (JIN *et al*., 2013; LI *et al*., 2011; PASZKO 2006; RIZZI *et al*., 2020; WANG *et al*., 2020). The Freundlich isotherm assumes that a heterogeneous, multilayer formation occurs on the carbon surface. However, this aspect does not exclude monolayer adsorption, which can also occur in the process (HENDRICKS, 2011).

Table 5.13 presents the results from the correlation test applying the Kendall method, analyzing the variables "GAC dosages" and "CBZ concentrations" at equilibrium for each matrix.

Table 5.13 - Result from application of the Kendall method for the variables GAC dosages and CBZ concentrations.

Matrix	Correlation coefficient – τ
DW	-1.00
FWTP	-1.00

The results show a strong negative correlation between GAC dosages and final CBZ concentrations for both DW and FWTP. This indicates an inverse relationship between the dosage of GAC and the CBZ concentration at equilibrium, i.e., the higher the dosage of adsorbent applied, the lower the remaining CBZ concentration.

Table 5.14 shows the significance test of the difference in results for the dosages of GAC within the same aqueous matrix. The test was applied to validate the dosages, certifying whether they would show different results to justify their use for the isotherm test.

Table 5.14 - Analysis of the significance of the difference in results for different dosages of GAC within the same matrix.

Matrix	p-value
DW	5.91×10^{-15} (<0.05)
FWTP	$8.10 \times 10^{-16.}$ (<0.05)

According to these results, the adopted doses of GAC (0.25, 0.50, 1.00, 2.00, and 5 g/L) presented significant differences in the final concentrations of CBZ after 24 h for both aqueous matrices. Thus, the experimental conditions used were validated by the statistical analysis and can be replicated in other similar experiments.

Table 5.15 shows the results of significance tests comparing the results measured in both aqueous matrices for each dosage of GAC. This methodology was used to analyze the interference of substances present in filtered water from the treatment plant in the adsorptive process.

Table 5.15 - Analysis of the difference between the aqueous matrices for the same GAC dosage (p< 0.05).

GAC dosage	0.25	0.50	1.00	2.00	5.00
p-value	<0.01	<0.01	0.01	<0.01	0.03

The results show that all dosages of GAC had significant differences when comparing deionized water with filtered water. It can be inferred that the adsorption process removed different fractions of CBZ for each dosage in DW and FWTP

matrixes. As the experimental conditions were identical (contact time of 24h, temperature of 25º C, and similar dosages of GAC), this difference was due to substances present in filtered but not in deionized water. From statistics, it can be concluded that substances present in FWTP interfered in the adsorption of the fungicide, corroborating the results obtained in isotherm tests.

5.2.4.5. Kinetics

The results of the experiments investigating the adsorption kinetics are presented in Table 5.16. For CBZ in deionized water, the second-order kinetics was the best fit for the adsorption process (R^2 = 0.94). The first-order and second-order kinetics fitted well for the experiment using the FWTP matrix (R^2 = 0.99). For comparison purposes, the pseudo-second-order model was adopted for the adsorption of CBZ on FWTP. The intraparticle diffusion played an essential role in the initial stages of the adsorption process (C = 0) in FWTP but not in DW (R^2 = 0.78).

Table 5.16 - Results of the CBZ kinetics adsorption experiments using deionized water and filtered water from the treatment plant.

Model	Parameter	CBZ in DW	CBZ in FWTP
First order	K_1 (t^{-1})	0.049	0.011
	q_e (mgCBZ/gGAC)	4.157	5.231
	R^2	0.94	0.99
Second order	K_2 (t^{-1})	0.017	0.002
	q_e (mgCBZ/gGAC)	4.462	6.745
	R^2	0.98	0.99
Intraparticle diffusion	k_{dt}	0.189	0.302
	C	1.419	0.000
	R^2	0.78	0.96

Equations 47 and 48 show the kinetic models that best fitted the adsorption of Carbendazim in deionized water and the FWTP matrix, respectively. Figure 5.8 shows the graphs obtained from these equations.

$$q_t = \frac{0.34 \text{ x } t}{1 + 0.08 \text{ x } t} \quad (47)$$

$$q_t = \frac{0{,}07 \text{ x } t}{1 + 0.01 \text{ x } t} \quad (48)$$

Figure 5.8 – Pseudo-second-order adsorption kinetics of CBZ on DW and FWTP.

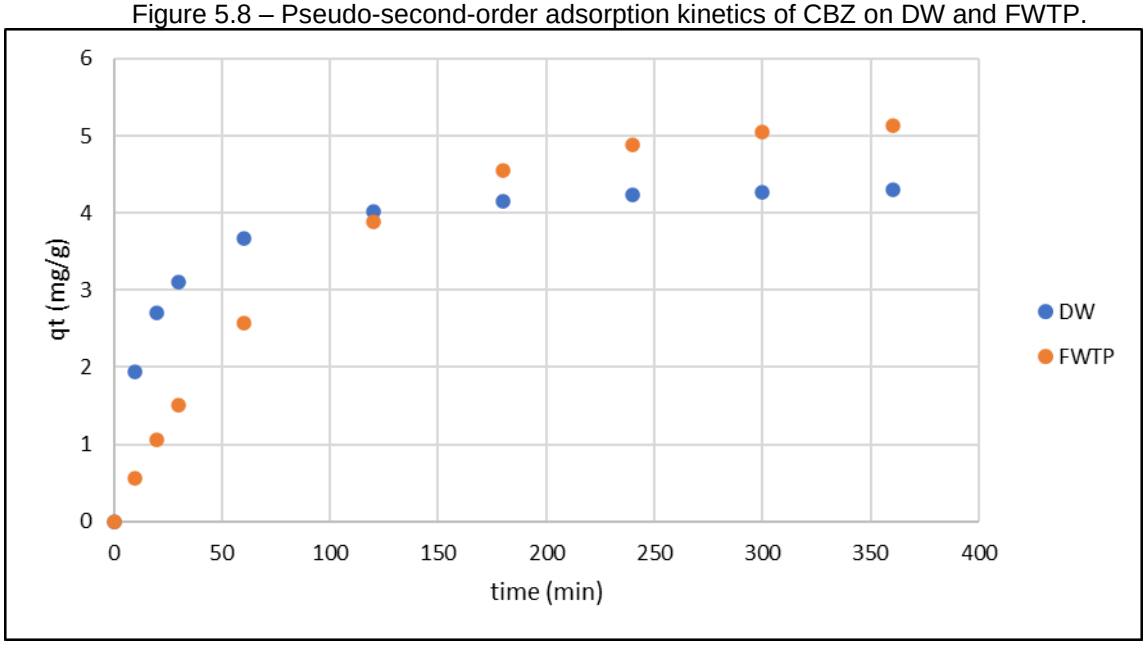

In the initial stages of the adsorptive process, the adsorption capacity of CBZ by GAC was higher on DW. However, over time the adsorption capacity of CBZ by GAC on FWTP increased and exceeded the value of q_t for DW for identical periods of the test. This may have been because the substances present in FWTP may have hindered the adsorption of CBZ, but the pores of the GAC remained available for the adsorption of the fungicide.

Hgeig, Novakovic & Mihajlovic (2019) found that the pseudo-second-order equation had the best fit for the adsorption of CBZ and herbicide Linuron on GAC. Using GAC as an adsorbent, the adsorption of the ß-blocker Atenolol was also best represented by pseudo-second-order kinetics. (HARO *et al*., 2017). Cao *et al*. (2011) found that the adsorption of the pesticide p,p'- and o,p'-Dichlorodiphenyltrichloroethane (DDT) in sediments also followed a pseudo-second-order kinetics. The same was identified for the adsorption of the insecticide Fenitrothion and the herbicide Trifluralin on organo-zeolites and activated carbon (LULE & ATALAY, 2014). The best fit of the pseudo-second-order equation for the adsorption of CBZ on DW and FWTP is similar to previous studies with the fungicide and other CEC, using activated carbon and other adsorbent types. In addition, it was observed that the pseudo-first-order equation also fitted well with the adsorption of CBZ. Other studies in the literature were not found to support the adsorption of CBZ as a pseudo-first-order kinetics process.

The intraparticle diffusion on GAC was stronger when the fungicide was diluted in FWTP when compared to DW. Besides, the deviation from the graph origin may

have occurred due to the difference in the mass transfer rate in the initial and final phases of adsorption for DW (AHMED & THEYDAN, 2012; DEL VECCHIO *et al*., 2019). The coefficient of determination for intraparticle diffusion (R^2 = 0.78) indicates that this model did not fit the adsorption of CBZ on GAC in DW as well as in FWTP (R^2 = 0.96). For DW, other interaction mechanisms must simultaneously control the adsorption process (HARO, 2019).

Applying the values of k_{di} and C from Table 5.16 to equation 39, the intraparticle diffusion model for FWTP is shown in Equation 49.

$$q_t = 0.30 \, x \, t^{0,5} \quad (49)$$

Figure 5.9 shows the relationship between the mass of CBZ adsorbed by unit mass of activated carbon and time, according to Equation 49. Two distinct steps of the adsorption of CBZ on GAC can be observed. The first step (Phase I) is related to the adsorption on the external surface of the adsorbent and represents the boundary layer effect, being linear and passing through the origin. The second region (Phase II) represents intraparticle diffusion. The phase representing the equilibrium in the adsorptive process, in which the amount adsorbed is constant (Phase III), was not observed (DEL VECCHIO *et al*., 2019; RUIZ *et al*., 2010). Hence, the phase related to intraparticle diffusion is more significant, exerting greater predominance in adsorption than the boundary layer effect (this may have occurred because the equilibrium was not reached).

Figure 5.9 - Graphic illustration of intraparticle diffusion in the adsorptive process of CBZ in GAC in filtered water.

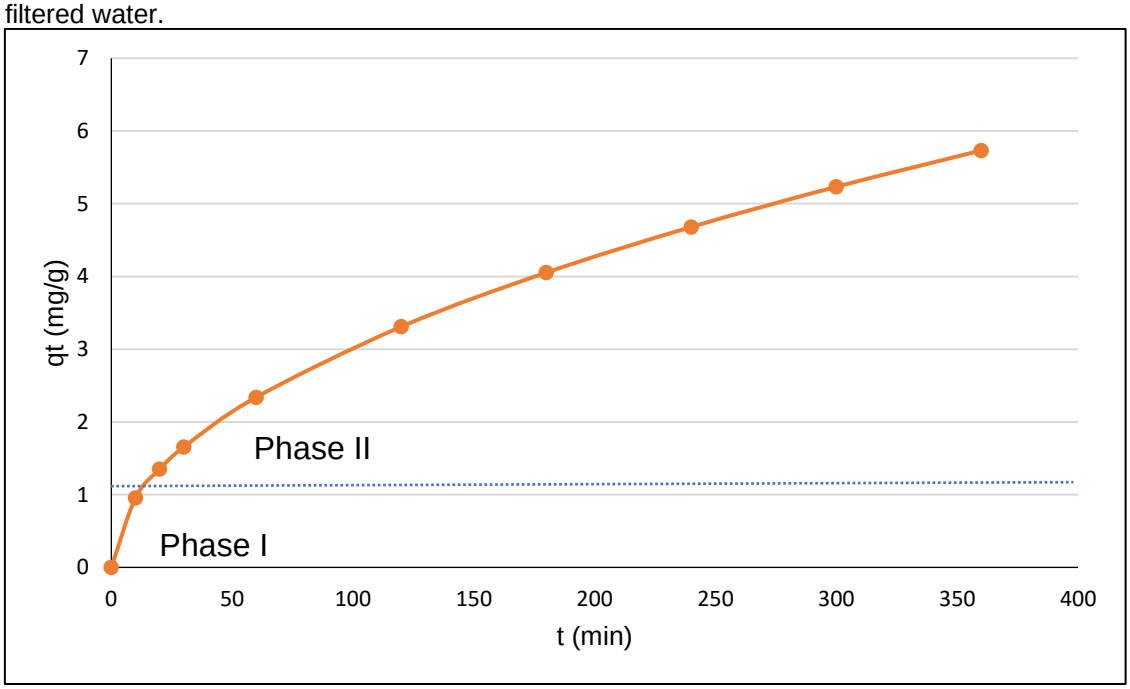

Larger GAC particles result in slower adsorption kinetics. In general, adsorption kinetics is inversely proportional to the square of the GAC particle diameter (KENNEDY *et al.,* 2015). GAC used in the experiments was microporous (Table 5.7). Thus, it is hypothesized that the carbon pores did not function as a limiting factor on the adsorption kinetics of CBZ.

A study by Hgeig, Novakovic, & Mihajlovic (2019) showed that the adsorption of CBZ on activated carbon also showed a high correlation coefficient for the fit of intraparticle diffusion. In this case, the model does not start from the origin of the initial adsorption stages. The authors concluded that adsorption on the external surface of the GAC exerted a more considerable influence in the initial stages, and intraparticle diffusion played a limiting role in adsorption. This conclusion differed from what was identified in the present study of CBZ adsorption on bone GAC.

Table 5.17 shows the results from the correlation test applying the Kendall method. It was analyzed the variables "Time" and "CBZ concentrations" for each matrix.

Table 5.17 - Result of applying the Kendall method for the variables time and CBZ concentrations.

Matrix	**Correlation coefficient – τ**
DW	-0.75
FWTP	-0.96

There is a negative correlation between the variables "time" and "CBZ concentrations". Thus, the longer the contact time, the lower the concentration of CBZ remaining in the solution for both matrices. This was already expected since previous studies used equilibrium times of 2 to 24 h for CBZ adsorption (JIN *et al*., 2013; LI *et al*., 2011; PASZKO, 2006; RIZZI *et al*., 2020; WANG *et al*., 2020). The correlation coefficient was higher in DW than in FWTP. This can be explained because in DW CBZ does not compete with other substances for adsorption.

Table 5.18 shows the results of the significance test performed for the results obtained for the contact times of CBZ with GAC within the same aqueous matrix. The approach was applied to validate the times employed, certifying whether they would show different results to justify their use for the kinetics test.

Table 5.18 - Analysis of the significance of the difference in results within the same matrix.

Matrix	**p-value**
DW	2.62×10^{-5} (<0.05)
FWTP	$1.30 \times 10^{-5.}$ (<0.05)

The p-value values showed that the contact times employed (0, 10, 20, 30, 60, 120, 180, 240, 300, and 360 min) presented significant differences in the final concentrations of CBZ for both aqueous matrices. Thus, the experimental conditions used were validated from the statistical point of view by presenting significant and distinct results. It can be replicated in other similar experiments as well as the methodology used in the isotherm study.

Table 5.19 shows the results of significance tests comparing the results obtained in the two aqueous matrices for each contact time of the CBZ with the applied dosage of GAC. This methodology was also used to analyze the interference of substances in the filtered water from the treatment plant in the adsorptive process.

Table 5.19 - Analysis of the difference between the aqueous matrices for the same GAC dosage (p< 0.05).

Time (min)	10	20	30	60	120	180	240	300	360
p-value	0.13	0.10	0.02	0.01	0.83	0.19	0.15	<0.01	<0.01

The results showed no significant differences in most of the time intervals collected. In the initial stages of adsorption, the removals of CBZ in DW and FWTP were similar (10 and 20 minutes). After 5 hours after the experiment began, the results showed a significant difference between the two tested conditions (DW and FWTP), showing the interference in adsorption.

5.2.4.6. Rapid Small-Scale Column Tests

Table 5.20 and Figure 5.10 shows the results measured in the Rapid Tests in Small-Scale Columns for each time the samples were collected.

Table 5.20 - RSSCT results for the Carbendazim (CBZ) tests in deionized (DW) and filtered water from the treatment plant (FWTP).

T (min)	DW	FWTP
	C/C0	C/C_0
0	0.00	0.00
60	0.00	0.03
120	0.01	0.05
180	0.03	0.11
240	0.02	0.10
300	0.04	0.11
360	0.05	0.13
1080	0.34	0.37
1140	0.42	0.42
1200	0.57	0.55
1260	0.67	0.65
1320	0.82	0.73
1380	0.92	0.79
1440	0.99	0.86
1500	1.00	0.95
1560	1.00	1.00
1620	1.00	1.00
1680	1.00	1.00

Figure 5.10 – RSSCT breakthrough curves of CBZ dissolved in DW and FWTP.

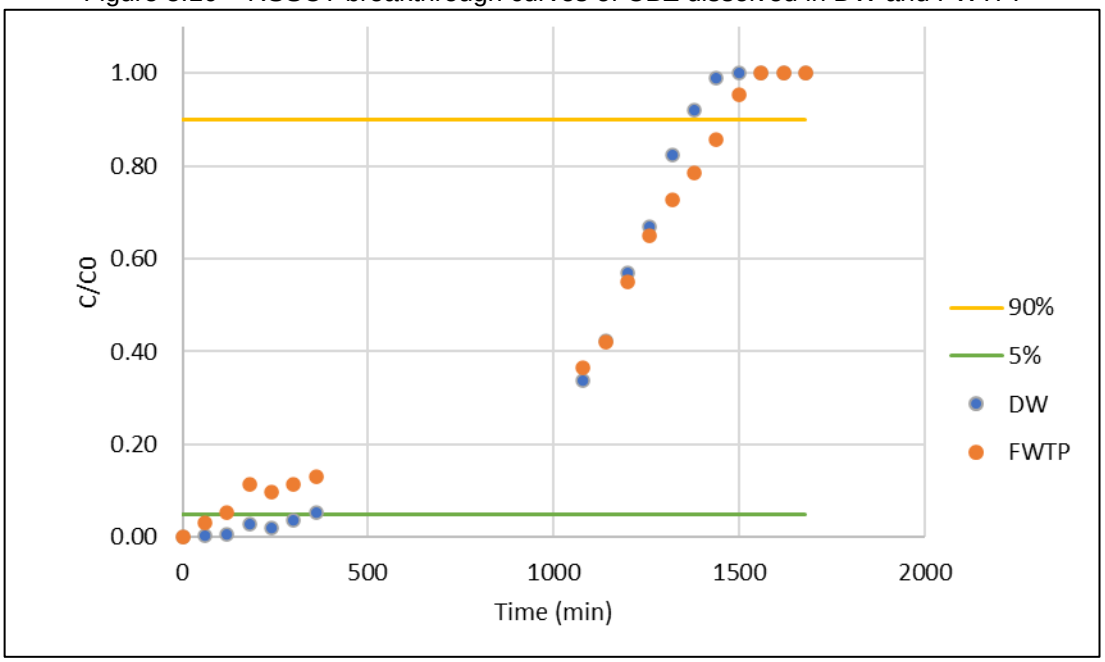

Analyzing the RSSCT results and comparing them with the kinetics data, it is observed that the breakthrough time is longer for the CBZ configuration in DW. In comparison, the saturation time is slightly longer for CBZ in FWTP (higher q_t of GAC over time, evidenced in kinetics tests). At the beginning of the adsorptive process, the adsorption capacity of CBZ by GAC was higher in the configuration with DW. However, the adsorption capacity of CBZ by GAC in FWTP water increases over time. This is evidenced in both kinetics and RSSCT tests. This particularity may be one reason for the longer time required to saturate the column of GAC in FWTP compared to the DW. There is a slight difference in adsorption velocity between the configurations analyzed, corroborated by the kinetics results.

It is possible that NOM could have sensibly improved the efficiency of GAC in removing CBZ. This is possible because some organic compounds change their fate in the presence of humic substances (CARTER & SUFFET, 1982). Such results have already been reported in previous studies with CEC in FWTP (COELHO *et al.*, 2020).

Table 5.21 summarizes the breakthrough and saturation times and shows the values of the specific transfer rates (STR) and carbon utilization rates (CUR) calculated by Equations 43 and 44. The table also shows the volumes of water treated at the breakthrough and saturation points, calculated by multiplying the flow rate (9.42 L/min) and the breakthrough and saturation times. The results were different for deionized and filtered water, indicating that the substances present in the FWTP interfered with the adsorption of CBZ in the GAC column compared to DW. This was also observed in the isotherm and adsorption kinetics tests.

Table 5.21 - Values of specific transfer and carbon utilization rates, based on the breakthrough and saturation times.

Tests	**Breakthrough time (min)**	**Treated volume at the breaking point (L)**	**Saturation time (min)**	**Treated volume at the saturation point (L)**	**STR (cm^3/g)**	**CUR (g/L)**
DW	360	3.39	1,440	13.56	110.77	9.03
FWTP	120	1.13	1,500	14.13	36.92	27.08

STR and CUR are parameters used to analyze the performance of the GAC in contaminant removal. The higher the STR values and, consequently, the lower the CUR values, the higher the efficiency of the GAC and the more economical its application in water treatment (KEMPISTY *et al*., 2022; KENNEDY *et al*., 2015). In this case, the highest GAC efficiency was in the CBZ removal in DW.

Coelho & Rozário (2019) used RSSCT to study the adsorption of 2,4-D on activated carbon. The initial concentration of 2,4-D was 7,0 mg/L, and the authors found a breakthrough time of 1,349 minutes (22 hours and 29 minutes) in ultrapure water. This value was higher than the breakthrough measured with CBZ in this study, implying higher STR and lower CUR. For this paper, the maximum 2,4-D value allowed by Brazilian legislation according to the Ministry of Health was adopted as the breaking point.

Mavaieie Jr. & Benetti (2021) used the same methodology to remove organic matter in water, measured by the total organic carbon concentration and absorbance to ultraviolet radiation at 254 nm. The column dimensions were identical to those used in this experiment. For an EBCT of 5 minutes, the breakthrough occurred at the experiment's initial stage.

Using the RSSCT method, Voltan, Dantas and Paschoalato (2016) obtained a CUR of 10.7 mg/L in removing the herbicides Diuron and Hexazinone by GAC (initial concentrations of 1.00 and 0.28 mg/L, respectively). For this paper, the maximum Diuron and Hexazinone values allowed by Brazilian legislation according to the Ministry of Health was adopted as the breaking point. Kennedy *et* al. (2015) identified CUR of 9 mg/L for the removal of 30 CEC with varying concentrations (8.10 to 2.70 mg/L) by full-scale GAC column. Although the RSSCT method has been applied to many contaminants, its specific use for CBZ removal was not found in the literature. CBZ removal by GAC, as measured in this study, was generally lower than for other contaminants, such as 2,4-D e Diuron. The resulting CUR values were in the magnitude of g/L, while in the articles reviewed, most showed CUR were in the order of mg/L.

Table 5.22 shows the results obtained from the correlation test applying the Kendall method to the measured RSSCT data, analyzing the variables "Time" and "CBZ concentrations" for each matrix.

Table 5.22 - Results from the correlation test applying the Kendall method to the variables time and CBZ concentration in the RSSCT.

Matrix	**Correlation coefficient – τ**
DW	0.80
FWTP	0.85

The values in Table 5.22 show a positive correlation between time and CBZ concentrations. This means that the more extended the RSSCT operation time, the

higher the concentration of CBZ effluent from the columns for both matrices. This fact was already expected since, over time, there was the filling of the adsorption sites of the GAC by CBZ and other solutes present in the sample for FWTP. The correlation coefficient obtained for both matrices was similar.

Table 5.23 shows the significance test for the results measured in the RSSCT at different sampling times within the same aqueous matrix. The approach was applied to validate the intervals employed, attesting whether they would show different results to justify their use for RSSCT.

Table 5.23 - Analysis of the significance of the difference in results within the same matrix.

Matrix	**p-value**
DW	6.24×10^{-8} (< <0.05)
FWTP	9.89×10^{-7} (< <0.05)

The p-values show that the time intervals used for collection (1h) presented significant differences in the effluent concentrations of CBZ for both aqueous matrices. Thus, the experimental conditions used were validated from the statistical point of view by presenting significant and distinct results with time.

Table 5.24 shows the results of significance tests comparing the concentrations measured in the two aqueous matrices for each collection time. This methodology was also used to analyze the interference of substances present in the filtered water of the FWTP in the adsorptive process.

Table 5.24 - Analysis of the difference between the aqueous matrices for the same GAC dosage ($p < 0.05$).

Time	p-value
0	-
60	0.74
120	0.04
180	0.02
240	0.15
300	0.08
360	0.08
1080	0.81
1140	0.62
1200	0.14
1260	0.05
1320	0.14
1380	0.10
1440	0.10
1500	0.10
1560	0.27
1620	0.82
1680	0.03

The results of the Kruskal-Wallis test shown in Table 5.24 indicated a statistically significant difference between the times of 120, 180, and 1680 min ($p < 0.05$). 120 min was the breaking point in the test with FWTP and the significant difference also observed in the sample that was in sequence (180 min) may indicate a change in the adsorption dynamics of CBZ on GAC in FWTP.

There was no significant difference, comparing DW and FWTP, in the times at which the breakthrough and saturation points were observed in DW (360 and 1,440 min, respectively) and the saturation point for FWTP (1,500 min). This fact shows that the dynamics of CBZ adsorption on GAC are similar at these points for the two matrices. Although saturation occurred earlier in DW than in FWTP, the difference between the matrices was insignificant. From a statistical point of view, the saturation points between the different matrices were similar. Thus, it can be considered that the column that received CBZ in DW had a better performance compared to FWTP, due to the similar saturation time and the longer time needed to reach the breaking point.

5.2.5. Conclusions

Isotherms, kinetics, and RSSCT tests showed that low concentrations of Carbendazim were achieved by adsorption in granular activated carbon made from bovine bones. The Freundlich isotherm fitted well with deionized and filtered water from the treatment plant. The model parameters changed according to the aqueous matrix, DW or FWTP. In both matrices, the Freundlich 1/n parameter indicated that the adsorption of CBZ in GAC was a favorable process. The adsorption capacity of CBZ on GAC was higher in the experiments using DW than in FWTP. This was expected since filtered water had more substances competing for the adsorptive sites of GAC. Besides the Freundlich isotherm, other models analyzed also fit the adsorption of CBZ in DW, as shown by their correlation coefficient. In filtered water, Freundlich's correlation was higher than other isotherm models.

For kinetics, it was found that the pseudo-second-order model was the best fit for the adsorption of CBZ on GAC in both matrices. The results showed that in the initial stages of the adsorptive process, the adsorption capacity of CBZ by GAC was higher in the configuration with DW. However, over time the adsorption capacity of CBZ by GAC in FWTP increased for the same experimental times. The same trend also occurred in the RSSCTs. This may have happened because the substances present in FWTP may have hindered the adsorption of CBZ, but the pores of the GAC were available for the adsorption of the fungicide. It is also possible that NOM could have sensibly improved the efficiency of CAG in removing CBZ in these experiments. The data indicated that the pore size of the GAC was not the limiting factor in the adsorption of CBZ. Intraparticle diffusion was more important in the adsorptive process occurring in FWTP than DW.

RSSCT showed that the time required to reach the breakthrough in DW was longer than in the FWTP matrix. However, the times to column saturation for DW and FWTP were similar. From statistics analysis, there was no significant difference between the saturation points for the RSSCT experiments in DW and FWTP.

The adsorption of CBZ diluted in FWTP showed that most parameters differed from the same data generated in the experiments when DW was used, applying the same experimental conditions. The substances in FWTP interfered with the adsorptive process. However, this interference did not compromise the adsorption of the fungicide on granular activated carbon.

The results of the study contributed to a better understanding of the dynamics of CBZ adsorption on GAC in two specific media, DW and FWTP. It showed that activated carbon can remove CBZ from contaminated water, making it safer for consumption.

5.3. ADSORPTION OF THE FUNGICIDE CARBENDAZIM ON ACTIVATED CARBON: ANALYSIS OF ISOTHERMS, KINETICS, RAPID SMALL-SCALE COLUMN TESTS AND IMPACTS OF THE ORGANIC MATTER

Highlights

- Bovine bone GAC removed Carbendazim in both aqueous matrices.
- Freundlich isotherm and pseudo-second-order equation fitted better the adsorption of CBZ on both matrices.
- CBZ breakthrough was achieved earlier in DWNOM, while column saturation occurred at similar times in both matrices.
- NOM interfered in CBZ adsorption but did not compromise the fungicide removal.

Graphical Abstract

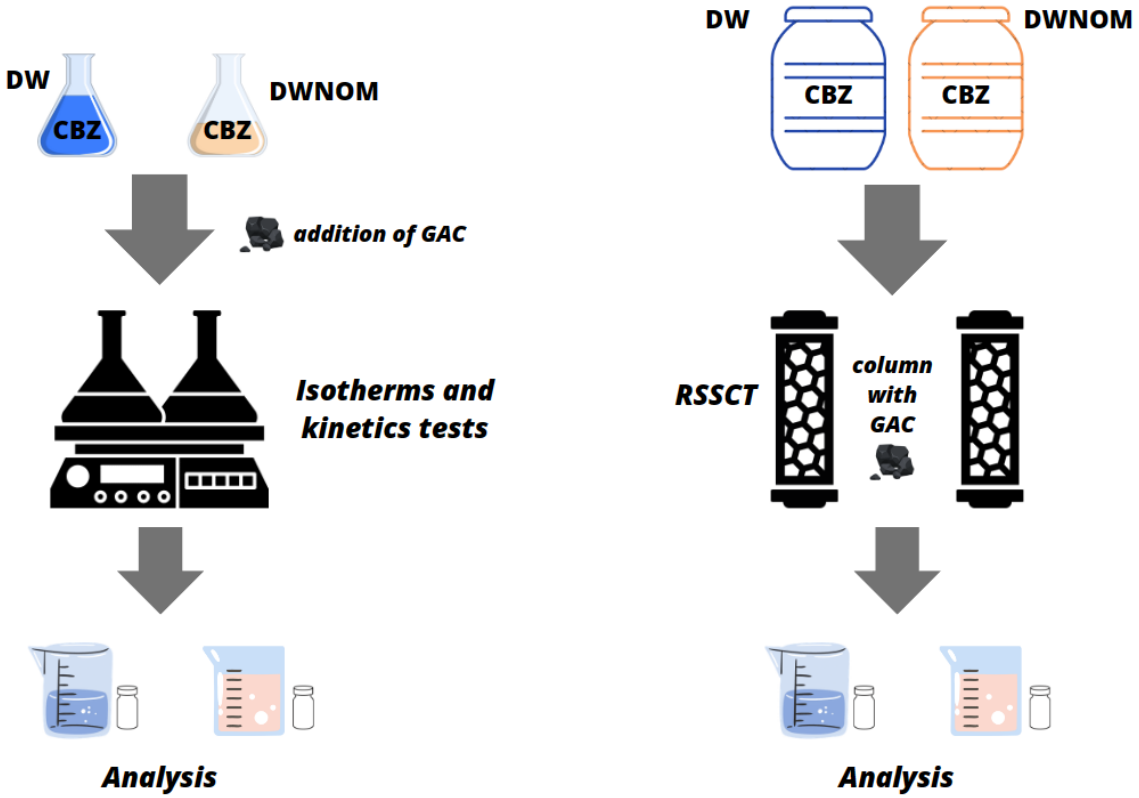

5.3.1. Abstract

The adsorption of the fungicide Carbendazim (CBZ) on granular activated carbon (GAC) made from bovine bone was investigated in deionized water (DW) and deionized water with the addition of natural organic matter (DWNOM). The study included tests of isotherms, kinetics, and Rapid Small-Scale Column Tests (RSSCT). Statistical methods were applied, and the measured parameters were compared to verify the interference of NOM in adsorption. The Freundlich model represented better the adsorption of the fungicide in both matrices, although other evaluated models also adjusted the data. For the kinetic study, all the evaluated models fitted well the CBZ adsorption in DWNOM, while the pseudo-second-order model fitted better in DW. The isotherm and kinetic studies showed the interference of NOM in the adsorption of CBZ through changes in the parameters of the applied models. In the RSSCT, the breakthrough time was faster in DWNOM than in DW. Different results were measured for saturation times, Specific Transfer Rate (STR), and Carbon Utilization Rate (CUR). Nevertheless, the CBZ concentrations of both matrices were considered statistically similar for most contact times. In the fixed bed experiments, the organic matter did not cause significant changes in the adsorption of CBZ in GAC. The presence of organic matter, under the conditions analyzed, may have improved the efficiency of GAC in adsorbing CBZ in isotherm, kinetic and RSSCT tests. The study showed that the impact of fouling was negligible under the applied conditions.

Keywords: Carbendazim, natural organic matter, granular activated carbon adsorption, isotherms, adsorption kinetics, rapid small-scale column tests.

5.3.2. Introduction

Contaminants of emerging concern (CEC) are chemical compounds that can affect human health and the environment. They are present at low concentrations in water bodies, sanitary sewage, and sometimes in treated water for human consumption (WRMA, 2019). CECs are released into the environment due to anthropic activities. One of these compounds is pesticides, substances that control pests considered harmful to crops and disease vectors (KÜMMERER, 2011). The presence of these compounds in the environment has a common origin, mainly agricultural activities. They reach water bodies after being dissolved or adsorbed to soil particles and transported by catchment runoff to surface waters or infiltration to groundwater (NOVOTNY, 2002; SELLAOUI *et al*., 2023).

Carbendazim (CBZ), a pesticide from the benzimidazole group (RAMA *et al*., 2014), is one of Brazil's most widely used pesticides. The Brazilian National Health Surveillance Agency (ANVISA) has banned this compound (ANVISA, 2022). However, its elimination is expected to be gradual since Brazilian farmers widely use CBZ in the plantations of beans, rice, soybeans, and other important agricultural products (PEDUZZI, 2022). Figure 5.11 shows the molecular structure of CBZ.

Figure 5.11 - Chemical structure of Carbendazim.

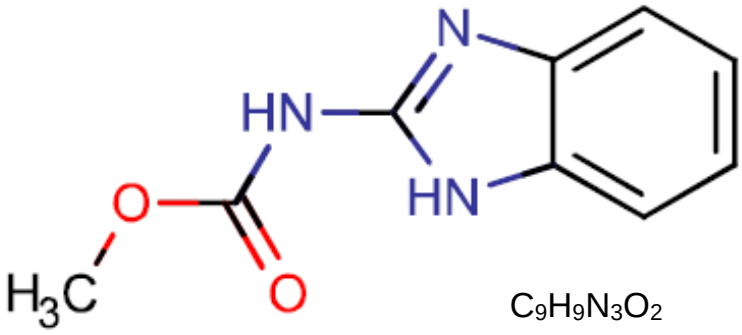

Source: Chemicalize (2021).

The toxicological re-evaluation conducted by ANVISA between 2020 and 2022 concluded that the fungicide has carcinogenic potential, induces germ cell mutations, and can cause reproductive toxicity in humans. The agency pointed out that it was not possible to find a safe dose threshold to humans for mutagenicity and reproductive toxicity characteristics (ANVISA, 2022). Carbendazim is on the Norman list of emerging substances with sufficient evidence of risk, requiring the adoption of mitigating measures (DULIO *et al*., 2016).

Several studies evaluated advanced water treatment technologies for removing and controlling health and environmentally harmful CEC, such as CBZ. The adsorption process has been used for several years to produce drinking water and treat domestic wastewater and industrial effluents. Activated carbon is the main adsorbent used for this purpose, both pulverized and granular, the latter being used in fixed beds. Dynamic adsorption (which occurs in fixed beds) can be employed in the removal of natural organic matter and CEC, with many studies proving its good performance in reducing these compounds in water (DOMERGUE *et al*., 2022; SELLAOUI *et al*., 2023). Several methodologies are employed in analyzing the adsorptive process, such as isotherms

and adsorption kinetics. In fixed-bed studies, Rapid Small Scale Column Tests (RSSCT) are often used (CRITTENDEN *et al*., 2012).

The adsorption isotherms are essential to evaluate activated carbon's performance in removing a specific adsorbate. They mathematically represent the relationship between the amount of adsorbate extracted by the adsorbent and the amount of adsorbate remaining in the liquid phase when the solution is in equilibrium at a given temperature (PICCIN *et al*., 2017). Kinetic models have been used to analyze experimental data to investigate adsorption mechanism and rate. The most studied models include the pseudo-first-order, the pseudo-second-order and the intraparticle diffusion models (HARO *et al*., 2021; HO & MCKAY, 1998).

RSSCT is one of the most widely used methods for estimating the performance of an activated carbon fixed bed column. This methodology involves the determination of breakthrough curves and other operating parameters from small-scale tests. Fixed-bed-based mass transfer models are applied to evaluate the performance of granular activated carbon (GAC) at full scale from RSSCT (CRITTENDEN *et al*., 1991). The shape and size of the breakthrough curve depend on several parameters, including adsorption rate, temperature, flow rate, bed length, contaminant concentration, presence of organic matter, and pH (DOMERGUE *et al*., 2022).

Under natural conditions and in treatment plants, natural organic matter (NOM) can be present in different concentrations. NOM is a complex mixture of organic compounds such as fulvic and humic acids, hydrophilic acids, and specific compounds such as carbohydrates and proteins, all of natural origin (SUMMERS *et al.*, 2011). Humic acids are the main constituents of NOM in natural waters. They are rich in aromatic carbon, phenolic structures and conjugated double bonds (Figure 5.12), with molecular weight ranging from 500 to more than 10,000 (SILLANPÄÄ, 2015; DUAN & GREGORY, 2003; THURMAN *et al*., 1982).

Figure 5.12 - Hypothetical molecular structure of humic acids.

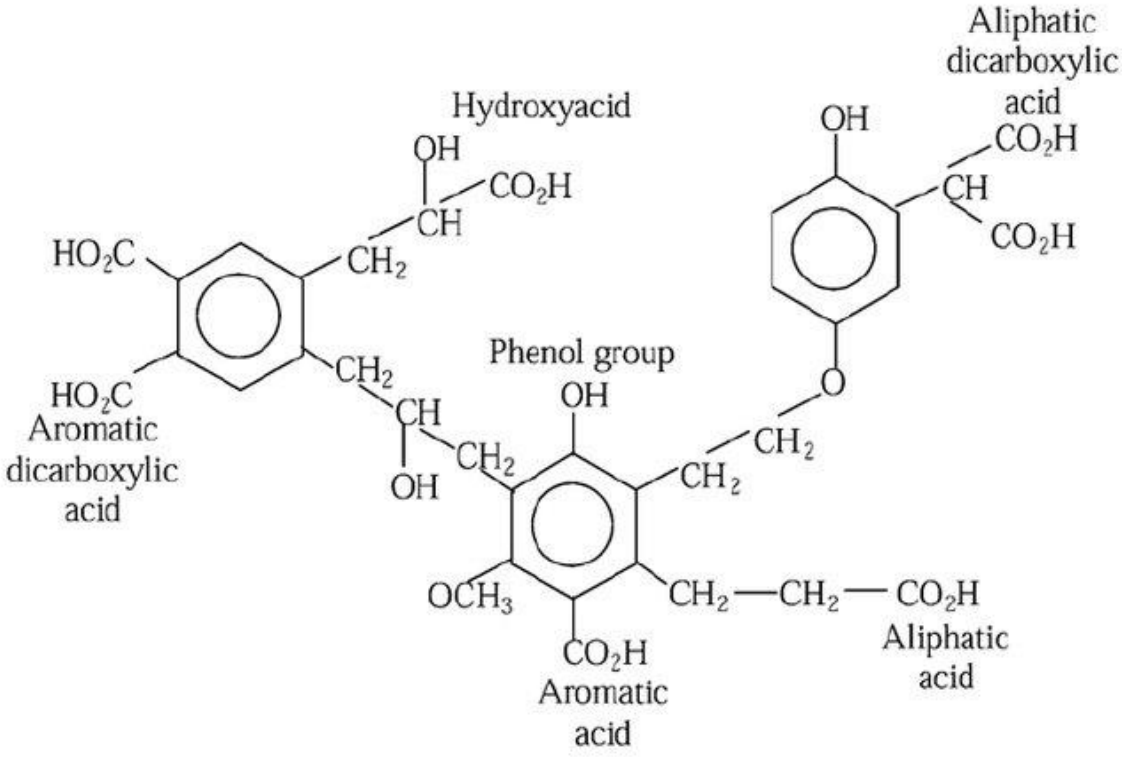

Source: Duan & Gregory (2003)

The study of the impact of natural organic matter on adsorption is of fundamental importance since, in most cases, it reduces the adsorption capacity of activated carbon and its performance in removing CEC and other compounds (DOMERGUE *et al*., 2022). This reduction in performance is due to its ability to compete for the adsorptive sites or pore blockage of the GAC (ERSAN *et al*., 2016). Therefore, the presence of NOM in the solution can affect activated carbon's performance in removing an adsorbate of interest.

This research investigated the removal of Carbendazim by adsorption on granular activated carbon through isotherms, adsorption kinetics, and RSSCT tests. The experiments were performed in two aqueous matrices, deionized water (DW) and deionized water solution with natural organic matter (DWNOM). Possible interference of NOM in the adsorption was investigated by comparing the results obtained in both matrices for each method tested (isotherms, kinetics, and RSSCT) and through statistical data analysis.

5.3.3. Methodology

5.3.3.1. Activated Carbon

Granular Activated Carbon (GAC) produced from bovine bones by the Bonechar Company was used in the experiments. Grain and pore sizes were, respectively, 60 x 80 mesh and 0.48 to 14.93 nm. Because of its pore size, it is characterized as strictly microporous (METCALF & EDDY, 2014). Table 5.25 presents the specifications of activated carbon according to company information (Bonechar, 2021). However, the point of zero charge (PZC), total specific surface area (BET), and pore volume values were determined in the laboratory.

The PZC was calculated by the 11 point method by varying the pH from 2 to 12 using 1 N solutions of HCl and NaOH (GIACOMNI *et al*., 2017). Total specific surface area analysis and pore volume quantification followed the BJH/DH method in a Quantachrome NovaWin equipment using the temperature of 77.350 K, molar mass of Nitrogen of 28.013 Kg/Kmol, cross-section of 16.20 Â², net density of 0.808 g/cc and Boer's method of calculation (DE BOER *et al*., 1966).

Table 5.25 - Bone GAC specifications provided by the manufacturer*. (Bonechar, 2021).

Properties	**Specifications**
Carbon	9 - 11%
Acid-soluble ash	< 3%
Insoluble ash	0.7
Tricalcium phosphate	70 - 76%
Calcium carbonate	7 - 9%
Calcium sulfate	0.1 – 0.2%
pH	8.5 – 9.5
Point of zero charge (PZC)	8.40
Total specific surface area (BET N^2)	57.78 m^2/ g
Carbon surface area	50 m^2/g
Iron	< 0.3%
Pore size	0.48 - 14.93 nm
Pore volume	0.0077 cm^3/g
Iodine number	93 mg/g
Humidity	< 5%
Apparent density	0.60 – 0.70 g/cm^3
Hardness	> 80
Aspect	Granulated and powdered solid
Smell	odorless

* Except Point of Zero Charge (PZC), BET specific surface area and pore volume

5.3.3.2. Solution with natural organic matter

To prepare the solution containing NOM, sodium salt of humic acid from Sigma-Aldrich was dissolved in deionized water to obtain a concentration of 5 mg/L organic matter at pH 7. This concentration range has been previously used in experiments with RSSCT in studies with other pesticides (PLATTNER *et al*., 2018). Table 5.26 presents the specifications of humic acid according to company information (SIGMA-ALDRICH, 2023).

Table 5.26 - Humic acid specifications.

Appearance	Form: flakes; Color: black, to, brown
Odor	odorless
pH	No data available
Melting point/freezing point	Melting point/range: > 300 °C
Initial boiling point and boiling range	> 640 °C at ca.1.013 hPa
Flammability (solid, gas)	The product is not flammable
Relative density	1,52 at 20 °C
Water solubility	369 g/l at 20 °C - Regulation (EC)
Partition coefficient: n-octanol/water	log Pow: ca.-2,08 at 23 °C - Bioaccumulation is not expected
Autoignition temperature	> 400 °C at 1.013 hPa

Source: Sigma-Aldrich (2023).

The NOM was quantified by Total Organic Carbon (TOC) analyses performed on a Shimadzu TOC-LCPH analyzer equipped with an automatic sample injector. The analyses were performed by thermal catalytic oxidation at 680°C on platinum-coated alumina beads with a continuous supply of oxygen flow. The non-purgeable organic carbon (NPOC) method was used, and all procedures followed the standard equipment manual.

5.3.3.3. Carbendazim

Carbendazim was purchased from Sigma-Aldrich, with a purity of 97%. The CBZ was initially dissolved in an acidic medium (pH between 2.7 and 3.0) with 1 N H_2SO_4 to accelerate the compound's dissolution. Afterwards, the pH of the solution was raised to a range between 7 and 8 by adding 1 N NaOH. The experiments were carried out in this pH range. For the analysis of CBZ, a Shimadzu LC20A High-Performance Liquid Chromatograph (CLAE - HPLC) equipped with a diode array detector (DAD, SPD-20AV) and autosampler (SIL-20A) was used. The concentration of CBZ used in the experiments was 5 mg/L, dissolved in deionized water (DW) and water containing organic matter (DWNOM). This concentration of CBZ was used due to better

monitoring of the adsorptive process and had already been used in similar experiments with higher concentrations (LI *et al*., 2022).

5.3.3.4. pH Test

Before the tests with natural organic matter, a study was conducted to identify the pH at which the activated carbon would perform best. This was done using 5 mg/L of CBZ in deionized water (DW) and a concentration of 1 g/L of bone GAC at pHs of 2, 4, 6, 8, and 10. To check if there was a significant difference between the pHs, the t-Student test was applied. An analysis using the Shapiro-Wilk test found that the results of this approach had a normal distribution. The test indicated that the performance of the GAC in CBZ removal at pH 8 did not differ significantly from that of the acidic medium. Therefore, all experiments were performed in the pH range between 7 and 8.

5.3.3.5. Isotherms

In the isotherm tests, variable concentrations of activated carbon (0.25; 0.50; 1.00; 2.00; and 5.00 g/L) were placed in Schott flasks containing 100 mL of water with a constant concentration of CBZ (5 mg/L). The flasks were placed in a water bath in a shaker equipment at 25º C for 24 hours. After this period, aliquots were removed from the flasks, separated on filters with size openings of 0.45 µm, and analyzed. The experiments were performed in triplicate in DW and DWNOM.

The results were analyzed to determine which isotherm, Langmuir, Freundlich, Sips, or Redlich-Peterson best fitted the experimental data (Equations 50 through 53). The parameters of the isotherms were determined using the nonlinear method with the Solver tool in Excel 2019.

$$q_e = q_{max.} \frac{b\,.\,C_e}{1 + b\,.\,C_e} \quad (50)$$

$$q_e = k_f\,.\,C_e^{\,1/n} \quad (51)$$

$$q_e = \frac{q_{max}.K_s.C_e^{\,1/ns}}{1 + K_s.C_e^{\,1/ns}} \quad (52)$$

$$q_e = \frac{k_{RP}.C_e}{1 + a_{RP}.C_e^{ß}} \quad (53)$$

Where: C_e = equilibrium concentration of CBZ in solution after adsorption (mg/L); q_e = adsorbed amount of CBZ at equilibrium (mg/g); $q_{máx}$ = maximum adsorption capacity

(mg/g); b = Langmuir equilibrium adsorption constant (L/mg); k_f = Freundlich constant, [(mg/g) (L/mg)$^{1/n}$]; $1/n$ = Freundlich intensity parameter; K_s = Sips equilibrium constant (L/mg)$^{1/ns}$; n_s = Sips exponent, dimensionless; a_{RP} = Redlich-Peterson equilibrium constant (L/mg)^{ß}; k_{RP} = constant incorporating the maximum sorption capacity and describing the adsorbent-adsorbate affinity (L/mg); and ß = exponent of the Redlich-Peterson isotherm, dimensionless.

5.3.3.6. Kinetics

The kinetics assays used a shaker with constant temperature of 25°C and pH between 7 and 8. Samples were collected in triplicate from Schott flasks containing 100 mL of solution with constant concentration of 1 g/L GAC and 5 mg/L CBZ. The assays were performed in DW and DWNOM, with sample collection at regular times of 0, 10, 20, 30, 60, 120, 180, 240, 300, and 360 minutes.

The kinetic parameters were calculated using the nonlinear method with Excel's Solver function. The pseudo-first-order, pseudo-second-order, and the intraparticle diffusion models (Equations 54 to 56, respectively) were tested. The intraparticle diffusion model considers that the linear coefficient C equals to zero if diffusion within the pore controls adsorption in the initial adsorption stages (HARO, 2017; ALLEN, MCKAY and KHADER, 1989).

$$q_t = q_e(1 - e^{-k_1 t}) \quad (54)$$

$$q_t = \frac{q_e{}^2 k_2 t}{1 + q_e k_2 t} \quad (55)$$

$$q_t = k_{di} \cdot t^{0,5} + C \quad (56)$$

Where: q_t = quantity of adsorbate removed per unit of adsorbent in time t (mg/g); q_e = quantity of adsorbate adsorbed per unit of adsorbent at equilibrium (mg/g); k_1 = first order rate constant (min^{-1}); t = contact time (min); k_2 = second-order rate constant (g/mg.min); k_{di} = intraparticle diffusion constant (mg/g.min^{0,5}).

5.3.3.7. Rapid Small Scale Column Tests

Standards from a full-scale column were applied to determine the parameters used in the RSSCT column, as described in Table 5.27. The Empty Bed Contact Time (EBCT) for the reduced scale was calculated using Equation 57.

$$\mathrm{EBCT}_{sc} = \mathrm{EBCT}_{lc} \cdot \left(\frac{\mathrm{d_{p.sc}}}{\mathrm{d_{p.lc}}}\right)^{2-\mathrm{x}} \quad (57)$$

Where: $\mathrm{EBCT_{sc}}$ = EBCT in the small-scale column (min); $\mathrm{EBCT_{lc}}$ = EBCT in the large column (min); $\mathrm{d_{p.sc}}$ = mean particle diameter of the small-scale column (mm); $\mathrm{d_{p.lc}}$ = mean particle diameter of the large-scale column (mm); x = coefficient of dependence of particle size on intraparticle diffusivity, being 0 when diffusivity is constant (CD) and 1 when diffusivity is proportional (PD) to particle size.

Crittenden *et al*. (2012) suggest using the hydraulic loading rate (HLR) in adsorbent beds in the range 120 to 360 m^3/m^2.day (0.083 m^3/m^2.min), and the EBCT between 5 and 30 minutes. The design parameters considered an EBCT of 5 min and HLR of 120 m^3/m^2.day for a real scale column. Applying this value in Equation 57, a time of 0.72 min was obtained for the reduced scale.

With the HLR and EBCT values, the reduced scale column height could be calculated using Equation 58.

$$\mathrm{H_{sc}} = \mathrm{HLR_{sc}} \cdot \mathrm{EBCT_{sc}} \quad (58)$$

Where: $\mathrm{H_{sc}}$ = small-scale bed height (m); $\mathrm{HLR_{sc}}$ = small-scale hydraulic loading rate, 120 m^3/m^2.day.

The flowrate of the reduced-scale adsorptive system was calculated using Equation 59. According to Summers *et al*. (2011), the flowrates for constant diffusivity (CD) and proportional diffusivity (PD) range from 50 to 150 mL/min and 5 to 20 mL/min, respectively. The operating flowrate of the system, 9.42 mL/min, characterized proportional diffusivity (X = 1 in Equation 57).

$$\mathrm{Q_{red}} = \mathrm{TAS_{red}} \cdot \mathrm{A_{red}} \quad (59)$$

Where: Q_{sc} = flowrate (mL/min); and A_{sc} = circular section area of the small-scale column (cm^2).

The internal diameter of the column used was 1.20 cm. Table 5.27 details the parameters designed for the RSSCT and the values corresponding to a full-scale column.

Table 5.27- RSSCT parameters and dimensions with the equivalent values for full-scale.

Parameter	Unit	Full Scale	Small-scale
GAC Granulometry	Mesh	8 x 30	60 x 80
The average diameter of the grains	mm	1.49	0.21
EBCT	Min	5	0.72
Hydraulic loading rate	$m^3/m^2.day$	120	120
	$m^3/m^2.h$	5.0	5.0
Flowrate	mL/min	-	9.42
Apparent density	g/cm^3	0.65	0.65
GAC bed volume	cm^3	-	6.82
GAC bed height	cm	-	6.03

From the results obtained in the RSSCT, it was possible to analyze the specific transfer rates (STR) and carbon utilization rates (CUR) through Equations 60 and 61.

$$\mathrm{STR} = \frac{\mathrm{t_{breakthrough}}}{\mathrm{EBCT}_{ls} \cdot \rho_{\mathrm{GAC}}} \tag{60}$$

$$\mathrm{CUR} = \frac{1}{\mathrm{STR}} \tag{61}$$

Where: STR = specific transfer rate (cm^3/g); ρ_{GAC} = density of bone GAC, equal to 0.65 g/cm^3; and CUR = carbon use rate (g/L).

The reduction in adsorption capacity caused by organic matter is known as fouling (CORWIN & SUMMERS, 2010). To evaluate this impact on the adsorption of CBZ on GAC, the Fouling Index equation (Equation 62) was used to compare the breakthrough curves of the experiments performed on a reduced scale (CORWIN & SUMMERS, 2010; KENNEDY *et al*., 2017).

$$FI = SF^{\gamma} = \left(\frac{\mathrm{d_{p.lc}}}{\mathrm{d_{p.sc}}}\right)^{\gamma} \tag{62}$$

Where FI = Fouling index; SF = Scaling factor; and γ = Fouling factor. As the comparison was performed between the reduced scales for both matrices, the ratio between the GAC diameters equals 1 ($\frac{\mathrm{d_{p.lc}}}{\mathrm{d_{p.sc}}}$ =1), as the same diameter range was used (60 x 80 mesh). The Fouling Index was calculated by nonlinear analysis using the Excel's Solver tool. Fixing $\frac{\mathrm{d_{p.lc}}}{\mathrm{d_{p.sc}}}$ =1, the value of γ was varied until a coefficient with the highest R^2 was found. Thus, the value of FI would be known, and the impact of fouling measured.

Due to the limitations of access and permanence in the laboratory at night, the analyses were not performed during this period. The experiments lasted 28 hours

because the saturation points had already been identified by the end of this period. To determine the breakthrough and saturation times, 5% and 90% of the initial CBZ concentration were considered. The experiments were performed in quadruplicate.

5.3.3.8. Statistical Treatment

Statistical analyses were performed to verify the interference of DWNOM in the adsorptive process compared to DW. The analysis included correlation, determination, and significance tests using R software version 4.0.4. Kendall's method was applied to identify the correlation between the applied GAC dosages and the remaining CBZ concentrations. For the significance tests in the RSSCTs, the Kruskal-Wallis method ($p < 0.05$) was used to compare the results for the different contact times in the DW and DWNOM matrices.

5.3.4. Results and discussion

5.3.4.1. Activated carbon characterization

The considerations in this topic refer to Table 5.25, which shows the GAC characterization.

The presence of calcium carbonate, calcium sulfate, and tricalcium phosphate in the GAC may be a factor favoring the adsorption of organic matter and consequently reducing the adsorption of CBZ. Bivalent cations such as calcium can interact with organic matter, increasing its adsorption capacity by forming complexes (SUMMERS, KNAPPE and SNOEYINK, 2011).

The density value is within the usual range for activated carbons manufactured from lignite and coconut shell (0.35 to 0.65 g/cm³) (SUMMERS, KNAPPE, and SNOEYINK, 2011). The specific surface area value, 57.78 m²/g is lower than that recommended by AWWA (2005) for adsorption by granular activated carbon in water supply systems (650 - 1,000 m²/g). This is also observed for the iodine number, whose recommended range is 600 to 1,100 mg/g (METCALF & EDDY, 2014). Although these parameters are indicators of the adsorptive capacity of activated carbon, the performance of GAC is generally best evaluated through isotherm and column experiments at the laboratory scale or pilot scale. This is particularly true for the removal of CEC in drinking water (SUMMERS, KNAPPE and SNOEYINK, 2011).

The experiments occurred in pH between 7 and 8, below the PZC value of 8.4 (Table 5.25). This pH value for PZC was also found in other studies for activated carbon (MIYITTAH *et al.*, 2016). Thus, the carbon surface showed slightly cationic characteristics, more prone to adsorb substances with anionic characteristics, such as organic matter.

The anionic form of CBZ predominated in the assays, considering its pKa of 4.53 ± 0.07 and pH of the medium between 7 and 8 (MAZELLIER *et al*., 2002). Thus, considering the configuration of the surface molecules of GAC and CBZ, there may be an electrostatic attraction between the compounds, favoring adsorption.

Crittenden *et al*. (2012) state that molecules with a molar mass of around 10^2 g/mol have a particle size of less than 0.01 nm. Considering that the molar mass of CBZ is 191.19 g/mol and the porosity of GAC varies between 0.48 - 14.93 nm, it can be concluded that the CBZ molecules could access the GAC pores.

Annex1 shows pictures of the GAC generated with Scanning Electron Microscopy, highlighting the grains and the GAC pores.

5.3.4.2. Isotherms

The results of the isotherm tests are presented in Figure 5.13 and Table 5.28. All the tested models fit the adsorption of CBZ in both DW and DWNOM. In deionized water, the Freundlich and Sips isotherms had R^2 of 0.9770 and 0.9759, respectively, slightly higher than Langmuir and Redlich-Peterson. For deionized water with organic matter, all models had the same R^2. Figure 5.13 shows that the presence of organic matter influenced the equilibrium concentrations for each mass of GAC used.

Figure 5.13 - Results of the tests for the DW and DWNOM experiments (means ± standard deviation, n=3).

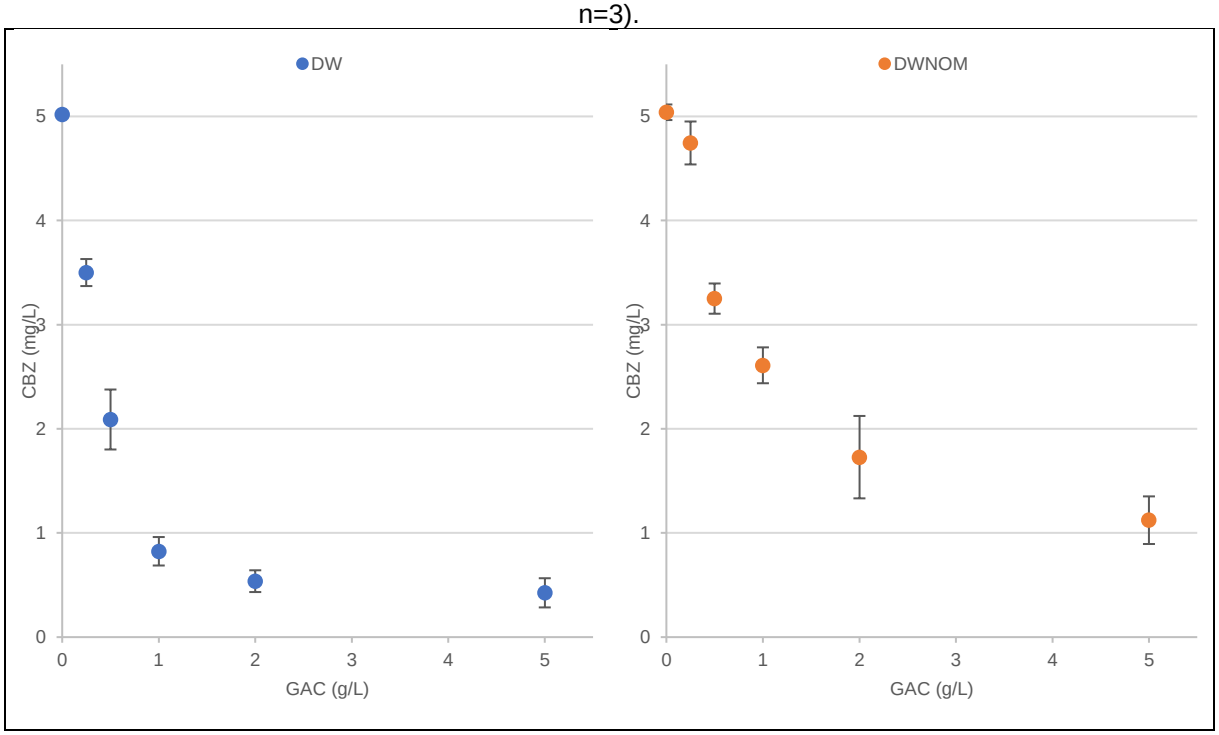

Table 5.28 - Parameter values and determination coefficients for the Freundlich, Langmuir, Sips, and Redlich-Peterson isotherms.

Model	Parameter	DW	DWNOM
Freundlich	K_f (mg/g)(L/mg)$^{1/n}$	60.49	17.09
	1/n	0.67	1.09
	R^2	0.98	0.91
Langmuir	$q_{máx}$ (mg/g)	159.10	564,423.77
	b (L/mg)	0.49	0.00
	R^2	0.97	0.91
Sips	$q_{máx}$ (mg/g)	159.10	869,460.22
	K_s (L/mg)$^{1/ns}$	0.49	2.18 x 10^{-5}
	ns	1.00	1.00
	R^2	0.98	0.91
Redlich-Peterson	a_{RP} (L/mg)^{ß}	0.00	0.00
	k_{RP} (L/mg)	32.72	19.24
	ß	0.00	0.00
	R^2	0.93	0.91

The Redlich Petterson ß value must be greater than 0 (0 < ß ≤ 1) (DEHGHANI, KARRI and LIMA, 2021). As the fitted model results in ß=0, it may be that this model does not adequately fit the adsorption of CBZ on GAC in DWNOM. The q_{max} values were very high for DWNOM. These values may indicate that the Langmuir isotherm is not the most adequate to represent the adsorption of CBZ on GAC for the analyzed conditions (ALMEIDA *et al*., 2023). Considering these particularities and the R^2 values, it was considered that the Freundlich model best describe the adsorption of Carbendazim on both matrices.

The Freundlich isotherm indicates the possibility of heterogeneous multilayer formation during adsorption (HARO *et al*., 2021; PICCIN *et al*., 2017). Thus, the adsorption of CBZ may also present this characteristic, with the formation of multilayers in both tested matrices.

For comparison purposes, the Freundlich isotherm was used to represent the adsorption of CBZ in both matrices. Equations 63 and 64 describe the Freundlich models for the adsorption of Carbendazim on DW and DWNOM, respectively. Figure 5.14 shows the graphs obtained from the equations.

$$q_e = 60.49 \text{ x } C_e^{0.67} \quad (63)$$

$$q_e = 17.09 \text{ x } C_e^{1.09} \quad (64)$$

Figure 5.14 - Freundlich isotherms for the adsorption of CBZ on DW and DWNOM.

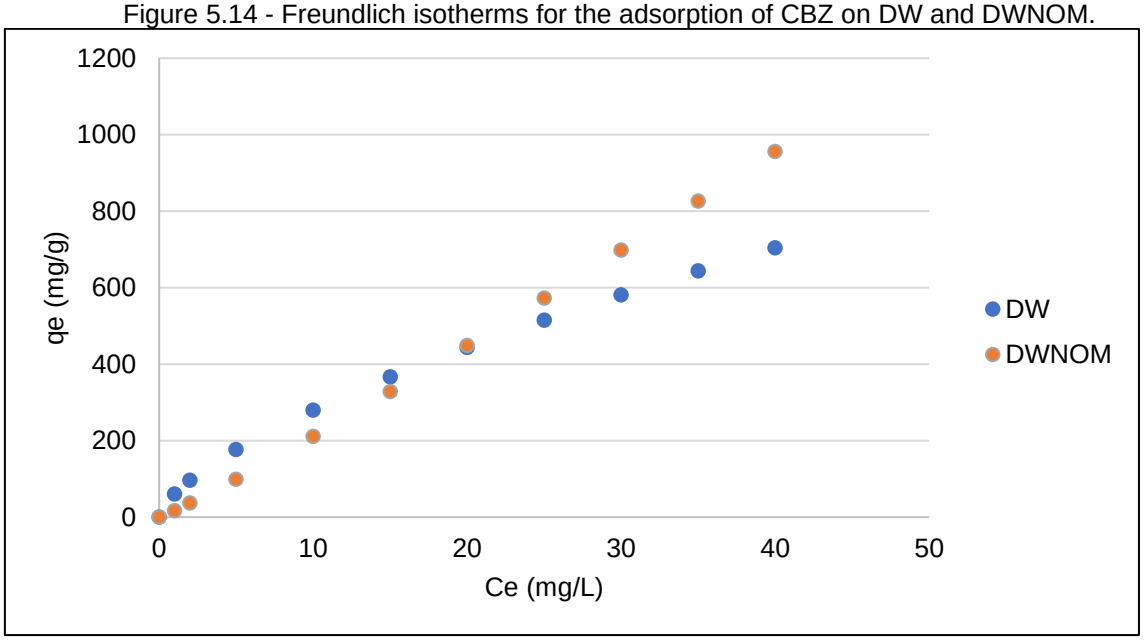

Figure 5.14 indicates that for the same equilibrium concentrations (Ce), the amount of CBZ adsorbed per gram of GAC (qe) is higher in deionized water than with the presence of organic matter up to a specific equilibrium concentration (20 mg/L). At this point, the Freundlich curve for CBZ in DWNOM crosses that of DW, indicating a change in the adsorption dynamics of CBZ in this medium. This crossing in q_e and C_e was also observed in kinetics and RSSCT. Although the adsorption was interfered with, the removal of CBZ was satisfactory in both matrices. Thus, bovine bone CAG was efficient in removing CBZ in DW and DWNOM.

There was a 72% reduction in the Freundlich constant (K_f) of the isotherm with DWNOM compared to DW. The reduction in K_f is interpreted as direct competition and

pore blocking of the activated carbon (PELEKANI & SNOEYINK, 1999). It was observed that the Freundlich intensity parameter (1/n) for adsorption on DW was less than unity, indicating that the adsorption of CBZ on bone GAC was a favorable process (ANFAR *et al*., 2020). This was also observed using other adsorbents (JIN *et al*., 2013; LI *et al*., 2011; PASZKO, 2006; RIZZI *et al*., 2020; WANG *et al*., 2020). For DWNOM, the 1/n value slightly above one (1.09) suggested that organic matter impacted the adsorptive process of CBZ in GAC. Changes in the value of "n" are interpreted as changes in the distribution of energy sites of the adsorbent (PELEKANI & SNOEYINK, 1999), which means that the presence of humic acid (NOM) may affected the distribution of the adsorptive sites of bovine bone GAC, changing the adsorption dynamics of CBZ and the shape of the Freundlich isotherm curve.

Table 5.29 presents the results of the correlation tests applying the Kendall method, analyzing the variables "GAC dosages" and "CBZ concentrations" at equilibrium for each matrix.

Table 5.29 - Result of applying the Kendall method to the isotherm test.

Matrix	**correlation coefficient (τ)**	**determination coefficient (τ^2)**
DW	-1.00	1.00
DWNOM	-0.60	0.36

The values indicated a strong negative correlation between the amount of GAC and the final concentration of CBZ in deionized water (DW). The adsorption of CBZ in DW was inversely proportional to the dosage of GAC, i.e., the greater the amount of adsorbent used, the lower the concentration of CBZ remaining in the solution. For DWNOM, the value of τ^2 was low. Although the inverse relationship between the adsorbate and the adsorbent remains, it was weaker than in DW.

5.3.4.3. Kinetics

The results of the experiments investigating the adsorption kinetics are shown in Figure 5.15 and Table 5.30. For both matrices, the pseudo-second-order kinetics best fitted the adsorption process (R^2 = 0.98 in DW and R^2 = 0.99 in DWNOM). The pseudo-first-order kinetics also fitted the adsorption of CBZ on GAC in both DW and DWNOM, with higher R^2 obtained in the medium with organic matter. Intraparticle diffusion was a determinant in the initial steps of the adsorption process in both matrices. A good fit was achieved in the adsorption of CBZ on GAC for DWNOM (R^2 = 0.93).

Figure 5.15 - Results of the kinetics tests for the experiments in deionized water (DW) and deionized water with organic matter (DWNOM) (means ± standard deviation, n=3).

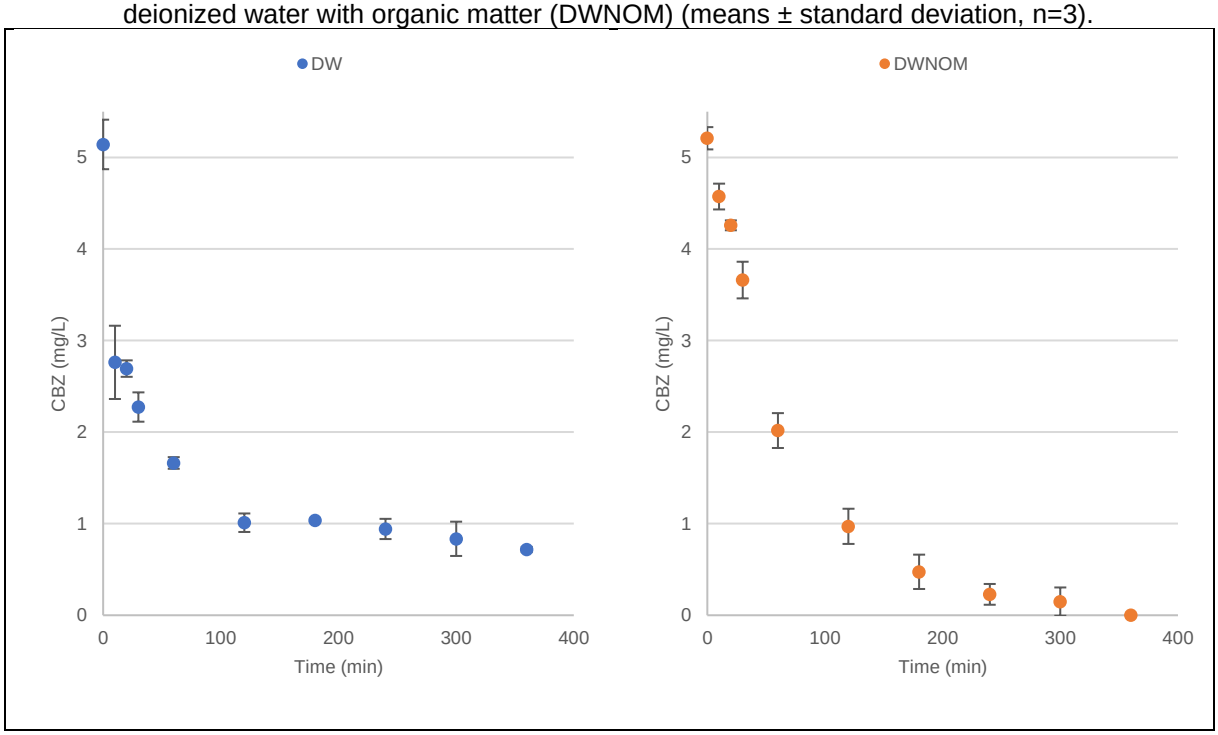

Table 5.30 - Parameter values and coefficients of determination for the pseudo-first-order and pseudo-second-order models and intraparticle diffusion.

Model	Parameter	CBZ in DW	CBZ in DWNOM
Pseudo-first-order	K_1 (t^{-1})	0.049	0.019
	q_e (mgCBZ/gGAC)	4.157	5.902
	R^2	0.94	0.99
Pseudo-second-order	K_2 (t^{-1})	0.017	0.003
	q_e (mgCBZ/gGAC)	4.462	6.987
	R^2	0.98	0.99
Intraparticle diffusion	K_{dt}	0.189	0.330
	C	1.419	0.615
	R^2	0.79	0.93

The pseudo-second-order kinetic models that best fitted Carbendazim's adsorption in DW and DWNOM are shown in Equations 65 and 66, respectively. Figure 5.16 shows the relations between q_t and t from these equations.

$$q_t = \frac{0.34 \text{ x } t}{1 + 0.08 \text{ x } t} \quad (65)$$

$$q_t = \frac{0.14 \text{ x } t}{1 + 0.02 \text{ x } t} \quad (66)$$

Figure 5.16 - Adsorption kinetics of CBZ in deionized water (DW) and deionized water with organic matter (DWNOM).

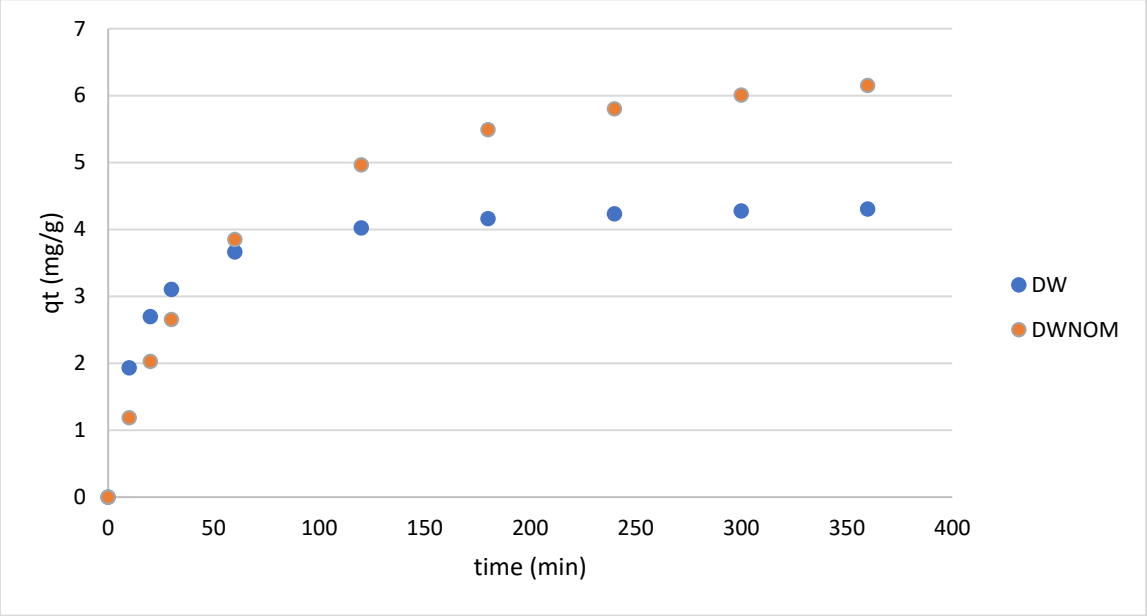

q_t = the amount of adsorbate removed per unit of adsorbent in time t, in mg/g.

The results showed that the adsorption capacity of CBZ by GAC was initially higher in DW. However, after approximately 60 minutes, the adsorption capacity of CBZ by GAC in DWNOM increases and exceeds the amount of CBZ adsorbed in DW for the same experimental times. The same occurred in the isotherm experiments, as illustrated in Figure 5.14. The explanation for this change in adsorption dynamics is uncertain. One hypothesis is that, because of their larger size and molecular weight, the organic matter particles may have dragged the CBZ molecules by adsorbing on the GAC surface, thus increasing the concentration removed from the fungicide. Zhu *et al.* (2023) showed that the presence of DOM enhanced the adsorption of heavy metals onto GAC at 5 mg/L DOM concentrations. Thus, another hypothesis is that NOM may have improved GAC's ability to adsorb fungicide.

The pseudo-second-order equation was also the best fit for the adsorption of CBZ and the herbicide Linuron on activated carbon (HGEIG *et al*., 2019). Similarly, the adsorption of atenolol on GAC was best represented by pseudo-second-order kinetics (HARO *et al*., 2017). Cao *et al*. (2011) found that the pseudo-second-order equation represented better the adsorption of p,p'- and o,p'-Dichloro-diphenyl-trichloroethane (DDT) in sediment. The same was identified for the adsorption of the insecticide Fenitrotione and the herbicide Trifluralin on organo-zeolites and activated carbon (LULE & ATALAY, 2014).

As for the GAC intraparticle diffusion, it was possible to infer that it was stronger in the adsorption of CBZ in DWNOM than DW. This can be attributed to the organic matter, which altered the adsorption dynamics of the fungicide and generated a deviation from the origin of the graph. The moderate coefficient of determination (0.79) showed that intraparticle diffusion was not a step determining the speed of adsorption of CBZ in GAC in DW.

Equation 67 represents the model of the intraparticle diffusion in DWNOM using the data shown in Table 5.30. Figure 5.17 shows the relation between q_t and t.

$$q_t = 0{,}33 \, . \, t^{0,5} + 0{,}62 \qquad (67)$$

Two distinct stages of the adsorptive process of CBZ on GAC can be observed. The first step (Phase I) was related to the adsorption on the adsorbent's external surface and represents the linear boundary layer effect. The second region (Phase II) represented intraparticle diffusion. The phase representing the equilibrium in adsorption, where the adsorbed amount is constant (Phase III), was not observed (DEL VECCHIO *et al*., 2019; HARO, 2017; RUIZ *et al*., 2010). Thus, for the adsorption of CBZ, the phase related to intraparticle diffusion exerted more influence on the adsorptive process than the boundary layer effect (this may have occurred because the equilibrium was not reached).

Figure 5.17 – Figure illustrating the intraparticle diffusion in the adsorption of CBZ on GAC in DWNOM, from Equation 67.

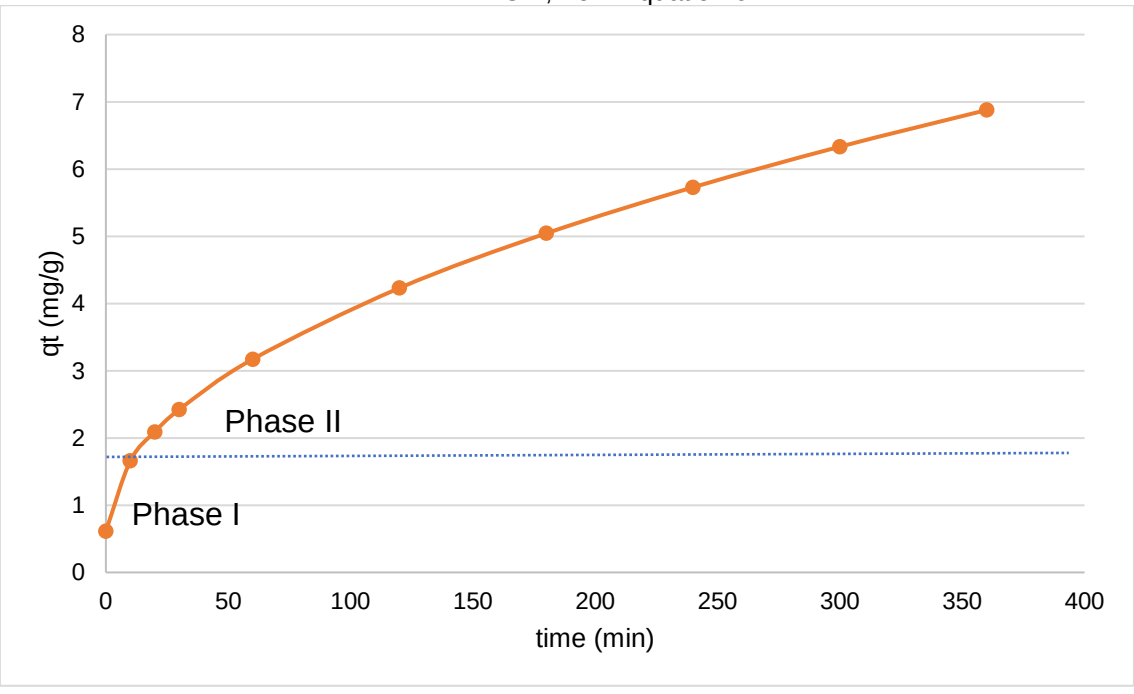

q_t = The amount of adsorbate removed per unit of the adsorbent in time t, mg/g.

The adsorption study of CBZ on activated carbon by Hgeig, Novakovic e Mihajlovic (2019) showed a high coefficient of determination when fitting the intraparticle diffusion equation. As in the present study, the equation did not start from the origin in the early stages of the adsorptive process. The authors concluded that adsorption on the surface of the GAC had the most significant influence at the beginning of the experiments, with intraparticle diffusion playing a limiting role in adsorption. In the present study, it was possible that the deviation from the origin occurred due to the difference in mass transfer rate between the initial and final stages of adsorption (AHMED & THEYDAN, 2012; DEL VECCHIO *et al*., 2019).

Larger GAC particles result in slower adsorption kinetics since this is inversely proportional to the square of the GAC particle diameter (Kennedy *et al*., 2015). According to the pore size and volume shown in Table 5.7, the GAC used in the experiments is strictly microporous. Thus, the change in adsorption dynamics is believed to be due exclusively to the organic matter, as the pores of the carbon did not act as a limiting factor on the adsorption kinetics of CBZ.

Table 5.31 shows Kendall's statistical test results in analyzing the variables "Time" and "CBZ concentrations" for each matrix.

Table 5.31 - Result of application of the Kendall test relating the variables time and CBZ concentrations in the kinetics assays.

Matrix	**Correlation coefficient (τ)**	**Determination coefficient (τ^2)**
DW	-0.75	0.56
DWNOM	-0.87	0.76

A moderate negative correlation between time and CBZ concentrations can be observed. In both matrices, the longer the contact time, the lower the concentration of CBZ remaining in the solution. This is consistent with previous studies that used 2 to 24 hours equilibrium times for CBZ adsorption (JIN *et al*., 2013; LI *et al*., 2011; PASZKO, 2006; RIZZI *et al*., 2020; WANG *et al*., 2020). Although contact time was the only variable factor (medium temperature, GAC concentration, pH, and CBZ concentration remained constant), a low τ^2 value was observed for DW. Figure 5.16 shows that there was no increase in the adsorption of CBZ in DW on CAG after a certain time, which might explain the low τ^2 value.

5.3.4.4. Rapid Small Scale Column Tests

Figure 5.18, 5.19 and Table 5.32 show the Rapid Small-Scale Columns Tests (RSSCT) results. The breakthrough time (5% C_o) was longer for the GAC column in the configuration of CBZ in DW. The column saturation time for CBZ adsorption (90% C_o) was higher with the presence of organic matter.

Figure 5.18 - Results of the small-scale column rapid tests (RSSCT) for deionized water (DW) and deionized water with organic matter (DWNOM) experiments (mean ± standard deviation, n= 4).

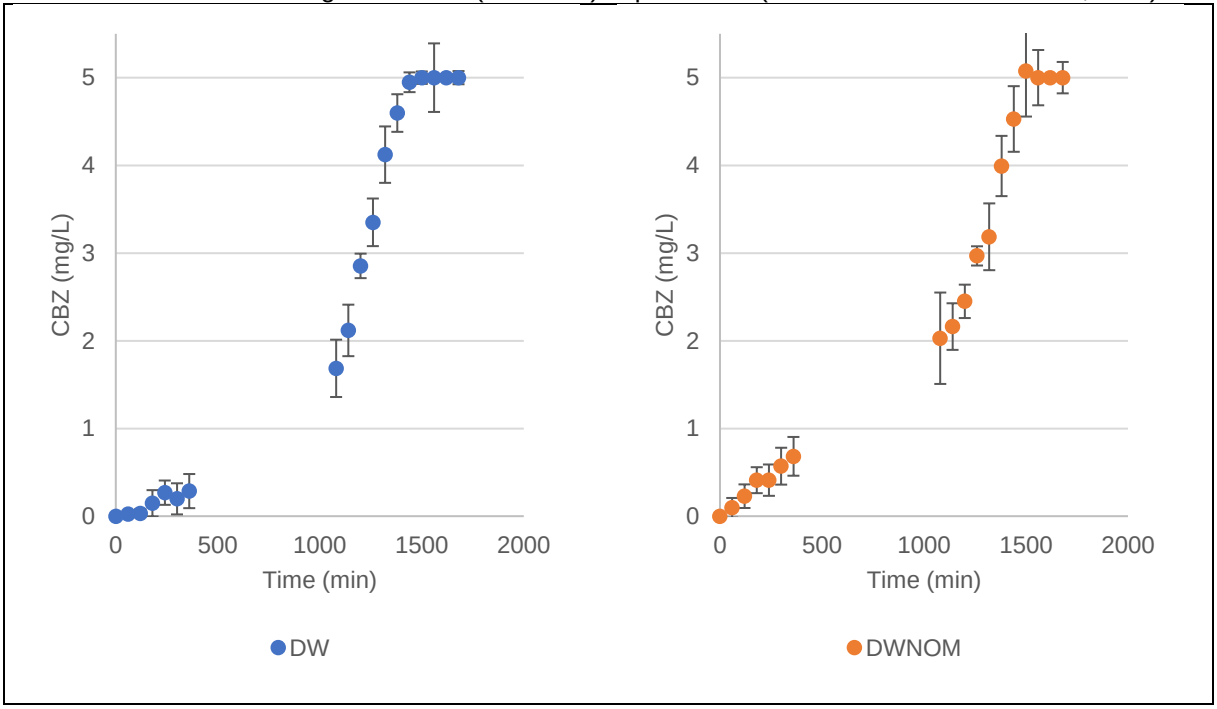

Table 5.32 - Relationship between final (C) and initial (Co) concentrations for each time collected in the RSSCT.

T (min)	CBZ in DW C/C_0	CBZ in DWNOM C/C_0
0	0.00	0.00
60	0.00	0.02
120	0.01	0.05
180	0.03	0.08
240	0.02	0.08
300	0.04	0.11
360	0.05	0.14
1080	0.34	0.41
1140	0.42	0.43
1200	0.57	0.49
1260	0.67	0.59
1320	0.82	0.64
1380	0.92	0.80
1440	0.99	0.91
1500	1.00	1.00
1560	1.00	1.00
1620	1.00	1.00
1680	1.00	1.00

Figure 5.19 – CBZ breakthrough curves obtained from the RSSCT for the experiments in deionized water (DW) and deionized water with organic matter (DWNOM).

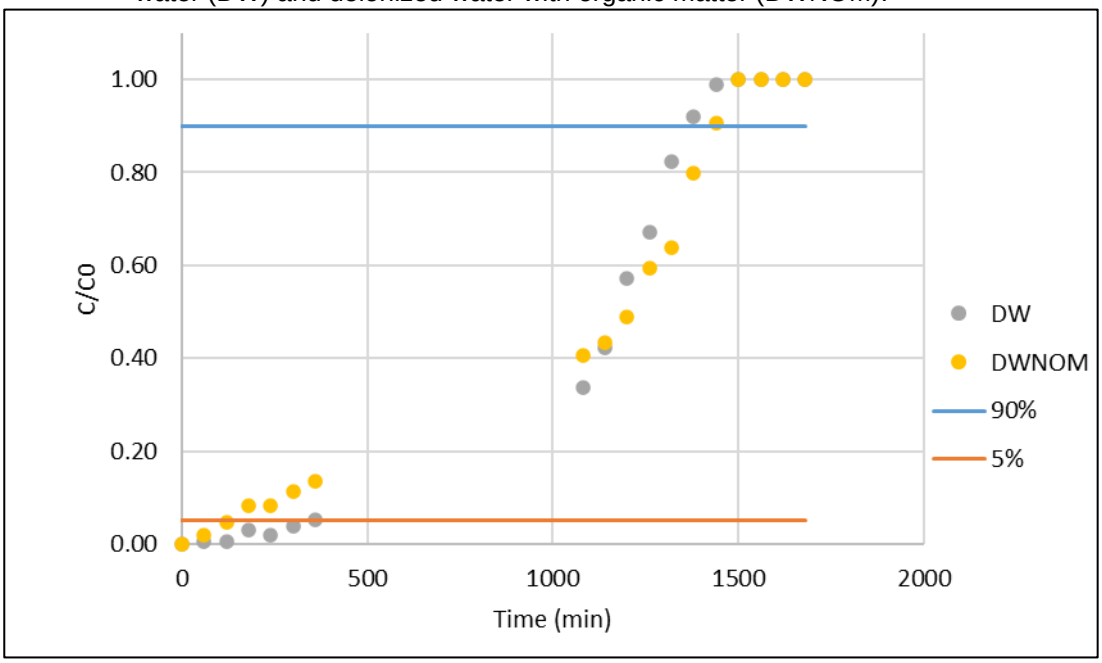

Figure 5.20 shows the breakthrough curve in the RSSCT test with the affluent containing only organic matter. NOM was present in the effluent of GAC column early in the column operation. This was also observed in tests performed by Mavaieie Jr. & Benetti (2021).

Figure 5.20 – NOM breakthrough curve in RSSCT test in DWNOM.

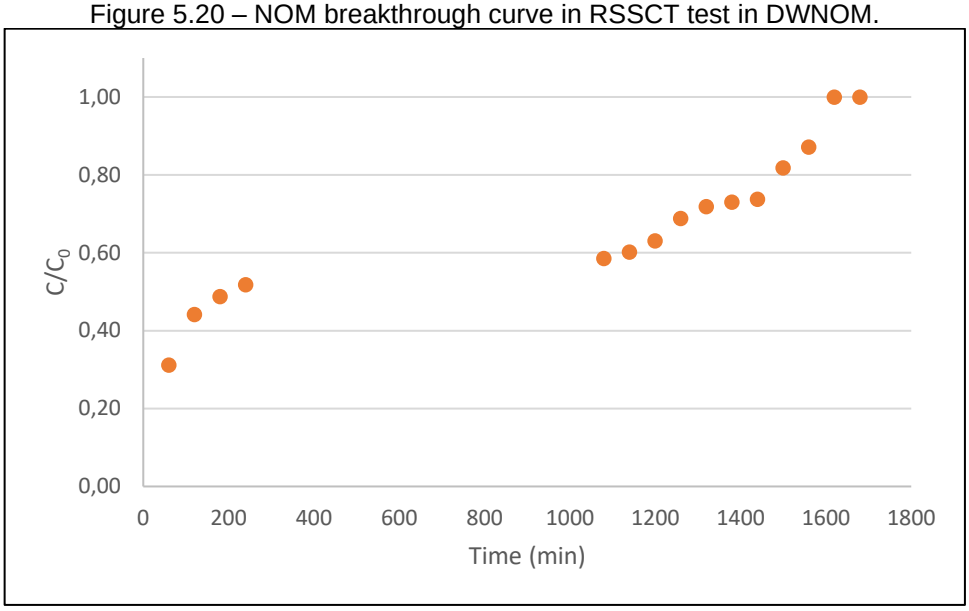

Table 5.33 presents the breakthrough and saturation times of the CBZ in DW and DWNOM. The Specific Transfer Rate (STR) and Carbon Utilization Rate (CUR) values calculated with Equations 60 and 61 are also presented. The results for DW and DWNOM were distinct, with organic matter influencing CBZ adsorption in the RSSCT assays.

Table 5.33 - Breakthrough times, saturation times, and values of specific transfer and carbon utilization rates in DW and DWNOM.

Tests	Breakthrough time (min)	Saturation time (min)	STR (cm^3/g)	CUR (g/L)
DW	360	1,440	110.8	9.0
DWNOM	120	1,500	36.9	27.1

DW = deionized water; DWNOM = deionized water with organic matter

STR and CUR are parameters used to analyze the performance of GAC in contaminant removal. The higher the STR values and, consequently, the lower the CUR values, the higher the efficiency of GAC and the more economical its application in water treatment (KEMPISTY *et al*., 2022; KENNEDY *et al*., 2015). The highest efficiency of GAC was in the configuration of CBZ in DW, in which there was no competition for the adsorption sites.

Specific adsorption studies of CBZ using RSSCT were not found in the literature. However, other substances have already been studied using this methodology. Coelho & Rozario (2019) reported the removal of the herbicide 2,4-D. They found a breaking point in ultrapure water of 1,349 minutes, higher than the time measured in the CBZ tests and, therefore, lower CUR. The authors used an initial 2,4-D concentration of 7 µg/L, EBCT of 0.72 min for reduced scale, a 6.5 mL/min flow rate,

and a GAC bed height of 6 cm. For this paper, the maximum 2,4-D value allowed by Brazilian legislation according to the Ministry of Health was adopted as the breaking point.

In another study, Voltan *et al*. (2016) evaluated the removal of the herbicides Diuron and Hexazinone in GAC and obtained a CUR of 10.7 mg/L. In this case, EBCT values ranged from 0.0251 to 0.0548 min, with a flow rate of 1.85 mL/min and a GAC bed height of 25 cm. For this paper, the maximum Diuron and Hexazinone values allowed by Brazilian legislation according to the Ministry of Health was adopted as the breaking point.

Comparing the results obtained for CUR, it is observed that the GAC showed lower performance in CBZ removal compared to the analyzed studies. Different operational conditions, such as GAC bed height, flow rates, EBCT, and initial concentrations of adsorbates, may have influenced the results.

As for the relationship between the experiments performed in RSSCT and the Fouling Index (Equation 62), it was observed that the Fouling Factor (ɣ) had no impact on the adsorption of CBZ, regardless of the values tested in the application of the method. The coefficient of determination (R^2) obtained was equal to 0.98 for all values of ɣ modeled by the Solver. The breakthrough curve of CBZ in deionized water in GAC multiplied by the values of each time with the Fouling Factor (SF) resulted in a breakthrough curve identical to the one obtained with the adsorption of the compound in DW without the addition of SF. Also, the breakthrough curve for the RSSCTs containing CBZ and natural organic matter showed a coefficient of determination of 0.98 relative to the adsorption curve of CBZ dissolved in DW. This indicates that the addition of a coefficient is not necessary. Thus, for the conditions analyzed, the impact of fouling on the adsorption dynamics of CBZ in GAC was considered negligible.

Table 5.34 shows the statistical test results applying the Kendall method to the data measured in the RSSCT trials, analyzing the variables "Time" and "CBZ concentrations" for each matrix.

Table 5.34 - Result of applying the Kendall method to the RSSCT.

Matrix	**Correlation coefficient (τ)**	**Determination coefficient (τ^2)**
DW	0.80	0.64
DWNOM	0.90	0.81

The values showed a moderate positive correlation between time and CBZ concentrations, indicating that the concentration of CBZ in the column effluent increases with operating time. This is the result of the filling of the adsorption sites by CBZ and organic matter.

Table 5.35 shows the results of the Kruskal-Wallis significance tests performed comparing the results measured in the two aqueous matrices for each collection time.

Table 5.35 - Analysis of the difference between CBZ concentrations dissolved in deionized water (DW) and with natural organic matter (DWNOM) for the same dosage of GAC ($p < 0.05$).

Time	p-value
0	-
60	0.54
120	0.04
180	0.08
240	0.25
300	0.08
360	0.08
1080	0.81
1140	0.62
1200	0.18
1260	0.08
1320	0.18
1380	0.18
1440	0.46
1500	0.65
1560	0.12
1620	0.48
1680	0.26

Table 5.35 shows that only at the time of 120 minutes there was a statistically significant difference ($p < 0.05$) between CBZ adsorption in DW and DWNOM. It is noted that 120 minutes was the breakthrough point in DWNOM, suggesting a change in the CBZ adsorption dynamics in this medium. On the other hand, the breakthrough and saturation times for the experiment in DW (360 and 1440 minutes, respectively) and the saturation point for DWNOM (1500 minutes) had no statistically significant differences. This trend is consistent with the fouling test results, which indicated that the impact of organic matter was negligible in a small-scale fixed bed.

Although the interference of organic matter on CBZ adsorption was detected through the distinct breakthrough and saturation times, STR and CUR, the final concentrations analyzed were statistically similar. Thus, it can be considered that the

column that received CBZ in DW had a better performance compared to DWNOM, due to the similar saturation time and the longer time needed to reach the breaking point.

5.3.4.5. General considerations on the impact of organic matter on CBZ adsorption

After performing the isotherms and kinetics tests, it was found that the presence of natural organic matter in the form of humic acid changed the adsorption parameters. This result was mainly due to the physicochemical properties and interactions between the organic matter, the pesticide, and the activated carbon. A possible explanation for this effect was the adsorption of larger molecules of NOM on the outer surface of the GAC, blocking the pore entrance and reducing the number of accessible adsorptive sites (DOMERGUE *et al*., 2022). This process may have decreased CBZ adsorption over time (MOUSSAVI *et al*., 2013). This interference was most evident in the isotherm experiments.

Because they have different molecular sizes, the competition for the sites observed in the experiments was mainly due to the pore size distribution of the GAC since the organic matter can occupy the macropores and mesopores, preventing the access of CBZ to the micropores of the adsorbent. Thus, the GAC's pore distribution controlled the competition mechanism (PELEKANI & SNOEYINK, 1999). Microcontaminants in drinking water are usually present in concentrations three to six orders of magnitude smaller than natural organic matter. This implies a reduced adsorption capacity in the presence of NOM (DOMERGUE *et al*., 2022)

Another interference factor in the adsorption process is the electrostatic interactions between the organic matter and the activated carbon, which can favor its adsorption. The organic matter in the form of humic acid is negatively charged in the pH range in which the experiments were performed. Thus, it can compete with the anions of the CBZ molecule for the activated carbon pores, which are positively charged (MOUSSAVI *et al*., 2013). As already verified in the characterization of the activated carbon, the presence of bivalent cations of the GAC may have favored these electrostatic interactions and enabled the adsorption of organic matter by this process.

It is possible that NOM could have improved the efficiency of GAC in removing CBZ. This is possible because some organic compounds change their fate in the presence of humic substances (CARTER & SUFFET, 1982). Guillossou *et al*. (2020) identified that a pre-equilibrium of 24 h between Organic micropollutants (OMP) and

dissolved organic matter (DOM) improved their removal onto powdered activated carbon. These results showed the formation of DOM-OMPs complexes in solution which increased the overall removal of OMPs, especially at short contact times. Similarly, Zhu *et al*. (2023) showed that the presence of DOM enhanced the adsorption of heavy metals onto GAC at 5 mg/L DOM concentrations. Our study did not include a pre-equilibrium period between CBZ and NOM. However, this may be a possibility for the increase in the adsorptive capacity of CBZ on GAC in DWNOM, especially in the RSSCT where the experiment time exceeded 24 hours.

CEC adsorption is mainly influenced by kinetic factors, which are affected by the interaction between NOM and trace molecules. As a result, NOM impacts the removal of target contaminants (DOMERGUE *et al*., 2022). Based on the obtained data and comparison with previous studies, it was observed that organic matter interacted with the adsorptive sites of bovine bone GAC, altering the adsorption dynamics of CBZ, especially in the batch experiments.

The fixed-bed experiments showed different results, reflected by breakthrough and saturation times, STR, and CUR values. However, the data generated were statistically similar, and there was no evidence of compromise in the efficiency of the activated carbon. The results of the kinetics and RSSCT tests may indicate an improvement in the adsorption of CBZ due to the presence of NOM. Therefore, this hypothesis is also valid for the data obtained. Furthermore, the fouling analysis showed that the effect of organic matter was negligible for small-scale fixed beds.

5.3.5. Conclusions

The isotherms, kinetics, and RSSCT experiments showed that activated carbon removed CBZ in both aqueous matrices. In the adsorption experiments for CBZ dissolved in deionized water with organic matter (DWNOM), the four isotherm models tested had equal determination coefficients (0.91). For CBZ dissolved in deionized water (DW), the Freundlich and Sips models had the highest determination coefficients (0.98). However, the Langmuir and Redlich-Peterson isotherms also fit the CBZ adsorption with coefficients of 0.97 and 0.93, respectively. The K_f and 1/n parameters of the Freundlich isotherm, which simultaneously fitted the adsorption of CBZ dissolved in DW and DWNOM, varied according to the matrix, evidencing the interference in adsorption by natural organic matter.

For the tests with kinetics, it was found that the pseudo-second-order model fitted best to the adsorption of CBZ on GAC in both matrices. The results showed that in the initial stages of adsorption, the adsorptive capacity was higher in the configuration in which CBZ was dissolved in DW. However, the adsorption capacity of CBZ dissolved in DWNOM increased during the same experimental times of CBZ in DW. The same occurred in RSSCT. Thus, the data show that the presence of organic matter, under the conditions analyzed, may have improved the efficiency of GAC in adsorbing CBZ in kinetics and RSSCT tests. Intraparticle diffusion was more intense in DWNOM than in DW, with adsorption on the outer surface of the GAC exerting a more significant influence. In both matrices, the pseudo-first-order model also adjusted well the data.

The RSSCT results showed that organic matter reduced the time required to reach a breakthrough compared to the pure aqueous matrix, evidencing a significant difference between the results. The concentrations of CBZ effluent from the GAC bed were different at all collection times analyzed, reflecting different saturation times, STR, and CUR. However, there was no statistically significant difference in the breakthrough curve for most of the data. The fouling study indicated that NOM did not significantly impact the CBZ breakthrough curve. Thus, even with differences between the fixed bed adsorption curves, the results were considered similar.

The results indicated that the presence of organic matter impacted the adsorption of CBZ, changing the dynamics in the isotherm and kinetics tests. This influence was evidenced in the different parameters obtained for all the methods tested. For the fixed-bed experiment, most of the results were statistically similar, although distinct data was observed. Despite having an impact on the adsorption of the fungicide, NOM may have improved the ability to remove CBZ, especially in the kinetics and RSSCT tests. This may have been due to a possible interaction between CBZ and humic acid.

Based on the isotherms, kinetics, and fixed-bed studies, it is concluded that granular activated carbon is a technique that can be used for the removal of the fungicide Carbendazim dissolved in aqueous matrices with natural organic matter, which is usually present in sources that serve as water supplies for human consumption.

6. CONSIDERAÇÕES FINAIS

Os resultados mostraram que a isoterma de Freundlich é a que melhor se ajusta à adsorção do CBZ em CAG. Dessa forma, a adsorção do fungicida ocorre predominantemente de forma heterogênea e em multicamadas. A maioria dos experimentos mostrou que a adsorção do composto é favorável. No experimento de adsorção do Carbendazim dissolvido em água deionizada em carvão de casca de coco, embora o parâmetro 1/n de Freundlich tenha sido maior que 1, o valor da Energia Livre de Gibbs indicou que a reação foi favorável (Artigo 1). Nos experimentos utilizando água filtrada da ETA e água deionizada com ácido húmico, os outros modelos de isotermas testados também mostraram bons ajustes.

A remoção do fungicida é caracterizada como um processo exotérmico. Além disso, a adsorção do CBZ é um processo espontâneo com predominância da fisiossorção e a presença de interações dipolo-dipolo entre a superfície do CAG e o fungicida. A variação da entropia mostrou que há uma redução do grau de desordem na interface adsorvente/solução, indicando que a adsorção do Carbendazim é um processo reversível e sem a transferência de elétrons.

Quanto à cinética de adsorção, o modelo de pseudo-segunda ordem é a que melhor se ajustou na adsorção do CBZ em CAG. Os experimentos mostraram que nos estágios iniciais, a adsorção do CBZ pelo carvão é maior em água deionizada. Contudo, no decorrer do processo, a capacidade adsortiva do CAG é maior em água filtrada da ETA e em água deionizada com matéria orgânica. A difusão intrapartícula exerceu maior influência na adsorção do CBZ em água da ETA. Os experimentos mostraram que o modelo de pseudo-primeira ordem também apresentou um bom ajuste na adsorção do CBZ no CAG em todas as matrizes aquosas analisadas.

Quanto aos experimentos em leito fixo com ERCER, observou-se que o tempo de ruptura foi maior para os experimentos em AD. Contudo, não houve diferença significativa entre os pontos de saturação obtidos para este meio e nos demais, em que houve competição pelos sítios adsortivos do CAG. Os valores de TUC e TTE mostraram que a coluna com aplicação de CBZ dissolvido somente em AD apresentou melhor desempenho do que nas outras matrizes. De forma geral, a MON na forma de ácido húmico e as substâncias presentes na água filtrada da ETA impactaram no tempo de ruptura na coluna de CAG mas a interferência não foi significativa nos tempos de saturação.

Analisando a competição do CBZ pelos sítios adsortivos do CAG com as substâncias presentes na água filtrada da ETA e com a matéria orgânica na forma de ácido húmico, observou-se que essa competição foi mais evidenciada nos estudos de isoterma e cinética de adsorção, em que houve a mudança de valores dos parâmetros obtidos. A competição pelos sítios adsortivos do CAG pode ter sido controlada principalmente pela distribuição dos tamanhos dos poros, uma vez que a matéria orgânica pode ocupar os macros e mesoporos do CAG, impedindo o acesso do CBZ aos microporos do adsorvente. As interações eletrostáticas entre a matéria orgânica e o carvão ativado também podem ter interferido na adsorção do CBZ, devido às características do CAG e dos compostos nas condições experimentais aplicadas.

Ainda, o contínuo contato do CBZ com a matéria orgânica, principalmente nos ERCER, pode ter favorecido uma combinação entre essas substâncias, melhorando a eficiência do CAG em remover o fungicida. Para os experimentos em leito fixo, a competição pelos sítios adsortivos do CAG não foi considerada significativa. O estudo do *fouling* mostrou que a MON não impactou significativamente a curva de ruptura do CBZ.

Por fim, observou-se que a mudança na dinâmica de adsorção do CBZ gerada pela competição com outras substâncias pelos sítios adsortivos do CAG não comprometeu a eficiência do adsorvente, que continuou removendo o fungicida em condições distintas. O estudo mostrou que a adsorção por carvão ativado granular é uma técnica avançada de tratamento de água eficaz na remoção do Carbendazim. A eficiência pode variar de acordo com o tipo de carvão ativado, com a forma de aplicação (em batelada ou em fluxo contínuo), concentração do adsorvente, temperatura, pH, além da presença de outras substâncias no meio em que o Carbendazim está dissolvido.

7. REFERENCIAS

ABDELHAMEED, R. M.; ABDEL-GAWAD, H.; SILVA, C. M.; ROCHA, J.; HEGAZI, B.; SILVA, A. M. S. Kinetic and equilibrium studies on the removal of 14 C-ethion residues from wastewater by copper-based metal – organic framework. **International Journal of Environmental Science and Technology**, v. 15, n. 11, p. 2283–2294, 2018.

AGÊNCIA NACIONAL DE VIGILÂNCIA SANITÁRIA (ANVISA). **Reavaliação toxicológica – ANVISA inicia a reavaliação do Carbendazim.** 2020. Disponível em: https://www.gov.br/anvisa/pt-br/assuntos/noticias-anvisa/2020/anvisa-inicia-a-reavaliacao-do-carbendazim. Acesso em 26 jan. 2021.

AGÊNCIA NACIONAL DE VIGILÂNCIA SANITÁRIA (ANVISA). **Programa de análise de resíduos de agrotóxicos em alimentos -PARA. Relatórios das amostras analisadas no período de 2017-2018**. Gerência Geral de Toxicologia. Brasília, 2019. Disponível em: http://portal.anvisa.gov.br/documents/111215/0/Relat%C3%B3rio+%E2%80%93+PARA+2017-2018_Final.pdf/e1d0c988-1e69-4054-9a31-70355109acc9. Acesso em 27 jan. 2020.

AGÊNCIA NACIONAL DE VIGILÂNCIA SANITÁRIA (ANVISA). **Relatório de atividades 2010**. Brasília-DF: Ministério da Saúde, 2010.

AGÊNCIA NACIONAL DE VIGILÂNCIA SANITÁRIA (ANVISA). **Carbendazim**. 2012. Disponível em: <http://portal.anvisa.gov.br/documents/111215/117782/c24.pdf/a019eb91-b52d-492d-8140-ae82f54d5698>. Acesso em 27 jan 2020.

AGÊNCIA NACIONAL DE VIGILÂNCIA SANITÁRIA (ANVISA). **Reavaliação toxicológica do Carbendazim**. 2022. Disponível em: https://www.gov.br/anvisa/pt-br/assuntos/noticias-anvisa/2020/anvisa-inicia-a-reavaliacao-do-carbendazim. Acesso em 26 nov 2022.

AHMED, M.J.; THEYDAN, S.K. Adsorption of cephalexin onto activated carbons from Albizia lebbeck seed pods by microwave-induced KOH and K2CO3 activations. **Chemical engineering journal**, v. 15, n. 211–212, p. 200–207, 2012.

ALAEE, M.; ARIAS, P.; SJÖDIN, A.; BERGMAN, A. An overview of commercially used brominated flame retardants, their applications, their use patterns in different countries/regions and possible modes of release. **Environment International**, v. 29, n. 6, p. 683–689, 2003.

ALBALADEJO, G. J.; ROS, J. A.; ROMERO, A.; NAVARRO, S. Effect of bromophenols on the taste and odor of drinking water obtained by seawater desalination in south-eastern Spain. **Desalination**, v. 307, p. 1–8, 2012.

ALLEN, S. J.; MCKAY, G.; KHADER, K. Y. H. Intraparticle Diffusion of a Basic Dye During Adsorption onto Sphagnum Peat. **Environmental Pollution**, v. 56, n.1, p. 39–50, 1989.

ALMEIDA, I. R.; SILVA, S. W.; TAVARES, L. C.; BENETTI, A. D. Carbendazim Adsorption on Granular Activated Carbon of coconut shell: Optimization and Thermodynamics. **Revista AIDIS de Ingeniería y Ciencias Ambientales: Investigación, desarrollo y práctica**, v. 16, n. 2, p. 456-476, 2023.

AMERICAN PUBLIC HEALTH ASSOCIATION; AMERICAN WATER WORKS

ASSOCIATION; WATER ENVIRONMENT FEDERATION. **Standard Methods for the Examination of Water and Wastewater**. 20th. ed. Washington, D.C.: American Public Health Association. Método 5220 C (Closed Reflux, Titrimetric Method). 1998.

AMERICAN SOCIETY FOR TESTING AND MATERIALS (ASTM) INTERNATIONAL. **Standard Practice for the Prediction of Contaminant Adsorption On GAC in Aqueous Systems Using Rapid Small-Scale Column Tests, D6586 − 03**. Reapproved (2014). ASTM Committee D-28 on Activated Carbon, 2014.

AMERICAN SOCIETY FOR TESTING AND MATERIALS (ASTM) INTERNATIONAL. **Standard Practice for determination of adsorptive capacity of activated carbon by aqueous phase isotherm technique, D3860 − 98**. 2nd edition. ASTM Committee D-28 on Activated Carbon, 2000.

AMERICAN WATER WORKS ASSOCIATION (AWWA). **Water Treatment Plant Design**. 4th ed. United States: McGraw-Hill. 972 p. 2005.

ANFAR, Z.; AHSAINE, H. A.; ZBAIR, M.; AMEDLOUS, A.; FAKIR, A. A. E.; JADA, A.; ALEM, N. E.. Recent trends on numerical investigations of response surface methodology for pollutants adsorption onto activated carbon materials: A review. **Critical Reviews in Environmental Science and Technology**, v.50, n.10, pp. 1043–1084. 2020.

ATKINS, P.; DE PAULA, J. **Atkins' physical chemistry**. New York: Oxford University Press, 2006.

AURIA, R.; FRERE, G.; MORALES, M.; ACUÑA, M.E.; REVAH, S. Influence of mixing and water addition on the removal rate of toluene vapors in a biofilter. **Biotechnology and Bioengineering**, v. 68, n.4, p. 448-455, 2000.

BARBOSA, A. M. C.; SOLANO, M. L. M.; UMBUZEIRO, G. A. Pesticides in Drinking Water – The Brazilian Monitoring Program. **Frontiers in Public Health**, v. 3, p. 1–10, 2015.

BARCELÓ, D.; HENNION, M.C. **Trace determination of pesticides and their degradation products in water, techniques and instrumentation in analytical chemistry**. 1st edition, v. 19. New York: Elsevier, 1997.

BASTOS, L. H. P. **Resíduos de agrotóxicos em amostras de leite: Uma avaliação visando a vigilância sanitária**. 2013. Tese (Doutorado em Vigilância Sanitária do Instituto Nacional de Controle de Qualidade em Saúde), Fundação Oswaldo Cruz, Rio de Janeiro, 2013. Disponível em: https://www.arca.fiocruz.br/bitstream/icict/36373/2/Tese_Lucia_Helena_Pinto_Bastos.pdf. Acesso em: 10 out. 2019.

BATOOL, F.; AKBAR, J.; IQBAL, S.; NOREEN, S.; NASIR, S.; BUKHARI, A. Study of Isothermal, Kinetic, and Thermodynamic Parameters for Adsorption of Cadmium: An Overview of Linear and Nonlinear Approach and Error Analysis. **Bioinorganic Chemistry and Applications**, v. 2018, 2018.

BENNER, J.; HELBLING, D. E.; KOHLER, H. P. E.; WITTEBOL, J.; KAISER, E.; PRASSE, C.; TERNES, T. A.; ALBERS, C. N.; AAMAND, J.; HOREMANS, B.; SPRINGAEL, D.; WALRAVENS, E.; BOON, N. Is biological treatment a viable alternative for micropollutant removal in drinking water treatment processes? **Water Research**, v. 47, n. 16, p. 5955–5976, 2013.

BENJAMIN, M. M.; LAWLER, D. F. **Water quality engineering: physical/chemical treatment processes**. 1st edition. Hoboken, New Jersey: Wiley & Sons, 2013.

BEZERRA, M. A.; SANTELLI, R. E.; OLIVEIRA, E. P.; VILLAR, L. S.; ESCALEIRA L. A. Response Surface Methodology (RSM) as a tool for optimization in analytical chemistry. **Talanta**, v. 76, n.5, p. 965–977, 2008.

BLYTHE, J. W.; HEITZ, A.; JOLL, C. A.; KAGI, R. I. Determination of trace concentrations of bromophenols in water using purge-and-trap after in situ acetylation. **Journal of Chromatography A**, v. 1102, n. 1–2, p. 73–83, 2006.

BONILLA-PETRICIOLET, A.; MENDOZA-CASTILLO, D. I.; REYNEL-ÁVILA, H. E. **Adsorption Processes for Water Treatment and Purification**. 1st edition. Springer International Publishing, 2017. *E-book*. Disponível em: https://doi.org/10.1007/978-3-319-58136-1. Acesso em 21 dez. 2020.

BRANDÃO, C. C. S.; SILVA, A. S. Remoção de cianotoxinas por adsorção em carvão ativado. *In*: PÁDUA, V. L. **Contribuição ao estudo da remoção de cianobactérias e microcontaminantes orgânicos por meio de técnicas de tratamento de água para consumo humano**. Rio de Janeiro: ABES, 2016. Cap. 10, p. 415-465.

BRASIL. **Monitoramento de Agrotóxicos (2014 - 2017)**. Ministério da Saúde. Disponível em: https://app.rios.org.br/index.php/s/ljppVjrP37ak8HE. Acesso em 10 abr. 2020.

BRASIL. **Portaria GM/MS nº 888, de Maio de 2021**. Altera o Anexo XX da Portaria de Consolidação GM/MS nº 5, de 28 de setembro de 2017, para dispor sobre os procedimentos de controle e de vigilância da qualidade da água para consumo humano e seu padrão de potabilidade. Brasília, DF: Gabinete do Ministro [2021].Disponível em: https://www.in.gov.br/en/web/dou/-/portaria-gm/ms-n-888-de-4-de-maio-de-2021-318461562. Acesso em: 23 nov. 2021.

BROZNIC, D.; DIDOVIC, M. P.; RIMAC, V.; MARINIC, J. Sorption and leaching potential of organophosphorus insecticide dimethoate in Croatian agricultural soils. **Chemosphere**, v. 273, p. 128563, 2021.

CAMPOS, L. C.; SU, M. F. J.; GRAHAM, N. J. D.; SMITH, S. R. Biomass development in slow sand filters. **Water Research**, v. 36, n. 18, p. 4543–4551, 2002.

CAO, X.; HAN, H.; YANG, G.; GONG, X.; JING, J. The sorption behavior of DDT onto sediment in the presence of surfactant cetyltrimethylammonium bromide. **Marine Pollution Bulletin**, v. 62, p. 2370–2376, 2011.

CARPENTER, C. M. G.; HELBLING, D. E. Removal of micropollutants in biofilters: Hydrodynamic effects on biofilm assembly and functioning. **Water Research**, v. 120, p. 211–221, 2017.

CARTER, C. W.; SUFFET, I. H. Binding of DDT to Dissolved Humic Materials. **Environmental Science and Technology**, v. 16, n. 11, p. 735-740, 1982.

CHEMICALIZE. **Carbendazim**. Disponível em: https://chemicalize.com/app/search/Carbendazim. Acesso em 19 abr. 2021.

CHEN, Y.; LI, J.; CHEN, L.; CHEN, S.; DIAO, W. Brominated flame retardants (BFRs) in waste electrical and electronic equipment (WEEE) plastics and printed circuit boards (PCBs). **Procedia Environmental Sciences**, v. 16, p. 552–559, 2012.

CHEN, J. P.; PEHKONEN, S. O.; LAU, C. C. Phorate and Terbufos adsorption onto four tropical soils. **Colloids and Surfaces A: Physicochemical and Engineering Aspects**, v. 240, n. 1–3), p. 55–61, 2004.

CHEN, J. P.; WU, S.; CHONG, K. H. Surface modification of a granular activated carbon by citric acid for enhancement of copper adsorption. **Carbon**, v. 41, n. 10, p. 1979–1986, 2003.

CHOI, G.; KIM, S.; KIM, S.; KIM, S.; CHOI, Y.; KIM, H. J.; LEE, J. J.; KIM, S. Y.; LEE, S.; MOON, H. B.; CHOI, S.; CHOI, K.; PARK, J. Occurrences of major polybrominated diphenyl ethers (PBDEs) in maternal and fetal cord blood sera in Korea. **Science of the Total Environment**, v. 491–492, p. 219–226, 2014.

COELHO, E. R. C.; BRITO, G. M.; LOUREIRO, L. F.; SCHETTINO JR., M. A.; FREITAS, J. C. C. 2,4-dichlorophenoxyacetic acid (2,4-D) micropollutant herbicide removing from water using granular and powdered activated carbons: a comparison applied for water treatment and health safety. **Journal of Environmental Science and Health, Part B**, v. 55, n. 4, p.361-375, 2020.

COELHO, E. R. C.; ROZÁRIO, A. Removal of 2,4-D in water samples by adsorption in fixed beds of granular activated carbon on reduced scale. **Engenharia Sanitaria e Ambiental**, v. 24, n. 3, p. 453–462, 2019.

COELHO, E. R. C.; VAZZOLER, H. Capacidade de adsorção frente as isotermas de Langmuir e Freundlich para atrazina em materiais zeolíticos e carbonosos utilizados em tratamento de água na remoção de matéria orgânica natural e sintética. *In*: Congresso Brasileiro de Engenharia Sanitária e Ambiental. **Anais.** Campo Grande, 2005. Nº 23, I-050.

COPENHAVER, M. D.; HOLLAND, B. Computation of the distribution of the maximum studentized range statistic with application to multiple significance testing of simple effects. **Journal of Statistical Computation and Simulation**, v. 30, n. 1, p. 1-15, 1988.

CORWIN, C.J.; SUMMERS, R.S. Scaling trace organic contaminant adsorption capacity by granular activated carbon. **Environmental. Science and Technology**. v. 44, p. 5403–5408, 2010. DOI: https://doi.org/10.1021/es9037462.

COUTINHO, C.; GALLI, A.; MAZO, L. H. Carbendazim e o meio ambiente: Degradacao e toxidez. **Revista de Ecotoxicologia e Meio Ambiente**, v. 16, p. 63-70, 2006.

COVACI, A.; VOORSPOELS, S.; D'SILVA, K.; HUWE, J.; HARRAD, S. Chapter 15 Brominated Flame Retardants as Food Contaminants. **Comprehensive Analytical Chemistry**, v. 51, n. 08, p. 507–570, 2008.

CRITTENDEN, J. C.; TRUSSEL, R. R.; HAND, D. W.; HOWE, K. J.; TEHOBANOGLOUS, G. **MWH's water treatment: principles and design**. 3rd edition, 1901 p. Hoboken, New Jersey: Wiley & Sons, 2012.

CRITTENDEN, J. C.; SANONGRAJ S.; BULLOCH J. L.; HAND, D. W.; ROGERS T. N.; SPETH, T. F.; ULMER, M. Correlation of aqueous-phase adsorption isotherms. **Environmental Science and Technology**, v. 33, n. 17, p. 2926–2933, 1999.

CRITTENDEN, J. C.; REDDY, P. S.; ARORA, H.; TRYNOSKI, J.; HAND, D. W.; PERRAM, D. L.; SUMMERS, R. S. Predicting GAC Performance With Rapid Small-

Scale Column Tests. **Journal American Water Works Association**, v. 83, n. 1, p. 77–87, 1991.

CRITTENDEN, J. C.; HAND, D. W.; ARORA, H.; LYKINS JR, B. W. Design Considerations for GAC Treatment of Organic Chemicals. **Journal American Water Works Association**, v. 79, n. 1, p. 74–82, 1987.

CRITTENDEN, J. C.; BERRIGAN, J. K.; HAND, D. W. Design tests for a constant diffusivity. **Journal Water Pollution Control Federation**, v. 58, n. 4, p. 312–319, 1986.

DA SILVA J. E.; RODRIGUES, F. I. L.; PACÍFICO, S. N.; SANTIAGO, L. F.; muniz, C. R.; SARAIVA, G. D.; NASCIMENTO, R. F.; SOUSA NETO, V. O. Estudo de Cinética e Equilíbrio de Adsorção Empregando a Casca do Coco Modificada Quimicamente para a Remoção de Pb (II) de Banho Sintético. **Revista Virtual de Química**, v. 10, n. 5, p. 1248–1262, 2018.

DAVIS, M. K.; CHEN, G. Graphing Kendall's τ. **Computational Statistics & Data Analysis**, v. 51, p. 2375-2378, 2007.

DE BOER, J.H.; LIPPENS, B.C.; LINSEN, B.G.; BROEKHOFF, J.C.P.; VAN DEN HEUVEL, A.; OSINGA, T.J., 1966. Thet-curve of multimolecular N2-adsorption. **Journal of Colloid and Interface Science**, v. 21, p. 405–414, 1966. DOI: https://doi.org/10.1016/0095-8522(66)90006-7

DE WIT, C. A.; ALAEE, M.; MUIR, D. C. G. Levels and trends of brominated flame retardants in the Arctic. **Chemosphere**, v. 64, n. 2, p. 209–233, 2006.

DEHGHANI, M. H.; KARRI, R. R.; LIMA, E. C. Adsorption: Fundamental aspects and applications of adsorption for effluent treatment. *In*: DEHGHANI, M. H.; KARRI, R. R.; LIMA, E. C. **Green Technologies for Defluorination of Water.** 1st edition. Elsevier, 2021. Chapter 3, p.41-88.

DEL VECCHIO, P.; HARO, N.K.; SOUZA, F.S.; MARCÍLIO, N.R.; FÉRIS, L.A. Ampicillin removal by adsorption onto activated carbon: Kinetics, equilibrium and thermodynamics. **Water Science & Technology**, v. 79, p. 2013–2021, 2019.

DELLE SITE, A. Factors affecting sorption of organic compounds in natural sorbent/water systems and sorption coefficients for selected pollutants. A review. **Journal of Physical and Chemical Reference Data**, v. 30, n. 1, p. 187–439, 2001.

DOMERGUE, L.; CIMETIÈRE, N.; GIRAUDET, S.; CLOIREC, P. LE. Adsorption onto granular activated carbons of a mixture of pesticides and their metabolites at trace concentrations in groundwater. **Journal of Environmental Chemical Engineering**, v. 10, n. 5, p. 108218, 2022. DOI: https://doi.org/10.1016/j.jece.2022.108218

DUAN, J.; GREGORY, J. Coagualtion by hydrolyzing metal salts. **Advanced Colloid Interface Science**, v.100-102, p. 475-502, 2003.

DULIO, V.; PETER .C.; OHE, VON DER, BOTTA, F.; IPOLYI, I., RUEDEL, H., SLOBODNIK, J. The NORMAN network ' s special view on prioritisation of biocides as emerging contaminants, **SETAC Europe annual meeting**, 2016.

ELOUAHLI, A.; ZBAIR, M.; ANFAR, Z.; AHSAINE, H. A.; KHALLOK, H.; CHOURAK, R.; HATIM, Z. Apatitic tricalcium phosphate powder : High sorption capacity of hexavalent chromium removal. **Surfaces and Interfaces**, v. 13, p. 139–147, 2018.

ENVIRONMENTAL PROTECTION AGENCY (EPA) US. IRC **Manual for Bench and Pilot-scale Treatment Studies**. Technical Support Division. Cincinnati, OH: EPA, 1996.

ERSAN, G.; KAYA, Y.; APUL, O.G.; KARANFIL, T. Adsorption of organic contaminants by graphene nanosheets, carbon nanotubes and granular activated carbons under natural organic matter preloading conditions. **Science of The Total Environment**, v. 565, p. 811–817. 2016. DOI: https://doi.org/10.1016/j.scitotenv.2016.03.224

EZECHIÁŠ, M.; COVINO, S.; CAJTHAML, T. Ecotoxicity and biodegradability of new brominated flame retardants: A review. **Ecotoxicology and Environmental Safety**, v. 110, p. 153–167, 2014.

FERNANDEZ, M.; RODRIGUEZ, R.; PICO, Y.; MANES, J. Liquid chromatographic-mass spectrometric determination of post-harvest fungicides in citrus fruits. **Journal of Chromatography A**., v. 912, n. 2, p. 301-310, 2001.

FOSTER, W. G.; GREGOROVICH, S.; MORRISON, K. M.; ATKINSON, S. A.; KUBWABO, C.; STEWART, B.; TEO, K. Human maternal and umbilical cord blood concentrations of polybrominated diphenyl ethers. **Chemosphere**, v. 84, n. 10, p. 1301–1309, 2011.

FREUNDLICH, H. M. F. Over the adsorption in solution. **The Journal of Physical Chemistry**, v. 57, p. 1100–1107. 1906.

FOO, K.Y.; HAMEED, B.H. Insights into the modeling of adsorption isotherm systems. **Chemical Engineering Journal**, v. 156, p. 2–10, 2010.

GIACOMNI, F.; MENEGAZZO, M.A.B.; DA SILVA, M.G.; DA SILVA, A.B.; DE BARROS, M.A.S.D. Importância da determinação do ponto de carga zero como característica de tingimento de fibras proteicas. **Revista Matéria**, v. 22, n. 2, 2017. https://doi.org/10.1590/S1517-707620170002.0159

GORZA, N. L. **Remoção de Agrotóxicos em uma Instalação Piloto de Tratamento de Águas de Abastecimento do Tipo Convencional, Associado à Pré-Oxidação e Adsorção em Carvão Ativado Granular**. 2012. Dissertação (Mestrado em Engenharia Ambiental), Universidade Federal do Espírito Santo, Vitória-ES, 2012. Disponível em: https://repositorio.ufes.br/bitstream/10/6127/1/Nadja%20Lima%20Gorza.pdf. Acesso em: 15 mar. 2020.

GROVER, D. P.; ZHOU, J. L.; FRICKERS, P. E.; READMAN, J. W. Improved removal of estrogenic and pharmaceutical compounds in sewage effluent by full scale granular activated carbon: Impact on receiving river water. **Journal of Hazardous Materials**, v. 185, n. 2–3, p. 1005–1011, 2011.

GUILLOSSOU, R.; LE ROUX, J.; MAILLER, R.; PEREIRA-DEROME, C. S.; VARRAULT, G.; BRESSY, A.; VULLIET, E.; MORLAY, C.; NAULEAU, F.; ROCHER, V.; GASPERI, J. Influence of dissolved organic matter on the removal of 12 organic micropollutants from wastewater effluent by powdered activated carbon adsorption. **Water Research**, v. 172, p. 115487, 2020.

GUO, S. ZHONG, S.; ZHANG, A. Privacy-preserving Kruskal–Wallis test. **Computer Methods and Programs in Biomedicine**, v. 112, n. 1, p. 135-145, 2013.

GUPTA, V. K.; GUPTA, B.; RASTOGI, A.; AGARWAL, S.; NAYAK A. Pesticides

removal from waste water by activated carbon prepared from waste rubber tire. **Water Research**, v. 45, n. 13, p. 4047–4055. doi: 10.1016/j.watres.2011.05.016., 2011.

HALLÉ, C.; HUCK, P. M.; PELDSZUS, S. Emerging contaminant removal by biofiltration: Temperature, concentration, and EBCT impacts. **Journal - American Water Works Association**, v. 107, n. 7, p. E364–E379, 2015.

HARO, N. K.; DÁVILA, I. V. J.; NUNES, K. G. P.; FRANCO, M. A. E.; MARCILIO, N. R.; FÉRIS, L. A. Kinetic, equilibrium and thermodynamic studies of the adsorption of paracetamol in activated carbon in batch model and fixed-bed column. **Applied Water Science**, v. 11, n. 2, p. 1–9, 2021.

HARO, N. K.; VECCHIO, P. D.; MARCILIO, N. R.; FÉRIS, L. A. Removal of atenolol by adsorption – Study of kinetics and equilibrium. **Journal of Cleaner Production**, v. 154, p. 214–219, 2017.

HARO, N. K. **Remoção dos fármacos Atenolol, Paracetamol e Ampicilina por adsorção em carvão ativado**. 2017. Tese (Doutorado em Engenharia Química), Universidade Federal do Rio Grande do Sul, Porto Alegre, 2017. Disponível em: https://www.lume.ufrgs.br/bitstream/handle/10183/172254/001058103.pdf?sequence=1&isAllowed=y. Acesso em 18 mar. 2020

HENDRICS, D. **Fundamentals of Water Treatment Unit Processes - Physical, Chemical, and Biological**. IWA Publishing. CRC Press. 2011.

HELWEG, A. Degradation and adsorption of Carbendazim and 2-aminobenzimidazole in soil. **Pesticide Science**, v. 8, n. 1, p. 71-78, 1977.

HGEIG, A.; NOVAKOVIĆ, M.; MIHAJLOVIĆ, I. Sorption of Carbendazim and linuron from aqueous solutions with activated carbon produced from spent coffee grounds: Equilibrium, kinetic and thermodynamic approach. **Journal of Environmental Science and Health - Part B Pesticides, Food Contaminants, and Agricultural Wastes**, v. 54, n. 4, p. 226–236, 2019.

HO, L.; GRASSET, C.; HOEFEL, D.; DIXON, M. B.; LEUSCH, F. D. L.; NEWCOMBE, G.; SAINT, C. P.; BROOKES, J. D. Assessing granular media filtration for the removal of chemical contaminants from wastewater. **Water Research**, v. 45, n. 11, p. 3461–3472, 2011.

HO, Y. S.; MCKAY, G. A. Comparison of chemisorption kinetic models applied to pollutant removal on various sorbents. **Process Safety and Environmental Protection**, v. 76, n. 4, 1998.

HO, Y. S. Review of second-order models for adsorption systems. **Journal of Hazardous Materials**, v. 136, n. 3, p. 681–689, 2006.

HOLLANDER, M.; WOLFE, D A. **Nonparametric Statistical Methods**. New York: John Wiley & Sons, p. 115–120, 1973.

HUCK, P. M.; SOZAŃSKI, M. M. Biological filtration for membrane pre-treatment and other applications: Towards the development of a practically-oriented performance parameter. **Journal of Water Supply: Research and Technology - Aqua**, v. 57, n. 4, p. 203–224, 2008.

HUNTER, W. J.; SHANER, D. L. Nitrogen limited biobarriers remove atrazine from contaminated water: Laboratory studies**. Journal of Contaminant Hydrology**, v. 103, n. 1–2, p. 29–37, 2009.

INOUE, K.; KAWAMOTO, K. Adsorption characteristics of carbonaceous adsorbents for organic pollutants in a model incineration exhaust gas. **Chemosphere**, v. 70, n. 3, p. 349–357, 2008.

INSTITUTO BRASILEIRO DO MEIO AMBIENTE E DOS RECURSOS NATURAIS RENOVÁVEIS (IBAMA). **Os 10 ingredientes ativos mais vendidos. Relatórios de comercialização de agrotóxicos**. Atualização de 01/11/2019. Disponível em: http://ibama.gov.br/agrotoxicos/relatorios-de-comercializacao-de-agrotoxicos. Acesso em 27 jan. 2020.

INTERNATIONAL PROGRAMME ON CHEMICAL SAFETY (ICPS). **Carbendazim**. World Health Organization (WHO). Disponível em: http://www.inchem.org/documents/icsc/icsc/eics1277.htm. Acesso em 13 abr. 2020.

INTERNATIONAL UNION OF PURE AND APPLIED CHEMISTRY (IUPAC). **THE PPDB.** Disponível em: http://sitem.herts.ac.uk/aeru/iupac/atoz.htm. Acesso em: 02 abr. 2020.

JIANG, J.; LI, W.; ZHANG, X.; LIU, J.; ZHU, X. A new approach to controlling halogenated DBPs by GAC adsorption of aromatic intermediates from chlorine disinfection : Effects of bromide and contact time. **Separation and Purification Technology**, v. 203, p. 260–267, 2018.

JIN, X.; REN, J.; WANG, B.; LU, Q.; YU, Y. Impact of coexistence of Carbendazim, atrazine, and imidacloprid on their adsorption, desorption, and mobility in soil. **Environmental Science and Pollution Research**, v. 20, n. 9, p. 6282–6289, 2013.

JOSS, A.; SIEGRIST, H.; TERNES, T. A. Are we about to upgrade wastewater treatment for removing organic micropollutants? **Water Science and Technology**, v. 57, n. 2, p. 251–255, 2008.

JULIANO, V. B. **Remoção dos compostos 2-metilisoborneol e geosmina da água de abastecimento por carvão ativado granular e ação microbiana**. 2010. Tese (Doutorado em Recursos Hídricos e Saneamento Ambiental), Universidade Federal do Rio Grande do Sul, Porto Alegre, 2010. Disponível em: https://lume.ufrgs.br/bitstream/handle/10183/32349/000769578.pdf?sequence=1&isAllowed=y. Acesso em: 08 jul. 2020.

KABIR, E. R.; RAHMAN, M. S.; RAHMAN, I. A review on endocrine disruptors and their possible impacts on human health. **Environmental Toxicology and Pharmacology**, v. 40, n. 1, p. 241–258, 2015.

KANJILAL, T.; PANDA, J.; DATTA S. Assessing Brevibacillus sp . C17 : An indigenous isolated bacterium as bioremediator for agrochemical effluent containing toxic Carbendazim. **Journal of Water Process Engineering**, v. 23, p. 174–185, 2018.

KAUFFMAN, D. D.; KATAN, J.; EDWARDS, D. F.; JORDAN, E. G. **Microbial adaptation and metabolism of pesticides**. Totowa: J. L. Hilton, 1985.

KEARNS, J.; DICKENSON, E.; KNAPPE, D. Enabling Organic Micropollutant Removal from Water by Full-Scale Biochar and Activated Carbon Adsorbers Using Predictions from Bench-Scale Column Data. **Environmental Engineering Science**, v. 37, n. 7, p. 459–471, 2020.

KEGEL, F. S.; RIETMAN, B. M.; VERLIEFDE, A. R. D. Reverse osmosis followed by activated carbon filtration for efficient removal of organic micropollutants from riverbank

filtrate. **Water Science and Technology**, v. 61, n. 10, p. 2603–2610, 2010.

KEMKER, C. **Conductivity, Salinity and Total Dissolved Solids**. Fundamentals of Environmental Measurements. Fondriest Environmental, *Inc*. 3 março, 2014. Disponível em: https://www.fondriest.com/environmental-measurements/parameters/water-quality/conductivity-salinity-tds/. Acesso em: 09 dez. 2020.

KEMPISTY, D.M.; AREVALO, E.; SPINELLI, A.M.; EDEBACK, V.; DICKENSON, E.R.V.; HUSTED, C.; HIGGINS, C.P.; SUMMERS, R.S.; KNAPPE, D.R.U. Granular activated carbon adsorption of perfluoroalkyl acids from ground and surface water. **Water Science**, v. 4, p. 1 – 14, 2022.

KENDALL, M. G. A new measure of rank correlation. **Biometrika**, v. 30, p. 81–93, 1938.

KENNEDY, A.M.; REINERT, A.M.; KNAPPE, D.R.U.; FERRER, I.; SUMMERS, R.S. Full- and pilot-scale GAC adsorption of organic micropollutants. **Water Research**, v. 68, p. 238–248, 2015.

KENNEDY, A.M.; REINERT, A.M.; KNAPPE, D.R.U.; SUMMERS, R.S. Prediction of Full-Scale GAC Adsorption of Organic Micropollutants. **Environmental Engineering Science**, v. 34, n. 734, p. 496–507. 2017. DOI: https://doi.org/10.1089/ees.2016.0525

KÜMMERER, K. **3.04 - Emerging Contaminants**. In Abbt-Braun, G., Ahuja, A., Aksoy, H., Amann, R.I., Amy, G., Anderson, E.I., Angelakis, A.N., Asano, T. (Eds), Treatise on Water Science, Elsevier, pp. 69–87. doi: 10.1016/B978-0-444-53199-5.00052-X. 2011

LAGERGREN, S. About the theory of so-called adsorption of soluble substances. **Kungliga Svenska Vetenskapsakademiens**, Handlingar, v. 24, p. 1–39, 1898.

LEWOYEHU, M. Comprehensive review on synthesis and application of activated carbon from agricultural residues for the remediation of venomous pollutants in wastewater. **Journal of Analytical and Applied Pyrolysis**, v. 159, 105279, 2021.

LI, G.; LI, J.; TAN, W.; YANG, M.; WANG, H.; WANG, X. Effectiveness and mechanisms of the adsorption of carbendazim from wastewater onto commercial activated carbon. **Chemosphere,** v. 304, p. 135231, 2022. DOI: https://doi.org/10.1016/j.chemosphere.2022.135231.

LI, L.; QUINLIVAN, P. A.; KNAPPE, D. R. U. Effects of activated carbon surface chemistry and pore structure on the adsorption of organic contaminants from aqueous solution. **Carbon**, v. 40, n. 12, p. 2085–2100, 2002.

LI, X.; ZHOU, Q.; WEI, S.; REN, W.; SUN, X. Adsorption and desorption of Carbendazim and cadmium in typical soils in northeastern China as affected by temperature. **Geoderma**, v. 160, n. 3–4, p. 347–354, 2011.

LIEBSCHER, E. Kendall regression coefficient. **Computational Statistics and Data Analysis**, v. 157, p. 107140, 2021.

LIMA, E. C.; GOMES, A. A.; TRAN, H. N. Comparison of the nonlinear and linear forms of the van't Hoff equation for calculation of adsorption thermodynamic parameters ($\Delta S°$ and $\Delta H°$). **Journal of Molecular Liquids**, v. 311, p. 113315, 2020.

LIMA, L. **Avaliação da remoção de sulfametoxazol, diclofenaco e 17β-estradiol em águas por adsorção em carvão ativado granular**. 2014. Dissertação (Mestrado em Engenharia Civil), Universidade Estadual Paulista, Ilha Solteira-SP, 2014. Disponível em: https://repositorio.unesp.br/handle/11449/126300. Acesso em 05 jun. 2020.

LOPES, B.; ARREBOLA, J. P.; SERAFIM, A.; COMPANY, R.; ROSA, J.; OLEA, N. Polychlorinated biphenyls (PCBs) and p,p'-dichlorodiphenyldichloroethylene (DDE) concentrations in maternal and umbilical cord serum in a human cohort from South Portugal. **Chemosphere**, v. 114, p. 291–302, 2014.

LOPES, T. S. A. **Avaliação da remoção de agrotóxicos por biorreator de membrana e pós-tratamentos de carvão ativado, osmose reversa e ozonização**. 2019. Dissertação (Mestrado em Engenharia Civil e Ambiental), Universidade Federal da Paraíba, João Pessoa, 2019. Disponível em: https://repositorio.ufpb.br/jspui/bitstream/123456789/15952/1/Arquivototal.pdf. Acesso em 20 dez. 2020.

LULE, G. M.; ATALAY, M. U. Comparison of fenitrothion and trifluralin adsorption on organo-zeolites and activated carbon. Part II: Thermodynamic parameters and the suitability of the kinetic models of pesticide adsorption. **Particulate Science and Technology**, v. 32, n. 4, p. 426–430, 2014.

MAATAOUI, Y. E.; M'RABET, M. E.; MAAROUFI, A.; OUDDA, H.; DAHCHOUR, A. Adsorption isotherm modeling of Carbendazim and flumetsulam onto homoionic-montmorillonite clays: comparison of linear and nonlinear models. **Turkish Journal of Chemistry**, v. 41, n. 4, p. 514–524, 2017.

MACHADO, R. M.; DA SILVA, S. W.; BERNARDES, A. M.; FERREIRA, J. Z. Degradation of Carbendazim in aqueous solution by different settings of photochemical and electrochemical oxidation processes. **Journal of Environmental Management**, v. 310, n. 114805, 2022.

MANSOURIIEH, N.; SOHRABI, M. R.; KHOSRAVI, M. Adsorption kinetics and thermodynamics of organophosphorus profenofos pesticide onto Fe/Ni bimetallic nanoparticles. **International Journal of Environmental Science and Technology**, v. 13, n. 5, p. 1393–1404, 2016.

MAVAIEIE JÚNIOR, P.A.; BENETTI, A.D. Remoção de carbono orgânico dissolvido de águas filtradas com tratamento complementar por pré-oxidação com ozônio e adsorção em carvão ativado. **Engenharia Sanitária e Ambiental**, v. 26, n. 6, p. 989–1001. 2021.

MAVAIEIE JÚNIOR, P. A. **Remoção de carbono orgânico dissolvido em águas de abastecimento por pré-oxidação e adsorção em carvão ativado granular**. 2019. Dissertação (Mestrado em Recursos Hídricos e Saneamento Ambiental), Instituto de Pesquisas Hidráulicas, Universidade Federal do Rio Grande do Sul, Porto Alegre. Acesso em 20. Jun. 2019.

MAZELLIER, P.; LEROY, É.; LEGUBE, B. Photochemical behavior of the fungicide carbendazim in dilute aqueous solution. **Journal of Photochemistry and Photobiology A: Chemistry**, v. 153, n. 1–3, p. 221-227, 2002.

MCKIE, M. J.; ANDREWS, S. A.; ANDREWS, R. C. Conventional drinking water treatment and direct biofiltration for the removal of pharmaceuticals and artificial

sweeteners: A pilot-scale approach. **Science of the Total Environment**, v. 544, p. 10–17, 2016.

MEREL, S.; BENZING, S.; GLEISER, C.; NAPOLI-DAVIS, G. D.; ZWIENER, C. Occurrence and overlooked sources of the biocide Carbendazim in wastewater and surface water. **Environmental Pollution**, v. 239, n. 2007, p. 512–521, 2018.

MERLE, T.; KNAPPE, D. R. U.; PRONK, W.; VOGLER, B.; HOLLENDER, J.; GUNTEN, U. V. Assessment of the breakthrough of micropollutants in full-scale granular activated carbon adsorbers by rapid small-scale column tests and a novel pilot-scale sampling approach. **Environmental Science: Water Research and Technology**, v. 6, n. 10, p. 2742–2751, 2020.

METCALF & EDDY. **Wastewater engineering - Treatment and resource recovery**. 5th ed. Boston: McGraw-Hill, 2014.

MIYITTAH, M.K.; TSYAWO, F.W.; KUMAH, K.K.; STANLEY, C.D.; RECHCIGL, J.E. Suitability of Two Methods for Determination of Point of Zero Charge (PZC) of Adsorbents in Soils. **Communications in Soil Science and Plant Analysis**, v. 47, p. 101–111, 2016.

MOUSSAVI, G.; HOSSEINI, H.; ALAHABADI, A. The investigation of diazinon pesticide removal from contaminated water by adsorption onto NH4Cl-induced activated carbon. **Chemical Engineering Journal**, v. 214, p. 172–179. 2013. DOI: https://doi.org/10.1016/j.cej.2012.10.034

NAGASE, H.; PATTANASUPONG, A.; SUGIMOATO, E.; INOUC, M.; HIRATA, K.; TANI, K.; NASU, M.; MIYAMOTO, K. Effect of environmental factors on performance of immobilized consortium system for degradation of Carbendazim and 2,4-dichlorophenoxyacetic acid in continuous culture. **Biochemical Engineering Journal**, v. 29, n. 1-2, p. 163-168, 2006.

NARBAITZ, R. M.; MCEWEN, J. Electrochemical regeneration of field spent GAC from two water treatment plants. **Water Research**, v. 46, n.15, p. 4852-4860, 2012.

NOVOTNY, V. **Water quality:** diffuse pollution and watershed management. New Jersey: Wiley, 2002.

NOWOTNY, N.; EPP, B.; SONNTAG, C. V.; FAHLENKAMP, H. Quantification and modeling of the elimination behavior of ecologically problematic wastewater micropollutants by adsorption on powdered and granulated activated carbon. **Environmental Science and Technology**, v. 41, n. 6, p. 2050–2055, 2007.

NEKOUEI, F.; NEKOUEI, S.; TYAGI, I.; GUPTA, V. K. Kinetic, thermodynamic and isotherm studies for acid blue 129 removal from liquids using copper oxide nanoparticle-modified activated carbon as a novel adsorbent. **Journal of Molecular Liquids**, v. 201, p. 124-133, 2015.

ÖBERG, K.; WARMAN, K.; ÖBERG, T. Distribution and Levels of Brominated Flame. **Chemosphere**, v. 48, p. 805–809, 2002.

OKOYE, C. C.; ONUKWULI, O. D.; OKEY-ONYESOLU, C. F.; NWOKEDI, I. C. Utilization of salt activated Raphia hookeri seeds as biosorbent for Erythrosine B dye removal: Kinetics and thermodynamics studies. **Journal of King Saud University – Science**, v. 31, n. 4, p. 849-858, 2019.

OMARA, M.; HOLSEN, T. M.; XIA, X.; PAGANO, J. J.; CRIMMINS, B. S.; HOPKE, P.

K. Comparison of PoraPak Rxn RP and XAD-2 adsorbents for monitoring dissolved hydrophobic organic contaminants. **Environmental Monitoring and Assessment**, v. 186, p. 7565–7577, 2014.

OSMARI, T. A.; GALLON, R.; SCHWAAB, M. COUTINHO, E. B.; SEVERO, J. B.; PINTO JR., J. C.Statistical analysis of linear and non-linear regression for the estimation of adsorption isotherm parameters. **Adsorption Science and Technology**, v. 31, n. 5, p. 433–458, 2013.

ÖZCAN, A. S.; ÖZCAN, A. Adsorption of acid dyes from aqueous solutions onto acid-activated bentonite. **Journal of Colloid and Interface Science**, v. 276, n. 1, p. 39–46, 2004.

PAREDES, L.; FERNANDEZ-FONTAINA, E.; LEMA, J. M.; OMIL, F.; CARBALLA, M. Understanding the fate of organic micropollutants in sand and granular activated carbon biofiltration systems. **Science of the Total Environment**, v. 551–552, p. 640–648, 2016.

PASZKO, T. Sorptive Behavior and Kinetics of Carbendazim in Mineral Soils. **Polish Journal of Environmental Studies**, v. 15, n. 3, p. 449–456, 2006.

PATTANASUPONG, A.; NAGASE, H.; INOUC, M.; TANI, K.; NASU, M.; HIRATA, K.; MIYAMOTO, K. Ability of a microbial consortium to remove pesticides, Carbendazim and 2,4-diclorophenoxyacetic acid. **World Journal of Microbiology & Biotechnology**, v. 20, p. 517-522, 2004.

PEDUZZI P. **Anvisa proíbe uso do fungicida carbendazim em produtos agrotóxicos.** Agência Brasil. Disponível em: <https://agenciabrasil.ebc.com.br/saude/noticia/2022-08/anvisa-proibe-uso-do-fungicida-carbendazim-em-produtos-agrotoxicos>. Acesso em 20. Out. 2022.

PELEKANI, C.; SNOEYINK, V.L. Competitive adsorption in natural water: Role of activated carbon pore size. **Water Research**, v. 33, n. 5, p. 1209–1219. 1999. DOI: https://doi.org/https://doi.org/10.1016/S0043-1354(98)00329-7

PEREIRA, A. R. **Remoção de Carbendazim de água por processo de clarificação acoplado à adsorção ou cloração**. 2018. Dissertação (Mestrado em Engenharia Ambiental), Universidade Federal de Outro Preto, Ouro Preto, 2018. Disponível em: https://www.repositorio.ufop.br/bitstream/123456789/9634/1/DISSERTA%C3%87%C3%83O_Remo%C3%A7%C3%A3oCarbendazim%C3%81gua.pdf. Acesso em 20. Jun. 2019.

PESTICIDE ACTION NETWORK (PAN). **Carbendazim: identification, toxicity, use, water pollution potential, ecological toxicity and regulatory information**. Disponível em: http://www.pesticideinfo.org/Detail_Chemical.jsp?Rec_Id=PRI1877#Toxicity. Acesso em 13 abr. 2020.

PICCIN, J. S.; CADAVAL JR., T. R. S.; PINTO, L. A. A. de.; DOTTO, G. L. Adsorption Isotherms in Liquid Phase: Experimental, Modeling, and Interpretations. *In*: BONILLA-PETRICIOLET, A.; MENDOZA-CASTILLO, D. I.; REYNEL-ÁVILA, H. E. **Adsorption Processes for Water Treatment and Purification**. 1st edition. Springer International Publishing, 2017. p. 19-51.

PLATTNER, J.; KAZNER, C.; NAIDU, G.; WINTGENS, T.; VIGNESWARAN, S. Removal of selected pesticides from groundwater by membrane distillation. **Environmental Science and Pollution Research**, v. 25, p. 20336–20347, 2018.

POLO, M.; LLOMPART, M.; GARCIA-JARES, C.; GOMEZ-NOYA, G.; BOLLAIN, M. H.; CELA, R. Development of a solid-phase microextraction method for the analysis of phenolic flame retardants in water samples. **Journal of Chromatography A**, v. 1124, n. 1–2, p. 11–21, 2006.

POURREZA, N.; RASTEGARZADEH, S.; LARKI, A. Determination of fungicide Carbendazim in water and soil samples using dispersive liquid-liquid microextraction and microvolume UV – vis spectrophotometry. **Talanta**, v. 134, p. 24–29, 2015.

PRETE, M. C.; DE OLIVEIRA, F. M.; TARLEY, C. R. T. Assessment on the performance of nano-carbon black as an alternative material for extraction of Carbendazim, tebuthiuron, hexazinone, diuron and ametryn. **Journal of Environmental Chemical Engineering**, v. 5, n. 1, p. 93–102, 2017.

PUBCHEM. **Carbendazim (Compound)**. Disponível em: https://pubchem.ncbi.nlm.nih.gov/compound/25429#section=NIOSH-Toxicity-Data. Acesso em 02 abr. 2020.

RAMA, E. M.; BORTOLAN, S.; VIEIRA, M. L.; GERARDIN, D. C. C.; MOREIRA, E. G. Reproductive and possible hormonal effects of Carbendazim. **Regulatory Toxicology and Pharmacology**, v. 69, n. 3, p. 476–486, 2014.

RAMA, E. M. **Avaliação do risco à saúde decorrente da exposição ocupacional e dietética ao agrotóxico Carbendazim no Brasil**. 2013. Dissertação (Mestrado em Toxicologia Aplicada à Vigilância Sanitária), Universidade Estadual de Londrina, Londrina, 2013. Disponível em: http://www.bibliotecadigital.uel.br/document/?code=vtls000185324. Acesso em 22 jun. 2019.

RATHI, B. S.; KUMAR, P. S. Application of adsorption process for effective removal of emerging contaminants from water and wastewater. **Environmental Pollution**, v. 280, p. 116995, 2021.

REINEKE, N.; BISELLI, S.; FRANKE, S.; FRANCKE, W.; HEINZEL, N.; HÜHNERFUSS, H.; IZNAGUEN, H.; KAMMANN, U.; THEOBALD, N.; VOBACH, M.; WOSNIOK, W. Brominated indoles and phenols in marine sediment and water extracts from the North and Baltic Seas-concentrations and effects. **Archives of Environmental Contamination and Toxicology**, v. 51, n. 2, p. 186–196, 2006.

REUNGOAT, J.; ESCHER, B. I.; MACOVA, M.; KELLER, J. Biofiltration of wastewater treatment plant effluent: Effective removal of pharmaceuticals and personal care products and reduction of toxicity. **Water Research**, v. 45, n. 9, p. 2751–2762, 2011.

RIFI, S. K.; SOUABI, S.; FELS, L. E.; DRIOUICH, A.; NASSRI, I.; HADDAJI, C.; HAFIDI, M. Optimization of coagulation process for treatment of olive oil mill wastewater using Moringa oleifera as a natural coagulant, CCD combined with RSM for treatment optimization. **Process Safety and Environmental Protection**, v. 162, p. 406-418, 2022.

RIZZI, V.; GUBITOSA, J.; FINI, P.; ROMITA, R.; AGOSTIANO, A.; NUZZO, S.; COSMA P. Commercial bentonite clay as low-cost and recyclable “natural” adsorbent for the Carbendazim removal / recover from water: Overview on the adsorption process

and preliminary photodegradation considerations. **Colloids and Surfaces A**, v. 602(April), p. 125060, 2020.

ROGERS, H. R. Sources, behavior and fate of organic contaminants during sewage treatment and in sewage sludges. **Science of the Total Environment**, v. 185, p. 3-26, 1996.

ROYSTON, J. P. Algorithm AS 181: The W test for Normality. **Applied Statistics**, v. 31, n. 2, p. 176–180, 1982.

RUIZ, B.; CABRITA, I.; MESTRE, A.S.; PARRA, J.B.; PIRES, J.; CARVALHO, A.P.; ANIA, C.O. Surface heterogeneity effects of activated carbons on the kinetics of paracetamol removal from aqueous solution. **Applied Surface Science**, v. 256, n. 17, p. 5171–5175., 2010.

RUTHVEN, D. M. **Principles of adsorption and adsorption processes**. New York: Wiley, 1984.

SALIM, N. A. A.; PUTEH, M. H.; KHAMIDUN, M. H.; FULAZZAKY, M. A.; ABDULLAH, N. H.; YUSOFF, A. R. M.; ZAINI, M. A. A.; AHMAD, N.; LAZIM, Z. M.; NUID, M. Interpretation of isotherm models for adsorption of ammonium onto granular activated carbon. **Biointerface Research in Applied Chemistry**, v. 11, n. 2, p. 9227–9241, 2021.

SEKULIĆ, M. T.; PAP, S.; STOJANOVIC, Z.; BOSKOVIC, N.; RADONIC, J.; KNUDSEN, T. S. Efficient removal of priority, hazardous priority and emerging pollutants with Prunus armeniaca functionalized biochar from aqueous wastes: Experimental optimization and modeling. **Science of the Total Environment**, v. 613–614, p. 736–750, 2018.

SELIN, Ş.; EMIK, S. Fast and highly efficient removal of 2,4-D using amino-functionalized poly (glycidyl methacrylate) adsorbent : Optimization , equilibrium, kinetic and thermodynamic studies. **Journal of Molecular Liquids**, v. 260, p. 195–202, 2018.

SILANPÄÄ, M. Natural organic matter in water: characterization and treatment methods. Amsterdan: Elsevier/IWA, 2015.

SILVA, C. M. M. S.; FAY, E. F.; MELO, I. S. Degradação do fungicida Carbendazim por Phanerochaete chrysosporium. **Fitopatologia Brasileira**, v. 21, n. 4, p. 498-496, 1996.

SIMPSON, D. R. Biofilm processes in biologically active carbon water purification. **Water Research**, v. 42, n. 12, p. 2839–2848, 2008.

SINGH, S.; SINGH, N.; KUMAR, V.; DATTA, S.; WANI, A. B.; SINGH, D.; SINGH, K.; SINGH, J. Toxicity, monitoring and biodegradation of the fungicide Carbendazim. **Environmental Chemistry Letters**, v. 14, p. 317–329 2016.

SNYDER, S. A.; ADHAM, S.; REDDING, A. M.; CANNON, F. S.; DECAROLIS, J.; OPPENHEIMER, J.; WERT, E. C. YOON, Y. Role of membranes and activated carbon in the removal of endocrine disruptors and pharmaceuticals. **Desalination**, v. 202, n. 1–3, p. 156–181, 2007.

STRID, A.; SMEDJE, G.; ATHANASSIADIS, I.; LINDGREN, T.; LUNDGREN, H.; JAKOBSSON, K.; BERGMAN, A. Brominated flame retardant exposure of aircraft personnel. **Chemosphere**, v. 116, p. 83–90, 2014.

SUMMERS, R.S.; KNAPPE, D.R.U.; SNOEYINK, V.L. Adsorption of organic compounds by activated carbon. *In*: EDZWALD, J.K. **Water quality and treatment: a handbook on drinking water**. 6th ed. New York: McGraw-Hill/American Water Works Association, 2011. Chapter 14.

SUZUKI, G.; TAKIGAMI, H.; WATANABE, M.; TAKAHASHI, S.; NOSE, K.; ASARI, M.; SAKAI, S. I. Identification of Brominated and Chlorinated Phenols as Potential Thyroid-Disrupting Compounds in Indoor Dusts. **Environmental Science and Technology**, v. 42, n. 5, p. 1794–1800, 2008.

TAMBOSI, J. L. **Remoção de fármacos e avaliação de seus produtos de degradação através de tecnologias avançadas de tratamento**. 2008. Tese (Doutorado em Engenharia Química), Universidade Federal de Santa Catarina, Florianópolis, 2008. Disponível em: https://repositorio.ufsc.br/handle/123456789/90956. Acesso em 25 jun. 2019.

TAKTAK, F.; İLBAY, Z.; ŞAHIN, S. Evaluation of 2,4-D removal via activated carbon from pomegranate husk / polymer composite hydrogel: Optimization of process parameters through face centered composite design'**. Korean Journal of Chemical Engineering**, v. 32, n. 9, p. 1879–1888, 2015.

TEIXEIRA, Marina Bergamaschi. **Remoção de Carbono Orgânico dissolvido de água de abastecimento por adsorção em carvão ativado granular**. 2014. Dissertação (Mestrado em Recursos Hídricos e Saneamento Ambiental), Universidade Federal do Rio Grande do Sul, Porto Alegre, 201a. Disponível em: https://www.lume.ufrgs.br/bitstream/handle/10183/119392/000970086.pdf?sequence=1&isAllowed=y. Acesso em 20. Jun. 2019.

THURMAN, E.; WERSHAW, R.L.; MALCOLM, R.L.; PINCKNEY, D.J. Molecular sizes of aquatic humic substances. **Organic Geochemistry**, v. 4, p. 27-35, 1982.

TOLOSA, I.; BAYONA, J. M.; ALBAIGÉS, J. Identification and occurrence of brominated and nitrated phenols in estuarine sediments. **Marine Pollution Bulletin**, v. 22, n. 12, p. 603–607, 1991.

TUKEY, J. W. One Degree of Freedom for Non-Additivity. **Biometrics - International Biometric Society,** v. 5, nº 3 p. 232-242, 1949.

VOLTAN, P. E. N.; DANTAS, A. D. B.; PASCHOALATO, C. F. R.; BERNARDO, L. D. Predição da performance de carvão ativado granular para remoção de herbicidas com ensaios em coluna de escala reduzida. **Engenharia Sanitaria e Ambiental**, v. 21, n. 2, p. 241–250, 2016.

WANG, T.; ZHANG, Z.; ZHANG, H.; ZHONG, X.; LIU, Y.; LIAO, S.; YUE, X.; ZHOU, G. Sorption of Carbendazim on activated carbons derived from rape straw and its mechanism. **The Royal Society of Chemistry Advances**, v. 9, p. 41745 – 41754, 2019.

WANG, T.; YU, C.; CHU, Q.; WANG, F.; LAN, T.; WANG, J. Adsorption behavior and mechanism of five pesticides on microplastics from agricultural polyethylene films. **Chemosphere**, v. 244, p. 125491, 2020.

WATER RESOURCES MISSION AREA (WRMA). **Emerging Contaminants**. 2019. Disponível em: https://www.usgs.gov/mission-areas/water-resources/science/emerging-contaminants. Acesso em 02 mai 2023

WEBER, W. J. MORRIS, J. C. Kinetics of adsorption on carbon from solution. **Journal of the Sanitary Engineering Division**, v. 89, n. 2, pp.31–60.

WEFER-ROEHL, A.; GRABER, E. R.; BORISOVER, M. D.; ADAR, E.; NATIV, R.; RONEN, Z. Sorption of organic contaminants in a fractured chalk formation. **Chemosphere**, v. 44, n. 5, p. 1121–1130, 2001.

WESTERHOFF, P. YOON, Y.; SNYDER, S.; WERT, E. Fate of endocrine-disruptor, pharmaceutical, and personal care product chemicals during simulated drinking water treatment processes. **Environmental Science and Technology**, v. 39, n. 17, p. 6649–6663, 2005.

WOODCOCK, D. **Microbial degradation of fungicides fumigantes and nematicides**. New York: Pesticide Microbiology, 1978.

WU, J. P.; GUAN, Y. T.; ZHANG, Y.; LUO, X. J.; ZHI, H.; CHEN, S. J.; MAI, B. X. Several current-use, non-PBDE brominated flame retardants are highly bioaccumulative: Evidence from field determined bioaccumulation factors. **Environment International**, v. 37, n. 1, p. 210–215, 2011.

YARDEN, O.; SALOMON, R.; KATAN, J.; AHARONSON, N. Involvement of fungi and bacteria in enhanced and nonenhanced biodegradation of Carbendazim and other benzimidazole in soil. **Canadian Journal of Microbiology**, v. 36, p. 15-36, 1990.

YARDEN, O.; AHARONSON, N.; KATAN, J. Accelerated microbial degradation of methyl benzimidazole-2-ylcarbamate in soil and its control. **Soil Biology and Biochemistry**, v. 19, p. 735-739, 1987.

YAMANAPPA, W.; SUDEEP, P. V.; SABU, M. K.; RAJAN, J. Non-Local means image denoising using Shapiro-Wilk Similarity measure. **IEEE Access**, v. 6, p. 66914-66922, 2018.

YU, Y.; ZHUANG, Y. Y.; WANG, Z. H.; QIU, M. Q. Adsorption of water-soluble dyes onto modified resin. **Chemosphere**, v. 54, n. 3, p. 425–430, 2004.

ZANELLA, O.; KLEIN, E. HARO, N. K.; CARDOSO, M. G. TESSARO, I. C.; FÉRIS, L. A. Equilibrium studies, kinetics and thermodynamics of anion removal by adsorption**. World Review of Science, Technology and Sustainable Development**, v. 12, n. 3, p. 193–218, 2016.

ZHILTSOVA, T.; MARTINS, N.; SILVA, M. R. F.; SILVA, C. F.; LOURENÇO, M. A. O.; TOBALDI, D. M.; COVITA, D.; SEABRA, M. P.; FERREIRA, P. Experimental and Computational Analysis of NOx Photocatalytic Abatement Using Carbon-Modified TiO2 Materials. **Catalysts**, v. 10, n. 2, p. 1–16, 2020.

ZHOU, Y.; ZHANG, L.; CHENG, Z. Removal of organic pollutants from aqueous solution using agricultural wastes: A review. **Journal of Molecular Liquids**, v. 212, p. 739–762, 2015.

ZHU, P.; SOTTORFF, I.; ZHANG, T.; HELMREICH, B. Adsorption of Heavy Metals and Biocides from Building Runoff onto Granular Activated Carbon—The Influence of Different Fractions of Dissolved Organic Matter. **Water**, v. 15, n. 11, p. 2099, 2023.

ZOLGHARNEIN, J.; SHAHMORADI, A.; GHASEMI, J. Pesticides Removal Using Conventional and Low-Cost Adsorbents: A Review. **Clean - Soil, Air, Water**, v. 39, n. 12, p. 1105–1119, 2011.

8. ANEXO 1 – IMAGENS DA MICROSCOPIA ELETRÔNICA DE VARREDURA

Nas imagens a seguir é possível ver os poros e a granulometria do CAG de Osso bovino, utilizado nos Artigos 2 e 3.


200 µm
410x
658 µm
15kV - Image
BSD Full
APR 08 2022 12:31
CAP

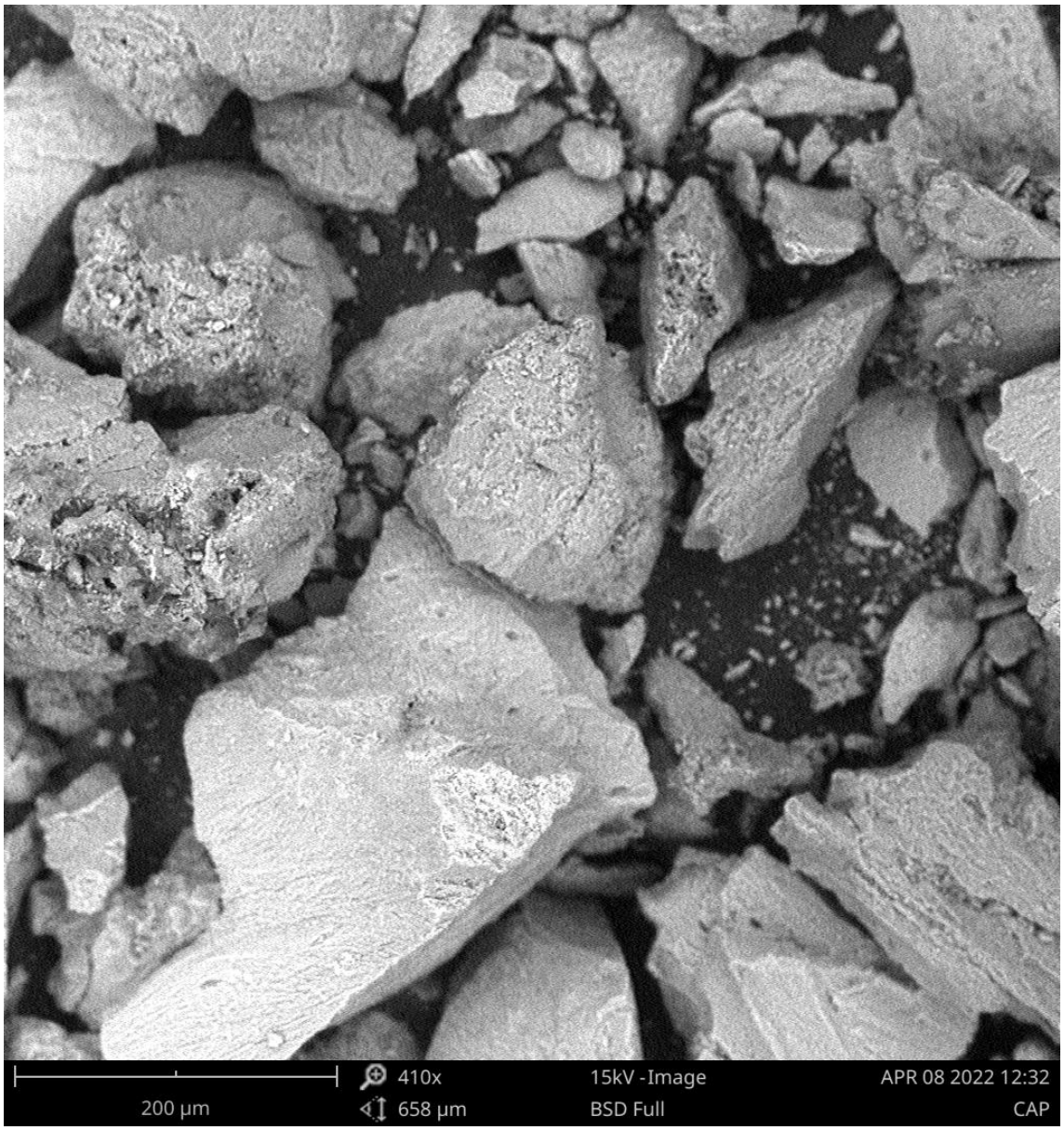
200 µm
410x
658 µm
15kV - Image
BSD Full
APR 08 2022 12:32
CAP


200 µm
410x
658 µm
15kV - Image
BSD Full
APR 08 2022 12:33
CAP


200 µm
410x
658 µm
15kV - Image
BSD Full
APR 08 2022 12:34
CAP